The Effect of Doxorubicin Administration on Skeletal Muscle

by

Sergio Fabris

Thesis submitted in partial fulfillment
of the requirements for the degree of
Doctor of Philosophy (PhD) in Biomolecular Sciences

Faculty of Graduate Studies
Laurentian University
Sudbury, Ontario

THESIS DEFENCE COMMITTEE/COMITÉ DE SOUTENANCE DE THÈSE
Laurentian Université/Université Laurentienne
Faculty of Graduate Studies/Faculté des études supérieures

Title of Thesis Titre de la thèse	The Effect of Doxorubicin Administration on Skeletal Muscle	
Name of Candidate Nom du candidat	Fabris, Sergio	
Degree Diplôme	Doctor of Philosophy	
Department/Program Département/Programme	Biomolecular Sciences	Date of Defence Date de la soutenance August 29, 2017

APPROVED/APPROUVÉ

Thesis Examiners/Examinateurs de thèse:

Dr. David MacLean
(Supervisor/Directeur(trice) de thèse)

Dr. Aseem Kumar
(Committee member/Membre du comité)

Dr. Amadeo Parissenti
(Committee member/Membre du comité)

Approved for the Faculty of Graduate Studies
Approuvé pour la Faculté des études supérieures
Dr. David Lesbarrères
Monsieur David Lesbarrères

Dr. Marina Mourtzakis Dean, Faculty of Graduate Studies
(External Examiner/Examinateur externe) Doyen, Faculté des études supérieures

Dr. Kabwe Nkongolo
(Internal Examiner/Examinateur interne)

ACCESSIBILITY CLAUSE AND PERMISSION TO USE

Abstract

Skeletal muscle (SM) is the largest organ in the human body and represents approximately 40% of the total body weight. Maintenance of SM mass and integrity is dependent on the delivery and removal of essential metabolic products as well as the dynamic balance between protein synthesis and degradation. The health and maintenance of skeletal muscle in cancer patients is of particular importance, as the significant loss of muscular mass is an indication of cachexia, a serious life-threatening condition. Doxorubicin (DOX) is a broad-spectrum anti-cancer chemotherapeutic and remains one of the most widely used chemotherapeutic agents for the treatment of solid tumors and hematological malignancies. The clinical use of DOX is limited by a well described dose-dependent and cumulative cardiotoxic side effect. The majority of DOX-related research remains focused on reducing cardiotoxicity while little is known of the effect of the drug on SM. Therefore, the purpose of the thesis was to study the effects of DOX chemotherapy on SM.

Study 1. The purpose of Study 1 was to examine the accumulation of doxorubicin (DOX) and its metabolite doxorubicinol (DOXol) in skeletal muscle of the rat up to 8 days after the administration of a 1.5 or 4.5 mg/kg i.p. dose. Subsequent to either dose, DOX and DOXol were observed in skeletal muscle throughout the length of the experiment. Interestingly an efflux of DOX was observed after 96 hrs, followed by an apparent re-uptake of the drug which coincided with a spike and rapid decrease of plasma DOX concentrations. The interstitial space within the muscle did not appear to play a significant rate limiting compartment for the uptake or release of DOX or DOXol from the tissue to

the circulation. Furthermore, there was no evidence that DOX preferentially accumulated in a specific muscle group with either dose.

Study 2. Study 2 examined intracellular and interstitial nitric oxide (NO) concentrations in the SM following the administration of DOX. A single dose of 1.5 or 4.5 mg/kg was administered intraperitoneally to male Sprague-Dawley rats and interstitial (IS) and intracellular (IC) NO was quantified every 24 up to 192 hrs. post injection. There was no significant difference in IC NO following the injection of 1.5 mg/kg DOX when compared to control, however the administration of 4.5 mg/kg DOX resulted in lower ($P<0.05$) concentrations of NO in the IC. Interestingly, a consistently higher ($P<0.05$) concentration of NO in the IS was established following the administration of 1.5 mg/kg compared to control while no significant changes in IS NO resulted from the administration of the 4.5 mg/kg dose. The fluctuation of IS and IC NO were not a result of substrate availability as arginine concentrations remained stable throughout the experiment.

Study 3. The purpose of Study 3 was to examine the effect of DOX administration on IC, IS and vascular concentrations of amino acids (AA) in SM of the rat up to 8 days after the administration of a 1.5 or 4.5 mg/kg i.p. dose. Intracellular total amino acids (TAA), essential amino acids (EAA) and branched-chain amino acids (BCAA) were significantly increased in each muscle group analyzed, following the 1.5 and 4.5 mg/kg doses compared to control. In the plasma, TAA were significantly increased compared to control where greater ($P>0.05$) concentrations were observed following the 1.5 mg/kg dose compared to the 4.5 mg/kg dose. Compared to control, the 1.5 mg/kg dose resulted in an increase ($P<0.05$) in interstitial TAA whereas the 4.5 mg/kg resulted in a sustained decrease ($P<0.05$).

These data represent the first concurrent investigation into the accumulation of DOX in the IC, IS and vascular spaces as well as the resulting effects on NO and AA concentrations in these communicating compartments. Overall, SM plays an important factor in the availability and metabolism of DOX and the effect of DOX on SM may play a more significant role in the therapeutic impact of DOX than previously considered. This thesis provides a substantial foundation for future studies focused on reducing DOX-induced skeletal muscle damage.

Acknowledgements

It is honor to have completed my doctoral thesis under the supervision of Dr. David MacLean. Your mentorship and guidance gave me the technical ability and confidence to conduct quality research. I am forever grateful for your insight and friendship, thank you Dr. MacLean.

I profoundly thank my parents who have provided me the opportunity to pursue my ambitions. My gratitude extends far beyond these words. For their endless support and interest in my thesis, I am proud to share this accomplishment with my family.

My friends, I thank you for always making yourselves available to share the good results or help me deal with the frustrations – each in your own unique way. Know you have all played a great role in the completion of my thesis.

Table of Contents

List of Abbreviations

AA – amino acids

ADP – adenosine diphosphate

AKR – aldo-keto reductase

AMP – adenosine monophosphate

ATP – adenosine triphosphate

ATPase – adenosine triphosphatase

BCAA – branched-chain amino acids

BCAT, BCAAT – branched-chain amino acid aminotransferase

BCKA – branched-chain ketoacids

BCKADH – branched-chain ketoacid dehydrogenase

CBR1 – carbonyl reductase 1

cGMP – cyclical guanosine monophosphate

CK – creatine kinase

Ctrl – control

DNA – deoxyribonucleic acid

DOX – Doxorubicin

DOXol – Doxorubicinol

EAA – essential amino acids

EF-2 – elongation factor 2

eNOS – endothelial nitric oxide synthase

GTP – guanosine triphosphate

HPLC – high performance liquid chromatography

IC – intracellular

IL-1 – interleukin 1

IL-6 – interleukin 6

IFNγ – interferon gamma

iNOS – inducible nitric oxide synthase

IP, i.p. – intraperitoneal

ISS, IS – interstitial space

IV – intravenous

JAK/STAT – janus kinase and signal transducer and activator of transcription

Jun-D – transcription factor Jun-D

KIC – α-ketoisocaporate

KIV – α-ketoisovolerate

KMV – α-keto-β-methylvalerate

MCK – muscle creatine kinase

mTOR – mamalian target of rapamycin

mTORC1 – mamalian target of rapamycin complex 1

mTORC2 – mamalian target of rapamycin complex 2

MyoD – myoblast determination protein

NADH – nicotinamide adenine dinucleotide

NF-κB – nuclear factor kappa-light-chain-enhancer of activated B cells

NH_3 – ammonia

nNOS – neuronal nitric oxide synthase

NO – nitric oxide

NOS – nitric oxide synthase

0_2^- – superoxide

$ONOO^-$ – peroxynitrites

PI3K – phosphoinositide 3 kinase

PIF – proteolysis inducing factor

PKG – protein kinase G

PL – plantaris

Rag – Ras-related GTP-binding protein

RALBP1 – RalA-binding protein 1

RG – red gastrocnemius

Rheb – ras-homolog enriched in the brain

ROS – radical oxygen species

rRNA – ribosomal ribonucleic acid

SM – skeletal muscle

SOL – soleus

SOP – statement of procedures

TAA – total amino acids

TCA cycle – tricarboxylic acid cycle

TNFα – tumor necrosis factor alpha

TOPII, TOP2A – topoisomerase II

UPP – ubiquitin proteasome pathway

UPR – unfolded protein response

WG – white gastrocnemius

List of Figures and Tables

Chapter II:

Chapter III:

Chapter IV:

CHAPTER I

1. Literature Review

1.1 Skeletal Muscle Energetics

Skeletal muscle represents the largest organ in the human body, consisting of approximately 40% of the total body weight. The mechanical role of skeletal muscle is essential to life and muscle contraction is dependent on the breakdown of adenosine triphosphate (ATP) by adenosine triphosphatase (ATPase) and the resulting release of free energy in form of inorganic phosphate (P_i). The contribution of three well established energy systems are primarily responsible for the replenishment of ATP stores (Baker, McCormick, & Robergs, 2010; Westerblad, Bruton, & Katz, 2010). The phosphagen system rapidly regenerates ATP by way of creatine kinase (CK), adenylate kinase and adenosine monophosphate (AMP) deaminase. The reversible enzymatic activity of CK allows for the rapid breakdown or synthesis of phosphocreatine during energy expenditure or storage, respectively. Additionally, adenylate kinase is a phosphotransferase that catalyzes a reaction that converts two adenosine diphosphate (ADP) molecules into a single ATP and AMP molecule. Equally important to the production of ATP is that of AMP, which activates phosphorylase and phosphofructokinase, two key enzymes in the initial phase of the glycolytic pathway. The glycolytic pathway regulates carbohydrate metabolism by catabolizing glycogen stores into glucose and promoting the uptake of glucose from the blood, (Pilegaard et al., 1999) producing a net yield of ATP as well as pyruvate and nicotinamide adenine dinucleotide (NADH). In the presence of oxygen, pyruvate is

shuttled to the mitochondria where it enters the TCA cycle and is oxidized to generate ATP. Similarly, in an aerobic state, NADH enters the mitochondria where it plays a key role in the electron transport chain. In the absence of sufficient oxygen, NADH is utilized by lactate dehydrogenase in the reaction to reduce pyruvate to lactate. Lactate reduction or removal from the cytosol into circulation prevents product inhibition of the glycolytic pathway, thus allowing the progression of glycolysis. Fatty acids, from intramuscular stores or deriving from the circulation, are also oxidized in the mitochondria following acyl-CoA synthase breakdown to Fatty-acyl CoA and subsequent metabolism by beta-oxidation and the TCA cycle to generate ATP. Central in the ability of skeletal muscle to produce energy from either aforementioned system is the delivery of oxygen, glucose and fatty acids and the removal of metabolic products such as lactate. As such, the vascular perfusion of the tissue is essential in its ability to produce energy and meet energetic demand.

1.2 Mediation of local perfusion: Nitric Oxide

Local vasoregulation in skeletal muscle is highly complex and involves several vasoactive compounds which function synergistically on the smooth muscle cells underlying the vascular endothelium to regulate the local vascular tone. The local perfusion of myocytes is equally important for the delivery of nutrients required for normal cell function, as it is for the removal of unwanted and potentially toxic metabolic byproducts. During any given physiological state, the local vascular tone in skeletal muscle is determined by the balance between competing intrinsic vasoconstrictive and

vasodilatory factors. Nitric oxide (NO) is a potent gaseous vasodilatory molecule endogenously produced in skeletal muscle (Archer et al., 1994; Calabrese et al., 2007; Riddell & Owen, 1999). In the presence of L-arginine (Arg), NADPH and molecular oxygen, NO is enzymatically produced by three nitric oxide synthase isoforms named after the cells in which they were originally purified. Endothelial NOS (eNOS) and neuronal NOS (nNOS) are constitutive calcium and calmodulin-dependent isoforms, whereas the macrophage or calcium calmodulin-independent isoform NOS is otherwise known as inducible NOS (iNOS) (Forstermann & Sessa, 2012; Stamler & Meissner, 2001). The constitutive isoforms of NOS (eNOS, nNOS) are activated by the influx of calcium ions from subsarcolemmal storage sites as a result of mechanical forces such as sheer stress or by other stimulatory compounds via cell surface receptors (Clifford & Hellsten, 2004; Furchgott, 1999). The increase of intracellular calcium leads to the dissociation of the inhibitory calveolin-NOS complex by calcium-bound calmodulin, resulting in the activation of NOS (Balligand, Feron, & Dessy, 2009; Michel, Feron, Sacks, & Michel, 1997; Weissman, Jones, Liu, & Gross, 2002). Independent of calcium-calmodulin, activation of iNOS is stimulated by tumor necrosis factor (TNFα), interferon gamma (IFNγ) and interleukins, which regulate iNOS expression via Janus kinase and Signal Transducer and Activator of Transcription (JAK/STAT) and nuclear factor kappa-light-chain-enhancer of activated B cells (NF-κB) pathways (Z. Yu, Zhang, & Kone, 2002). Once in the vascular smooth muscle, NO activates soluble guanylate cyclase, which catalyzes the dephosphorylation of guanosine triphosphate (GTP) to cyclical guanosine monophosphate (cGMP) that inhibits calcium entry to the cell, activates K^+ channels and activates myosin light chain phosphatase via protein kinase G (PKG) to cause relaxation

of the smooth muscle and local vasodilation (Ahn, Foster, Cable, Pitts, & Sybertz, 1991; Ghofrani, Osterloh, & Grimminger, 2006). Irrespective of the activated NOS isoform, synthesized NO diffuses from the cell in which it was produced through the interstitial space, in order to promote vasodilation through its effects on vascular smooth muscle.

1.3 Skeletal Muscle Interstitial Space

In skeletal muscle, the interstitial space represents an important compartment located between the vasculature and the tissue. Water makes up 60% the total body mass of an adolescent male, where the intracellular compartment contains two thirds of the total body water and the remaining one third is held in the extracellular compartment. Interstitial fluid represents approximately 75% of the extracellular fluid volume. As such, a 70 kg adolescent male contains ~10.5 L of interstitial fluid. The interstitial fluid provides a medium for the diffusion of various metabolic substances and their byproducts between the capillary network and the cell. Additionally, the interstitial compartment has been shown to play a functional role in the integration and regulation of various metabolic and vasoactive substances (Leuenberger, Johnson, Loomis, Gray, & MacLean, 2008; MacLean, Bangsbo, & Saltin, 1999; MacLean, Sinoway, & Leuenberger, 1998; MacLean, Vickery, & Sinoway, 2001).

First described by Delgado et al., (Delgado, DeFeudis, Roth, Ryugo, & Mitruka, 1972) the microdialysis technique is a unique analytical procedure that allows for the direct *in vivo* investigation of metabolic compounds in the interstitial space. The microdialysis probe is composed of a tubular semipermeable dialysis membrane through which a solution

is perfused (termed perfusate) at a constant rate. Once inserted into the tissue, the dialysis membrane is integrated with the interstitial fluid. Substances that are of greater concentration in the interstitial fluid in comparison to the perfusate at the permeable surface of the membrane diffuse through the membrane and into the perfusate for collection. The flux of molecules into the perfusate is defined by the diffusional pathlength of molecules in the interstitial fluid, which is affected by intrinsic tortuosity and the volume of interstitial fluid as it relates to the tissue (MacLean et al., 1999; Nicholson & Phillips, 1981). This has been eloquently described by the modification of Fick's law of diffusion by MacLean *et al.* (MacLean et al., 1999)

$$\mathrm{J} = -D_p/\lambda^2 \cdot V_O/\mathrm{V} \cdot \nabla \mathrm{c}$$

where J is the microscopic flux, $-D_p/\lambda^2$ is the diffusion coefficient in perfusate where tortuosity is λ, V_O/V is the volume fraction and $\nabla \mathrm{c}$ is the concentration gradient. Once collected, various analytical techniques can be performed to quantify the molecules under investigation. Therefore, the microdialysis technique allows for the determination of vasoactive molecules responsible for the modulation of the local vascular tone as well as the transport kinetics of important metabolic substances, such as amino acids, between the vascular and intracellular compartments.

1.4 Amino Acid Metabolism in Skeletal Muscle

As the largest organ in the body, the maintenance of healthy skeletal muscle plays a critical role in whole body metabolic homeostasis (Clausen, 1986; Juel, 1996; Levy,

1999; Sinacore & Gulve, 1993). Conservation of skeletal muscle mass and integrity is dependent on the continuous and dynamic balance between protein synthesis and degradation, and central to this process is the availability of amino acids in the free amino acid pool (Rennie, Wackerhage, Spangenburg, & Booth, 2004). In humans, approximately 130 gms of free amino acids are present in the skeletal muscle intracellular space (Wagenmakers, 1998) and, in addition to its role in muscle protein turnover, it participates in numerous metabolic reactions that take place throughout the body (Felig, 1973; Wolfe, 2006). The branched-chain amino acids (BCAA) valine (Val), leucine (Leu) and isoleucine (Iso) are the dominant essential amino acids oxidized in skeletal muscle. The metabolic roles of BCAAs in energy production and protein synthesis regulation in skeletal muscle are well established (Brosnan & Brosnan, 2006; Cole, 2015; T.E. Graham, 1995; MacLean, Graham, & Saltin, 1994).

The catabolism of BCAA is a two step enzymatic process, first of which involves transamination of the amino acid and the second an oxidative decarboxylation of the deaminated product (Harper, Miller, & Block, 1984; Milan, 2011). The mitochondrial branched-chain amino acid aminotransferase (BCAAT) isoenzyme is primarily repsonbile for initiating BCAA catabolism (T. R. Hall, Wallin, Reinhart, & Hutson, 1993). The reversible activity of the BCAAT transfers an amino group from BCAA to 2-oxoglutarate to form branched-chain ketoacids (BCKA) α-ketoisocaporate (KIC), α-keto-β-methylvalerate (KMV) and α-ketoisovolerate (KIV) from Leu, Iso and Val, respectively. In the subsequent flux-generating step, the BCKA undergo irreversible oxidative decarboxilation by the enzymatic activity of branched-chain ketoacid dehydrogenase (BCKADH) complex to form isovaleryl-CoA, 3- methylbutyryl-CoA and isobutyryl-CoA

from KIC, KMV and KIV, respectively (Cole, 2015; Matthews et al., 1981). The resulting intermediates are further catabolized to produce acetoacetate, acetyl-CoA, proprionyl-CoA and succinyl-CoA end products, which enter the TCA cycle for ATP production.

The potent anabolic effect of BCAA in skeletal muscle has been well established (Armsey & Grime, 2002; Blomstrand, Eliasson, Karlsson, & Kohnke, 2006; Chromiak & Antonio, 2002; Koopman et al., 2006; Volpi, Kobayashi, Sheffield-Moore, Mittendorfer, & Wolfe, 2003). BCAA-induced stimulation of protein synthesis has been primarily attributed to the activation of the mamalian target of rapamycin (mTOR). A highly conserved serine threonine kinase, mTOR is comprised of two distinct mutiprotein complexes mTORC1 and mTORC2 (Catania, Binder, & Cota, 2011; M. N. Hall, 2008). The mTORC1 complex includes mTOR, Raptor, Deptor, PRAS40 and mLST8/GβL. Intramuscular amino acid availability increases levels of Ca^{2+} which activates mTORC1 signaling via Ca^{2+}/calmodulin-mediate activation of phosphoinositide 3-kinase (PI3K) (Gulati et al., 2008; Nobukuni et al., 2005). The potent BCAA-mediated stimulation of protein synthesis has been primarily attributed to the Leu regulated activation of mTORC1 by inducing the interaction of Ras-related GTP-binding protein (Rag) with ras-homolog enriched in the brain (Rheb) (Kimball & Jefferson, 2006; Norton & Layman, 2006). Perturbation of the dynamic balance between protein anabolism and catabolism, where net protein breakdown is greater than that of synthesis in skeletal muscle, can result in a cachectic, or muscle wasting condition.

1.5 Cancer Cachexia

Cachexia is a serious, life-threatening condition associated with several pathologies including cancer (Esper & Harb, 2005; K. C. Fearon, Glass, & Guttridge, 2012; Porporato, 2016). Recently, a consensus definition of cancer cachexia has been reached and it is stated as follows:

> "Cancer cachexia is defi ned as a multifactorial syndrome characterised by an ongoing loss of skeletal muscle mass (with or without loss of fat mass) that cannot be fully reversed by conventional nutritional support and leads to progressive functional impairment. The pathophysiology is characterised by a negative protein and energy balance driven by a variable combination of reduced food intake and abnormal metabolism (K. Fearon et al., 2011)."

Cancer cachexia affects 50-80% of cancer patients and accounts for approximately 20% of cancer-related deaths (Argiles, Busquets, Stemmler, & Lopez-Soriano, 2014; Tisdale, 2002). Cachectic patients with greater than 15% weight loss exhibit impaired physiological function and a drastic reduction in quality of life. Patient death normally occurs when weight loss exceeds 30% (Tisdale, 2002). Additionally, cachectic patients are less tolerant to chemotherapy, radiation therapy and the response to these therapeutic strategies are significantly reduced (K. C. Fearon & Baracos, 2010; Vaughan, Martin, & Lewandowski, 2013). Attempts at reversing cachexia through nutritional strategies have yielded little success indicating that, unlike anorexia, a decrease in caloric intake is not the primary cause of the condition (Evans et al., 2008). Despite being a systemic condition, skeletal muscle is the major target of wasting in cachectic patients. Several proinflammatory cytokines

have been associated with the pathogenesis of cachexia, primarily TNFα via the NF-κB pathway, IFNγ, interleukin-1 and -6 (IL-1, IL-6) (Acharyya et al., 2004; Baltgalvis et al., 2008; Han, Weinman, Boldogh, Walker, & Brasier, 1999; Uehara, Sekiya, Takasugi, Namiki, & Arimura, 1989). Within the tissue the lysosomal, calcium-dependent and ubiquitin-dependent pathways as well as the proteolysis inducing factor (PIF) have been identified as responsible for the intracellular breakdown of protein. While the lysosomal and calcium-dependent pathways contribute to approximately 20% of total protein breakdown and PIF is a key component of proteolysis, it is the activation of the ubiquitin proteasome pathway (UPP) that plays a major role in muscle wasting (Biolo et al., 2000; Lorite, Thompson, Drake, Carling, & Tisdale, 1998; Mitch & Goldberg, 1996; Temparis et al., 1994; Williams, Sun, Fischer, & Hasselgren, 1999). Significant research has been performed to elucidate the role of endogenously produced host and tumor-derived factors responsible for the progression of cancer related muscle wasting. However, Wang *et al.* (H. Wang et al., 2015) demonstrated that muscle in tumor bearing mice treated with docetaxel (a chemotherapy agent) underwent atrophy more severely (1.5 fold) than those treated with tumor cells alone. This indicates that chemotherapy significantly contributes to the onset of cachexia. Very little research has focused on delineating host-derived and chemotherapy-derived factors, or the possible synergy between the two, in the onset and progression of the cachectic condition in cancer patients. Further research into these mechanisms would greatly improve our understanding of the pathophysiology and would also provide important insights into possible targets for strategies directed at minimizing muscle wasting.

1.6 Doxorubicin Chemotherapy

Since its discovery in 1969 (Arcamone et al., 1969), Doxorubicin (DOX) remains one of the most widely used chemotherapeutic agents for the treatment of solid tumors and hematological malignancies (Weiss, 1992). Doxorubicin is an anthracycline antibiotic with antineoplastic properties first isolated from cultures of *Streptomyces peucetius* var. *caesius*. The highly lipophilic nature of DOX is due to a naphthacenequinone nucleus which is linked to a hydrophilic amino sugar, daunosamine, through a glycosidic bond at ring atom 7. Additionally, DOX contains acidic and basic functions in the ring phenolic groups and in the sugar group, respectively, and is therefore both an amphoteric and amphiphilic molecule thus allowing it to bind to cell membranes and proteins. Protonation of the amino group of the sugar, forming DOX hydrochloride, increases the aqueous solubility of the molecule for administration (Mohan & Rapoport, 2010).

Doxorubicin induced cytotoxicity has been attributed to DNA intercalation, topoisomerase II (TOPII) inhibition and formation of radical oxygen species (ROS). As a planar molecule, DOX preferentially intercalates between neighboring DNA base pairs forming a covalent bond between DOX and guanine on one strand of DNA and a hydrogen bond between DOX and guanine on the opposing strand, significantly effecting DNA replication (Chaires, Fox, Herrera, Britt, & Waring, 1987; Chen, Gresh, & Pullman, 1986; Coldwell, Cutts, Ognibene, Henderson, & Phillips, 2008; Minotti, Menna, Salvatorelli, Cairo, & Gianni, 2004; Momparler, Karon, Siegel, & Avila, 1976; Yang, Teves, Kemp, & Henikoff, 2014). Topoisomerase II is a highly conserved enzyme that regulates DNA topology by releasing torsional stress formed during DNA transcription and is the key component in the decatenation of replicated DNA during mitosis (Carpenter & Porter,

2004; Pommier, Leo, Zhang, & Marchand, 2010). Inhibition of TOPII constrains DNA and increases torsional stress resulting in double-strand DNA breakages and subsequent cell death (Gewirtz, 1999). The presence of a quinone ring in the chemical structure of DOX allows for the one-electron reduction of the drug mediated by oxoreductive enzymes xanthine oxidase, NADH dehydrogenase and cytochrome P450 reductase. This reduction converts the quinone to a semiquinone free radical which, in the presence of oxygen, undergoes redox cycling to form hydroxyl radicals, superoxides and peroxides causing lipid peroxidation, DNA damage and cell death (Doroshow, 1983; Gewirtz, 1999; M. A. Graham, Newell, Butler, Hoey, & Patterson, 1987; Singal, Li, Kumar, Danelisen, & Iliskovic, 2000). Taken together, the formation of DOX-DNA adducts, TOPII inhibition and ROS formation have been identified as the significant mechanisms responsible for DOX-related cellular toxicity.

Despite its potent toxicity, the clinical use of DOX as a cancer chemotherapeutic is limited by a well described dose-dependent and cumulative cardiotoxic side effect leading to the development of congestive heart failure (Lefrak, Pitha, Rosenheim, & Gottlieb, 1973; Singal & Iliskovic, 1998). Doxorubicin-related cardiotoxicity has been shown to be mediated by its primary circulating alcohol metabolite, Doxorubicinol (DOXol), catalyzed by the enzymatic activity of carbonyl reductase-1 (CBR1) carbonyl reduction of DOX (Kassner et al., 2008). Potent DOXol-dependent inhibition of the sarcoplasmic reticulum calcium pump, the sarcolemmal Na^+/K^+ pump and mitochondrial F_0F_1 proton pump in cardiomyocytes effectively compromises systolic and diastolic cardiac function (Boucek et al., 1987; Minotti et al., 1998; Olson et al., 1988).

The impetus to identify and elucidate the underlying mechanisms leading to cardiotoxicity has focused DOX-related research to cardiomyocytes. However, off-target cytotoxicity is not limited to cardiomyocytes and recent studies have described the effect of DOX on skeletal muscle. Hayward *et al.* have reported that the exposure of skeletal muscle to DOX resulted in a significant and progressive decline in muscular function (Hayward et al., 2013). Additionally, a decline in maximal twitch force and rate of force generation as well as an increase in muscular fatigue have also been shown following the administration of DOX (Gilliam & St Clair, 2011; van Norren et al., 2009). Furthermore, in clinical practice, it has been shown that chemotherapy can alter insulin sensitivity (Chala et al., 2006; Feng et al., 2013). Insulin is considered to be the main anabolic hormone in the body and plays a particularly important role in skeletal muscle where it promotes the synthesis and inhibits the degradation of protein and glycogen in the tissue. De Lima Junior *et al.* (de Lima Junior et al., 2016) have reported that treatment with DOX caused hyperglycaemia and insulin resistance mimicking conditions that are similar to cachexia. It is important to acknowledge that skeletal muscle health, maintenance and function have an influence on a cancer patient's prognosis and quality of life. Therefore, further investigations into the underlying mechanisms which leads to skeletal muscle dysfunction is undeniably warranted.

2. Thesis Purpose

The importance of skeletal muscle health and function in the quality of life and positive prognosis of cancer patients is well established. However, little is known regarding the effect of chemotherapeutic treatment on essential metabolic mechanisms responsible for the maintenance of skeletal muscle. In this thesis, the concurrent determination of DOX in the plasma, the intramuscular and interstitial space will provide novel insights into the accumulation of the drug in these tissues as well as its effect on the systemic availability of the drug. In addition, the concurrent measurement of NO concentrations in these compartments will allow be us to determine if the perfusion of the tissue plays a role in the uptake and/or retention of the drug in the muscle. Lastly, the study of the free amino acid pool in the muscle following Dox administration will permit us to assess the possible contribution this drug has to non-host induced muscle wasting. Ultimately, the aims of this thesis are designed to elucidate the effects that Doxorubicin has on skeletal muscle following its administration.

2.1 Objectives

I. Quantify the accumulation of Doxorubicin and its metabolite Doxorubicinol in the plasma, interstitial space, and within skeletal muscle of the rats. This will determine to what extent skeletal muscle may act as a reservoir or sink for the accumulation of the drug following administration.

II. Examine the effect of Doxorubicin administration on nitric oxide concentrations in skeletal muscle. As a local mediator of vascular tone, the

assessment of changes in nitric oxide concentration may suggest that tissue perfusion is disrupted by chemotherapy drugs, which could in turn affect the updake and/or retention.

III. Investigate the amino acid response in skeletal muscle following the administration of Doxorubicin. This will help us determine whether Doxorubicin affects amino acid pools in muscle that may contribute to non-host induced cachexia.

CHAPTER II

(Study 1)

Skeletal Muscle an Active Compartment in the Sequestering and Metabolism of Doxorubicin Chemotherapy.

3. Study 1 Objective: Describe and quantify the accumulation of Doxorubicin and its metabolite, Doxorubicinol, in rat skeletal muscle.

4. Overview of Study 1

To study the effect of DOX chemotherapy on skeletal muscle, the first objective was to determine the uptake and retention of the drug in the tissue. As an amphiphilic molecule, administered DOX effectively diffuses from the vasculature into the interstitial space where cellular uptake occurs. The chemical nature of DOX allows for the passive diffusion of DOX through the cytoplasmic membrane and into the intracellular space. This study investigates the accumulation of DOX and its major metabolite, DOXol, in skeletal muscle following its administration in the rat. Additionally, the relationship between the muscular, interstitial and vascular compartments as it relates to the diffusional pathway and systemic availability of DOX and DOXol is examined. This study represents the first time that the accumulation of DOX and DOXol have been quantified in skeletal muscle up to 8 days following the administration of the drug. In addition, it is also the first time that the

relationship between the muscular, interstitial and vascular compartments have been examined concurrently following DOX administration.

5. Skeletal Muscle an Active Compartment in the Sequestering and Metabolism of Doxorubicin Chemotherapy.

(Original Research)

Sergio Fabris, David A. MacLean

[Published in *PLoS ONE*]

Fabris, S., & MacLean, D. A. (2015). Skeletal Muscle an Active Compartment in the Sequestering and Metabolism of Doxorubicin Chemotherapy. *PLoS One*, 10(9), e0139070. doi: 10.1371/journal.pone.0139070

Contributions: Experiments where conceived, designed and conducted by Sergio Fabris. Sergio Fabris performed the analysis of the data and wrote the manuscript.

5.1 Abstract

Doxorubicin remains one of the most widely used chemotherapeutic agents however its effect on healthy tissue, such as skeletal muscle, remains poorly understood. The purpose of the current study was to examine the accumulation of doxorubicin (DOX) and its metabolite doxorubicinol (DOXol) in skeletal muscle of the rat up to 8 days after the administration of a 1.5 or 4.5 mg kg-1 i.p. dose. Subsequent to either dose, DOX and DOXol were observed in skeletal muscle throughout the length of the experiment. Interestingly an efflux of DOX was examined after 96 hours, followed by an apparent re-uptake of the drug which coincided with a spike and rapid decrease of plasma DOX concentrations. The interstitial space within the muscle did not appear to play a significant rate limiting compartment for the uptake or release of DOX or DOXol from the tissue to the circulation. Furthermore, there was no evidence that DOX preferentially accumulated in a specific muscle group with either dose. It appears that the sequestering of drug in skeletal muscle plays an acute and important role in the systemic availability and metabolism of DOX which may have a greater impact on the clinical outcome than previously considered.

5.2 Introduction

Doxorubicin (DOX) is one of the most widely used chemotherapeutic agents for the treatment of solid tumors and hematological malignancies. DOX induced cytotoxicity has been attributed to the inhibition of DNA replication and RNA transcription via DNA intercalation, inhibition of topoisomerase II (TOP2A) resulting in TOP2-mediated DNA damage, the formation of reactive oxygen species and hydrogen peroxide (Minotti et al., 2004; Momparler et al., 1976; S. Wang et al., 2004). Although effective, DOX is strongly limited by a dose-dependent and cumulative cardiotoxic side effect which has been primarily attributed to its metabolite Doxorubicinol (DOXol) (Minotti et al., 1998; Olson et al., 1988). DOXol is ten times more cytotoxic than DOX and highly cardiotoxic as a result of its potent inhibition of the sarcoplasmic reticulum calcium pump, the sarcolemmal Na^+/K^+ pump and the mitochondrial F_0F_1 proton pump (Boucek et al., 1987; Olson et al., 1988)

To date, much of the research remains focused on reducing the cardiotoxic effect related to the use of DOX. However, recent studies have reported that the exposure of skeletal muscle to DOX causes significant physiological effects including a progressive decline in muscular function (Hayward et al., 2013), a decline in maximal twitch force and rate of force generation (Gilliam & St Clair, 2011) as well as increased muscular fatigue (van Norren et al., 2009). Cellular dysfunction has been shown to be related to a significant increase in mitochondrial reactive oxygen species (Smuder, Kavazis, Min, & Powers, 2011b). In addition, upregulated autophagy and apoptotic pathways are believed to be primarily responsible for the DOX-induced decrease in muscle mass (Gilliam & St Clair, 2011; Smuder, Kavazis, Min, & Powers, 2011a; A. P. Yu et al., 2014). Despite the growing

evidence suggesting a DOX related myotoxicity, the effect of DOX on skeletal muscle metabolism and function has received little attention.

In skeletal muscle, the interstitial space represents an important compartment located between the vasculature and the tissue. It has been shown to play a functional role in the regulation and integration of various metabolic substances (Leuenberger et al., 2008; MacLean et al., 1999; MacLean, Sinoway, et al., 1998). Microdialysis is used to directly measure these substances in the interstitial space *in vivo*. The microdialysis technique, first described by Delgado *et al.* (Delgado et al., 1972), is based on the principle of simple diffusion through a semipermeable membrane which allows for the direct measurement of compounds, including DOX and DOXol, located within the interstitial space directly at the tissue level. To date, not only has DOX and DOXol not been thoroughly examined in the vascular, interstitial and muscular compartments, but the relationship between these compartments has never been investigated. Therefore, the purpose of the current study was to investigate the accumulation of DOX and DOXol in skeletal muscle and examine the relationship between the muscular, interstitial and vascular compartments following administration of DOX in the rat. Overall, our results clearly indicate that DOX and DOXol is sequestered in the skeletal muscle and that there were no differences in the sequestering of the drug or its metabolite in muscle groups containing predominantly fast or slow muscle fibers. Therefore, it appears that skeletal muscle plays an acute and important role in the systemic availability and metabolism of DOX.

5.3 Results

Plasma DOX. The administration of 1.5 mg kg-1 DOX elevated ($P<0.05$) arterial concentrations of DOX throughout the experiment, with the highest concentration observed after 96 (41.4±17.9 nM) and 192 hours (20.3±7.5 nM) post injection as compared to baseline. Similarly, circulating concentrations were elevated ($P<0.05$) throughout the experiment following the administration of 4.5 mg kg-1 DOX. When compared to the 1.5 mg kg-1 dose, the concentration of DOX was greater ($P<0.05$) following the 4.5 mg kg-1 dose after 24 (300±77 %), 72 (609±119 %), 120 (288±0 %) and 144 (845±147 %) hours (Fig 1A)

Plasma DOXol. Following the administration of 1.5 mg/kg, DOXol was measurable ($P<0.05$) after 24 hours (1.24±0.25 nM) and remained measurable throughout the experiment. In comparison to the initial concentration observed after 24 hours, the levels were decreased ($P<0.05$) by 51±10 %, 49±11 % and 48±12 % after 72, 120 and 144 hours respectively. The 4.5 mg kg-1 dose resulted in an initial DOXol increase ($P<0.05$) after 24 hours (1.26±0.17 nM) which remained stable for the remainder of the experiment. Despite the fluctuation difference of DOXol in both doses, the 4.5 mg kg-1 dose was observed to be elevated ($P<0.05$) after 48 (213±7 %) and 72 (157±6 %) hours as compared to the 1.5 mg kg-1 dose (Fig 1B).

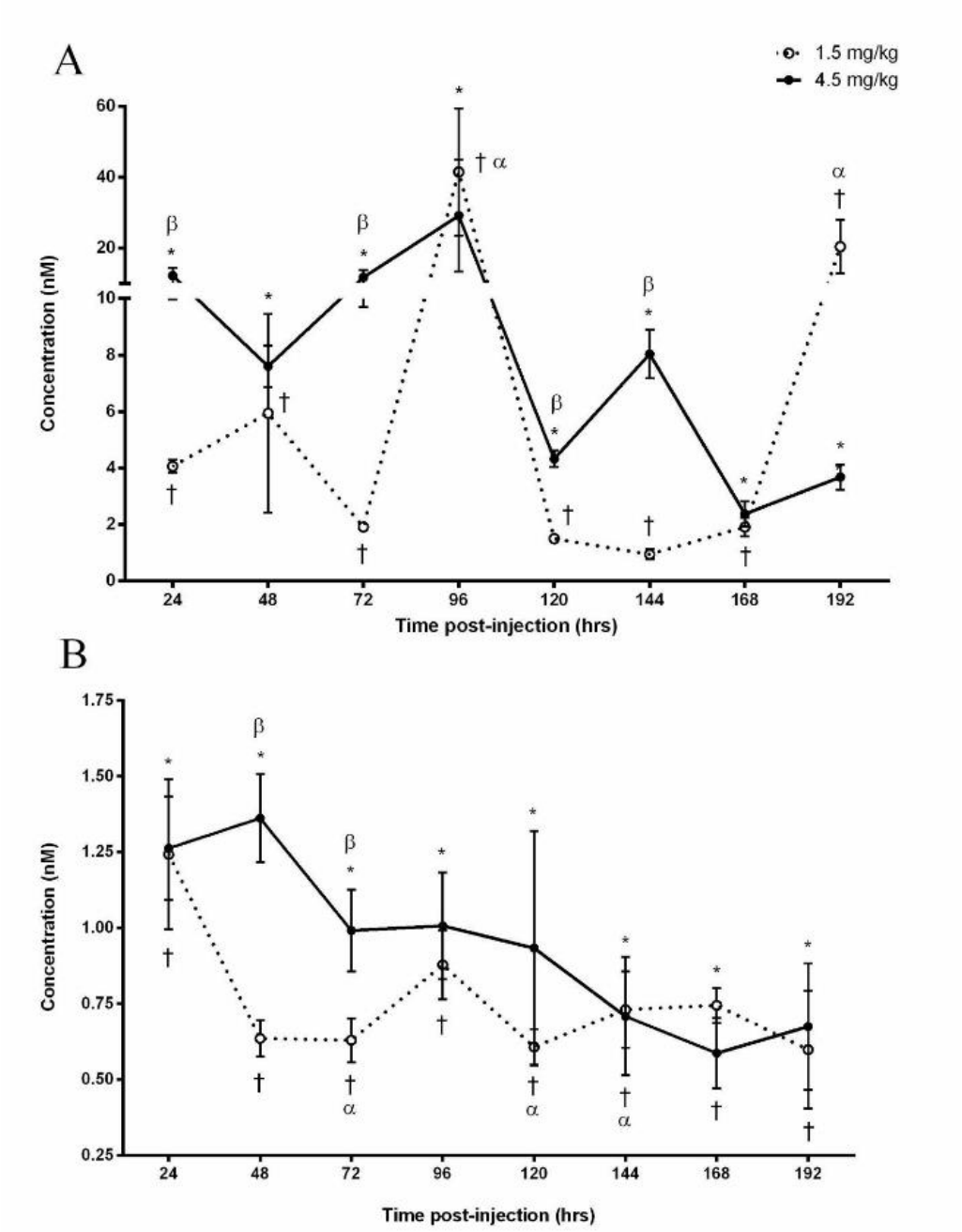

Fig 1. Doxorubicin (A) and Doxorubicinol (B) concentrations in the arterial plasma following the IP administration of 1.5 or 4.5 mg kg-1 Doxorubicin. (A) Significance compared to baseline for the 1.5 mg kg-1 dose is denoted by † and 4.5 mg kg-1 by *. α Denotes an increase ($P<0.05$) compared to 24, 48, 72, 120, 144 and 168 hours as a result of the 1.5 mg kg-1 dose. β Denotes difference ($P<0.05$) between administered doses. (B) Significance compared to baseline for the 1.5 mg kg-1 dose is denoted by † and 4.5 mg kg-1 by *. α Denotes a decrease ($P<0.05$) compared to 24 hours. β Denotes difference ($P<0.05$) between administered doses.

Skeletal Muscle DOX. Following the 1.5 mg kg-1 dose, DOX was detectable in the WG at each time point ($P<0.05$) with the exception of 96 and 168 hours. Additionally, these concentrations were elevated ($P<0.05$) after 48 (0.78±0.24 μmol/kg), 72 (0.32±0.1 μmol/kg) and 120 (1.23±0.56 μmol/kg) hours post-injection (Fig 2A). The administration of 4.5 mg kg-1 dose resulted in measurable ($P<0.05$) DOX concentrations at each time point. When compared to 48 hours (1.62±0.61 μmol/kg), 10 and 20-fold decreases ($P<0.05$) were observed after 24 and 96 hours, respectively (Fig 2B).

With the exception of the 96 hour time point, the concentration of DOX was measurable ($P<0.05$) RG at each time point of the experiment following the administration of 1.5 mg kg-1 dose with an initial tissue concentration of 0.90±0.43 μmol/kg after 24 hours (Fig 2A). DOX was measurable ($P<0.05$) at the 48, 72, 120, 144, 168 and 192 hour time points following the administration of the 4.5 mg kg-1 dose. The concentration of DOX significantly decreased 200-fold after 168 hours and 26-fold after 192 hours when compared to the 72 hour (4.13±2.16 μmol/kg) time point (Fig 2B).

Subsequent to the 1.5 mg kg-1 dose, DOX concentrations in the PL were measurable at each time point and were elevated ($P<0.05$) to 1.38±0.44 μmol/kg after 48 hours. Concentrations subsequently decreased ($P<0.05$) after 120 (726±0 %), 144 (690±6 %), 168 (575±0.2 %) and 192 hour (675±1 %) in comparison to the 48 hour time-point (Fig 2A). The administration of 4.5 mg kg-1 resulted in measurable concentrations of DOX after 72 hours (0.14±0.06 μmol/kg, $P<0.05$) which remained consistent for the remainder of the experiment (Fig 2B).

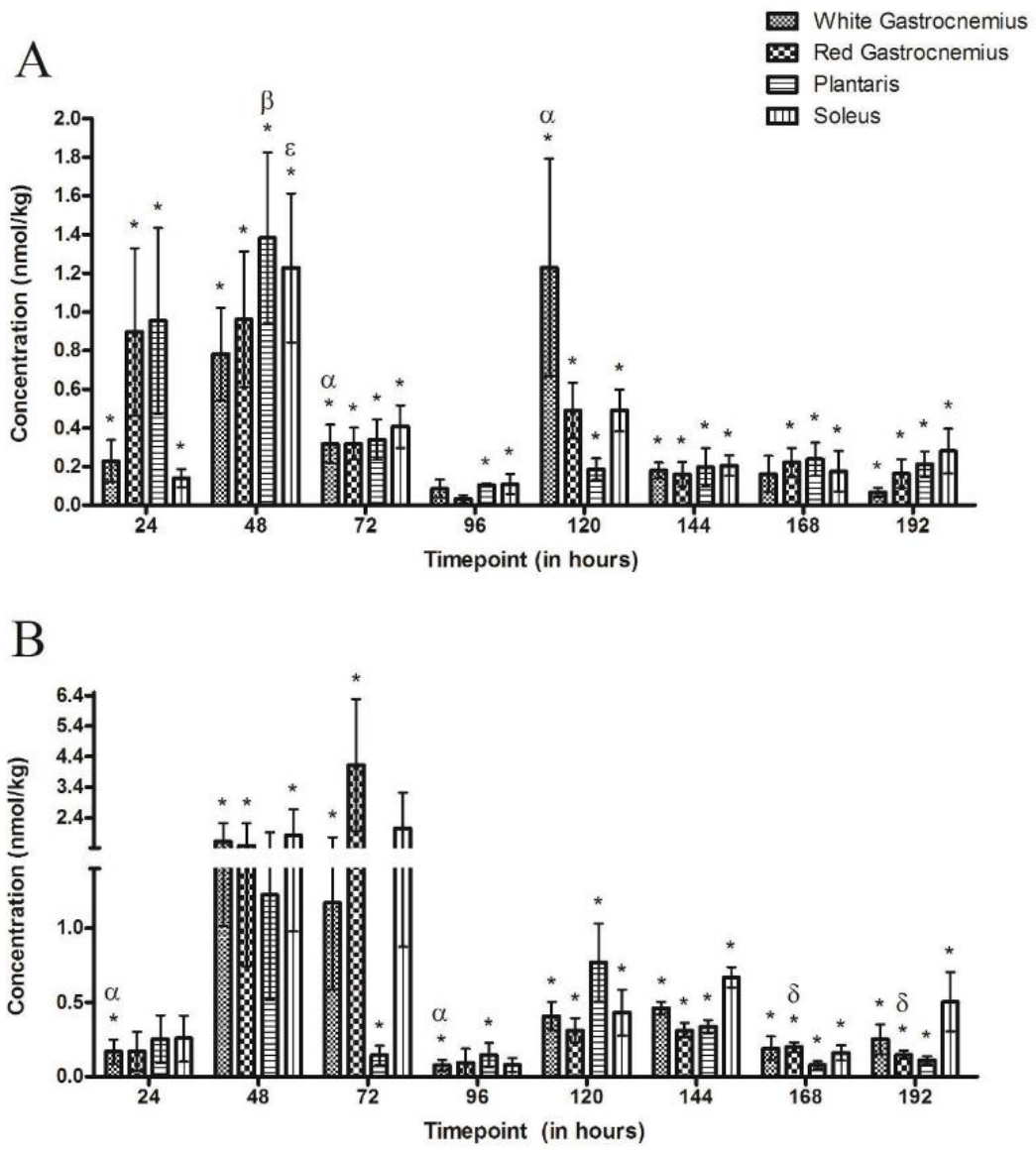

Fig 2. Doxorubicin concentrations in skeletal muscle groups following the IP administration of (A) 1.5 mg kg-1 or (B) 4.5 mg kg-1 of Doxorubicin. (A) * Denotes significance when compared to baseline for all muscle groups. α Indicates the highest points of accumulation of DOX ($P<0.05$) in the white gastrocnemius, β Indicates the highest point of accumulation ($P<0.05$) in the plantaris and ε Indicates the point of greatest accumulation of DOX ($P<0.05$) in the soleus. (B) * Denotes significance when compared to baseline for all muscle groups. α Denotes a decrease ($P<0.05$) compared to 48 hours in the white gastrocnemius and δ denotes a significant decrease compared to 72 hours in the red gastrocnemius. There are no significant differences between muscle types at any time point in either administered doses.

The administration of 1.5 mg kg-1 DOX resulted in measurable concentrations of DOX within the SOL at each time point with the highest ($P<0.05$) concentration (1.23±0.39 μmol/kg) occurring after 48 hours (Fig 2A). DOX was measurable ($P<0.05$) in the SOL at each time point with the exception of the 24, 72 and 96 hour time points following the 4.5 mg kg-1 dose (Fig 2B).

Interestingly, no consistent differences between intracellular DOX concentrations were observed throughout the course of the experiment when comparing muscle groups at either the administration of 1.5 or 4.5 mg kg-1 dose. Furthermore, there were no significant dose-dependent differences in DOX concentrations at any time point when comparing administered doses.

Skeletal Muscle DOXol. DOXol was measurable ($P<0.05$) in the WG after 72, 144 and 192 hours as a result of the administered 1.5 mg kg-1 dose (Fig 3A). The administration of 4.5 mg kg-1 dose resulted in measureable ($P<0.05$) DOXol concentrations after 48, 72, 120, 144 and 192 hours (Fig 3B).

The administration of 1.5 mg kg-1 dose resulted in measurable DOXol concentrations ($P<0.05$) in the RG after 48, 72, 120, 144 and 192 hours (Fig 3A). The 4.5 mg kg-1 dose resulted in measurable ($P<0.05$) tissue concentrations of DOXol at 48, 72, 144, 168 and 192 hours (Fig 3B).

The 1.5 mg kg-1 dose resulted in measurable ($P<0.05$) concentrations of DOXol in the PL after 24, 48, 72, 120 and 192 hours (Fig 3A), whereas the 4.5 mg kg-1 dose resulted in measurable ($P<0.05$) levels of DOXol after 24, 120, 144, 168 and 192 hour (Fig 3B).

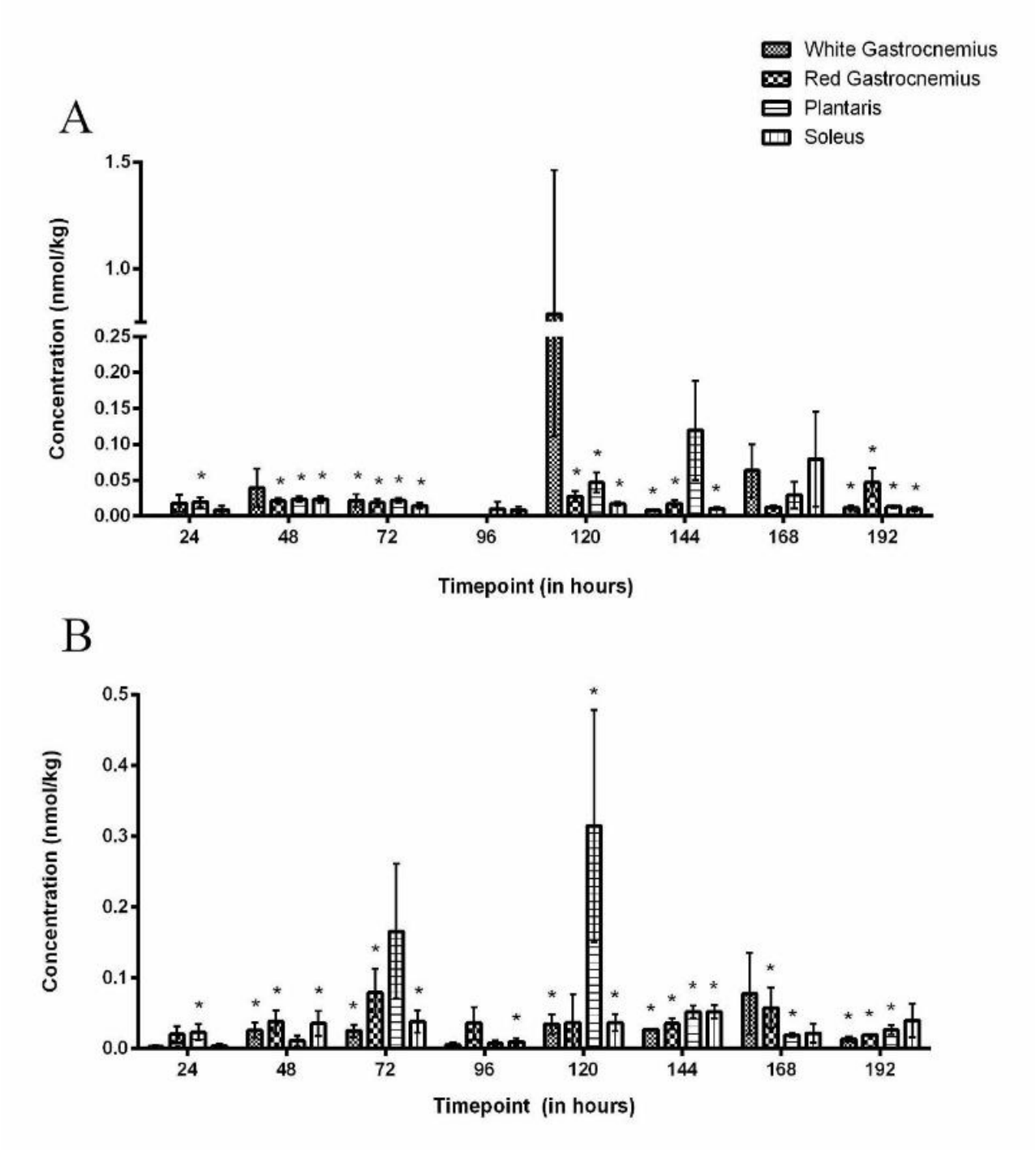

Fig 3. Doxorubicinol concentrations in skeletal muscle groups following the IP administration of (A) 1.5 mg kg-1 or (B) 4.5 mg kg-1 of Doxorubicin. * Denotes significance when compared to baseline for all muscle groups. There are no significant differences between muscle types at any time point in either administered doses.

DOXol was measurable ($P<0.05$) in the SOL after 48, 72, 120, 144 and 192 hours following the 1.5 mg kg-1 dose (Fig 3A). Similarly, DOXol was measurable ($P<0.05$) after 48, 72, 96, 120 and 144 hours post-injection of the 4.5 mg kg-1 dose (Fig 3B).

Interestingly, there were no consistent differences between DOXol concentrations when comparing muscle groups following the 1.5 mg kg-1 or 4.5 mg kg-1 dose. Additionally, there were no significant dose-dependent differences in DOXol concentrations at any time point when comparing administered doses.

Interstitial DOX. Following the 1.5 mg kg-1 dose, interstitial DOX concentrations were measurable ($P<0.05$) after 48 hours (0.58±0.28 nM) then decreased until 120 hours (0.24±0.1 nM; $P<0.05$) where levels remained stable for the remainder of the experiment. Similarly, as a result of the 4.5 mg/kg, DOX was measurable ($P<0.05$) after 48 hours (0.4±0.18 nM) and decreased until 96 hours (0.44±0.18 nM; $P<0.05$) where concentrations remained stable for the remainder of the experiment. There were no significant differences in interstitial DOX concentrations at any time point when comparing between administered doses (Fig 4A).

Interstitial DOXol. Interstitial DOXol concentrations were measurable ($P<0.05$) after 48, 144 and 192 hours post-administration of the 1.5mg kg-1 dose. Subsequent to the 4.5 mg kg-1 dose, DOXol was measurable after 48 hours (0.16±0.07 nM) and remained stable for the remainder of the experiment. There were no significant differences between interstitial DOXol concentrations between doses (Fig 4B).

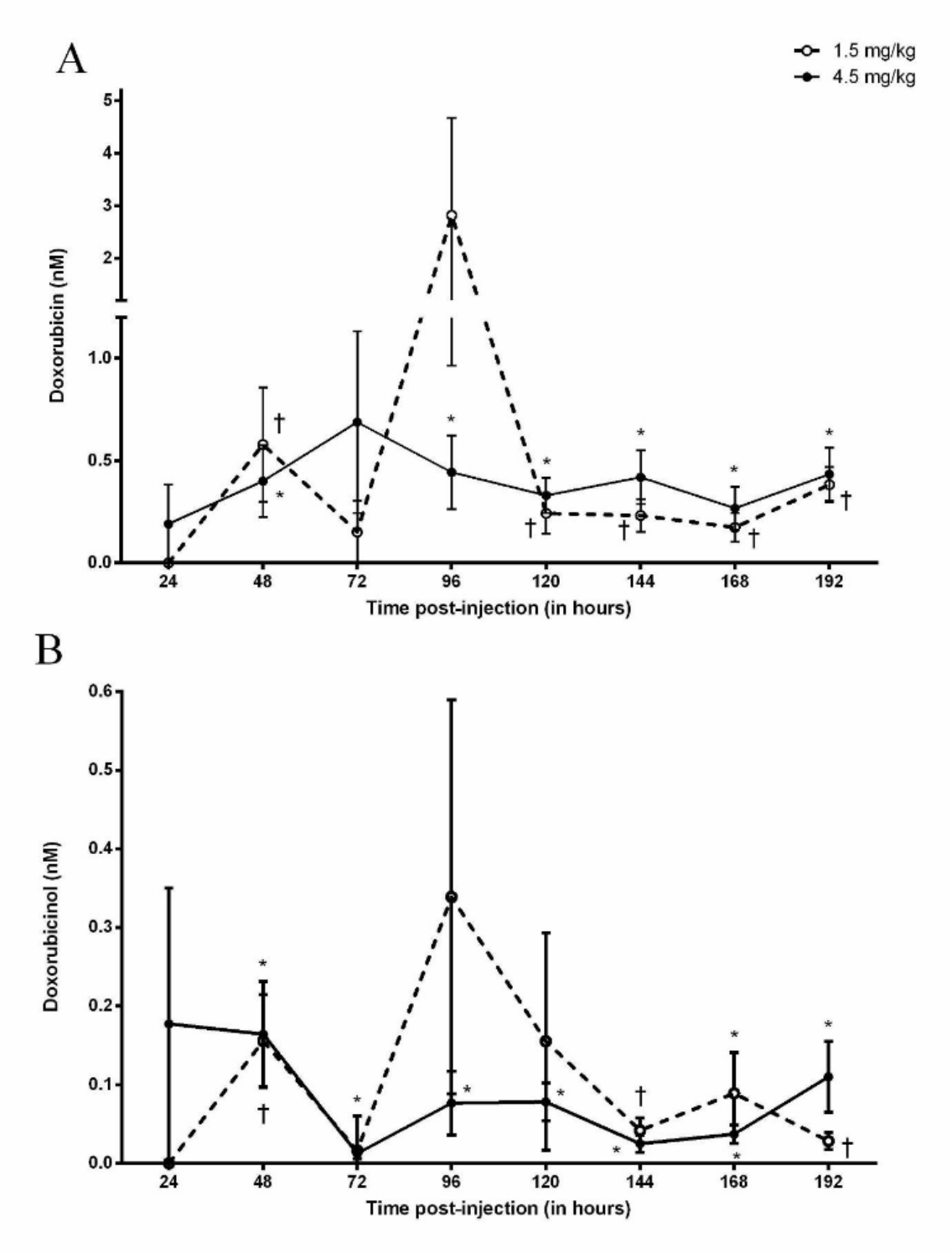

Fig 4. Doxorubicin (A) and Doxorubicinol (B) concentrations in the interstitial space of skeletal muscle following the IP administration of 1.5 or 4.5 mg kg-1 Doxorubicin. † Designates significance compared to baseline for the 1.5 mg kg-1 dose. * Designates significance compared to baseline for the 4.5 mg kg-1 dose.

5.4 Discussion

The focus of the current study was to investigate the accumulation of DOX and DOXol in skeletal muscle and examine the relationship between the muscular, interstitial and vascular compartments following the administration of DOX in the rat. A major finding in this study was the apparent role that skeletal muscle plays in the sequestering of DOX following its administration. This was made evident as plasma DOX levels were inversely proportional to skeletal muscle concentrations (data presented Figs 1 and 2). A static pool of DOX was established in the interstitial space which maintained in dynamic equilibrium between the vasculature and skeletal muscle which did not change over time or with an increase in dose. As such, the interstitial space does not appear to represent a rate limiting factor in the diffusion kinetics of the drug. Furthermore, the relationship between the three compartments was impartial to muscle groups predominantly composed of different fiber types. Hence, it appears that skeletal muscle plays an acute and important role in the systemic distribution of DOX and may have a greater impact on drug availability than previously considered.

DOX was administered IP in order to simulate previous studies that have examined the cardiotoxic effects of DOX in the rat (Guerra et al., 2005; Jensen, Acton, & Peters, 1984; Teraoka, Hirano, Yamaguchi, & Yamashina, 2000; Yen, Oberley, Vichitbandha, Ho, & St Clair, 1996). A single low dose of DOX was used in order to minimize the drug-induced risk of cardiotoxicity. For example, previous studies have utilized a variety of concentrations and treatment regimens documenting significant cardiomyocyte damage. Iqbal et al. (Iqbal, Dubey, Anwer, Ashish, & Pillai, 2008) administered a single 20 mg kg-1 dose IP and observed the induction of acute cardiotoxicity after 48 hours and up to 7 days

post administration. A study by Nagi et al. (Nagi & Mansour, 2000) reported that a single dose of 15 mg kg-1 IP induced cardiotoxicity after 24 and 48 hours and Jensen et al. (Jensen et al., 1984) noted that a 10 mg kg-1 or less total dosage did not cause cardiac failure. Although Arola et al. (Arola et al., 2000) reported minor cardiomyocyte apoptosis after 3 days following the injection of 1.5 mg kg-1 and 5 mg/kg, it remains unclear whether this significantly altered cardiac performance. Cumulative doses have been studied where 1 mg kg-1 (IP) was administered 15 times over 3 weeks resulted in cardiac dysfunction (Teraoka et al., 2000) and 1.5 mg kg-1 weekly for 9 weeks resulted in severe cardiomyopathy (Guerra et al., 2005). What these studies have in common is the focus on the long term effects of DOX where, to our knowledge, little or no attention has been given to the early stages of DOX accumulation in skeletal muscle. As such the current study investigated DOX concentrations 24 hours sequentially up to 192 hours. With the aforementioned factors taken into consideration, the concentrations used in this study provided a dose-related experimental contrast while minimizing the drug-induced risk of cardiac dysfunction associated with the higher doses. Additionally, the time frame allows for the examination of acute DOX accumulation in skeletal muscle as well as the dynamic between the circulation and the interstitial space within the skeletal muscle.

This study represents the first time that sequential measurements of plasma DOX concentrations have been made for 8 days (192 hours) after IP administration. Despite the threefold increase in administered dose from 1.5 mg kg-1 to 4.5 mg/kg, a stable circulating concentration of DOX was maintained throughout the 8 days with the exception of a spike in concentration after 4 days (96 hours). This stable concentration may be attributed to the enzymatic breakdown of DOX once in the circulation. It is well known that DOX is

enzymatically reduced to a number of metabolites (Thorn et al., 2011). The reduction of DOX to its major metabolite, DOXol (Mordente, Meucci, Silvestrini, Martorana, & Giardina, 2009) by way of carbonyl reductase-1 (Kassner et al., 2008), carbonyl reductase-3 (Bains et al., 2010) or aldo-keto reductases (Heibein, Guo, Sprowl, Maclean, & Parissenti, 2012) is of particular clinical importance as it is 10 times more cytotoxic than DOX (Mahnik, Rizovski, Fuerhacker, & Mader, 2006) and has been identified to be responsible for the cardiotoxic effect related to DOX therapy (Olson et al., 1988). DOXol concentrations in the plasma did not have the same degree of variability within the dose groups or degree of dose response as that observed in the DOX concentrations. What is interesting, however, is that despite the increase in DOXol concentrations between doses after 48 and 72 hours, concentrations remained constant for the remainder of the experiment indicating that the breakdown of DOX to DOXol does not complement the increase in administered dose. This would indicate that a threshold in the enzymatic breakdown of DOX to DOXol may exist and a maximal rate was achieved 24 hours after drug administration which resulted in a constant circulating concentration of the cytotoxic metabolite. The persistent circulation of DOX represents a significant clinical importance as the repeated administration of DOX may further increase circulating concentrations of the drug and its toxic metabolite above that established by the initial dose. While this may be beneficial in assuring the delivery to the tumor, increasing the drug and, as a result, its toxic metabolite may have a greater impact on healthy tissue.

The current study proposes that the persistent circulating concentration of DOX is attributed to the acute sequestering of the drug in the skeletal muscle which is primarily responsible for the timely release of the drug back into the circulation. Previous studies

have focused on the accumulation of DOX in the heart, liver, spleen, lung, brain and kidney (Arnold, Slack, & Straubinger, 2004; Ciaccio et al., 1993; Sacco et al., 2003; Shin, Matsunaga, & Fujiwara, 2010; van Asperen, van Tellingen, Tijssen, Schinkel, & Beijnen, 1999). However very few have investigated the accumulation in skeletal muscle (Doroshow, Tallent, & Schechter, 1985; Gibson, Quinn, Pfannenstiel, Hydock, & Hayward, 2013; Hayward et al., 2013). The accumulation of DOX was observed in the muscle at each time point regardless of the administered dose. What was most surprising was the consistent efflux of DOX at 96 hours which was quickly followed by a re-accumulation after 120 hours with both doses. The rapid elimination of DOX from the skeletal muscle coincides with the notable increases seen in plasma as previously discussed. To our knowledge no mechanisms to date have been identified that may explain these results, although these data may indicate an active survival mechanism by the skeletal muscle in order to export DOX from the cytosol once a toxic concentration has been attained. As previously mentioned, a constant rate of DOX breakdown from the circulation may have been established after 24 hours of drug administration. As such, the sequestering of DOX in skeletal muscle may occur to assist in minimizing the toxic circulating concentrations while being subjected to the rate limiting enzymatic breakdown by the liver. It is also possible that after approximately 72 hours the sequestration of DOX into the skeletal muscle by way of passive diffusion (Skovsgaard & Nissen, 1982), a threshold limit may have been achieved. The subsequent transcription of transport proteins such as RALBP1 (Awasthi et al., 2008) and/or P-glycoprotein (Georges, Bradley, Gariepy, & Ling, 1990) required for the active export of DOX may be initiated resulting in the efflux of DOX back into the circulation. The opportunistic release of drug back into the circulation and

subsequent breakdown reduces toxicity both at tissue and systemic level. The apparent re-uptake of DOX into the skeletal muscle tissue may be a function of the rapid reintroduction of DOX into the circulation and resulting diffusion back into the tissue. DOXol was measurable in skeletal muscle up to 8 days, regardless of the administered dose. Although quantifiable, the accumulation of DOXol was minimal up to 96 hours which corresponds to the aforementioned metabolic breakdown of DOX. To our knowledge, data regarding the accumulation of DOXol in skeletal muscle remains limited (B. J. Cusack, Young, Driskell, & Olson, 1993; Mushlin et al., 1993; Peters, Gordon, Kashiwase, & Acton, 1981) and the mechanisms involved in the apparent accumulation of DOXol in the skeletal muscle remains poorly understood. It may be possible that DOXol enters the cell by passive diffusion, in a similar process as that of DOX. In support of this notion, the constant circulating concentration of DOXol that was established after 96 hours would explain the increased accumulation in skeletal muscle. It is also possible that the accumulated concentration of DOX in skeletal muscle is broken down to DOXol at a steady rate by the presence of carbonyl reductase-1 resulting in a constant rate within the tissue (Kassner et al., 2008; Lim et al., 2013). Given the well-established cytotoxic nature of DOXol, more research is necessary to understand the role that skeletal muscle plays in the accumulation and metabolism of this metabolite. It should be noted that the route of administration as well as the inherent individual differences of drug uptake from the gut may have contributed to these results. Alternative routes such as IV may yield a distinct contrast in concentrations between doses. Furthermore, as a limitation of the experimental procedures, these data are not paired as the same measurements were not made from the same rat over the course of the experiment (192 hours). Skeletal muscle represents

approximately 40% of the body mass and constitutes an important compartment which appears to play a major role in the sequestering of DOX. The resulting accumulation of the drug in the muscle may have a more immediate impact on the tissue than previously believed. More concerningly, the apparent sequestering may significantly limit the amount of drug intended for the target tissue (i.e. tumor) upon repeated administration while inadvertently increasing concentrations while unnecessarily elevating DOXol in the healthy tissue.

The interstitial space within the skeletal muscle did not appear to represent a significant rate limiting compartment for the uptake or release of DOX or DOXol from the tissue to the circulation irrespective of the dose. Interstitial DOX and DOXol concentrations were stable throughout the experiment as well as comparable between the two doses. This suggests that the rate of appearance of DOX and DOXol in the interstitial space from the vasculature appears to be matched by the rate of disappearance of the drug and its metabolite from the interstitial space into the muscle. A dynamic equilibrium appears to form resulting in no net accumulation in the interstitial space. This is further supported by the finding that the reciprocal efflux of DOX and DOXol from the muscle back into the plasma at 96 hours did not result in any significant accumulation of these compounds in the interstitial space, suggesting that the dynamic equilibrium is sustained in both directions. Additionally, these data demonstrate that the microdialysis technique is an effective tool for the *in vivo* analysis of drug concentrations within the extracellular fluid of skeletal muscle, and as such, may be an important tool in the assessment of drug delivery kinetics.

Muscle groups which differ in fiber type distribution were examined to further investigate the factors involved in the accumulation of DOX and DOXol within skeletal muscle. The SOL predominantly consists of ~97 % of Type I fibers whereas the WG is ~88 % Type IIB fibers (Bloemberg & Quadrilatero, 2012). The RG (~39 % Type I, ~30 % Type IIA) and PL (~45 % Type IIX, ~21 % Type IIA) are considered as a mixed based on the distribution of fiber types (Bloemberg & Quadrilatero, 2012). Interestingly, there was no evidence that DOX preferentially accumulated in a specific muscle group at either the 1.5 mg kg-1 or 4.5 mg kg-1 dose. Additionally, no differences in DOX concentrations were observed when comparing levels between the two doses. It has previously been shown that once in the cytosol DOX has a high affinity for cardiolipin (Goormaghtigh, Huart, Praet, Brasseur, & Ruysschaert, 1990), an important phospholipid expressed in the mitochondrial membrane. It would be expected that a preferential accumulation of DOX would occur in the oxidative Type I muscle as it relies heavily on mitochondrial activity as compared to the Type II glycolytic muscle. Though, the current data supports the contention proposed by Anderson *et al.* (Anderson, Xiong, & Arriaga, 2004) who has reported a high degree of variability of the accumulation of DOX in the mitochondria. It is well known that the capillary network within the skeletal muscle differs greatly between fiber types where the capillary to fiber ratio is significantly higher in Type I muscle compared to that of Type II (Erzen, Janacek, & Kubinova, 2011; Murakami et al., 2010). In the current study, it does not appear that the difference in perfusion of the tissue plays a role in the accumulation of DOX in the skeletal muscle**.** The data in the current study represent basal muscle conditions as there was minimal muscle exertion over the course of the experiment. Muscle stimulation or exercise may expose fiber type differences in the accumulation of DOX and,

as such, further study is required to better explore this possibility. There was some individual variation in DOXol accumulation amongst the muscle groups but overall there was no difference between muscle groups regardless of the administered dose. As previously noted, the mechanisms responsible for the influx and efflux of DOXol from skeletal muscle has not yet been elucidated and even less is known about the commonalities shared between fiber types leading to the results seen in this study. Considering the resemblance of data between DOXol and DOX, it is within reason to believe that muscle fiber types do not affect DOXol accumulation in basal conditions. Further study is required to explore the possible role that increased muscle use may have on accumulation.

Overall, this study clearly shows that skeletal muscle plays an important role in the metabolism of DOX and may significantly alter its therapeutic impact. The rapid and sustained accumulation of the drug in the muscle as a result of a single injection may initiate factors leading to the characteristic dysfunction previously described. Furthermore, the apparent sequestering of the drug in the muscle effectively reduces systemic concentrations and favors metabolic breakdown. In turn, this decreases the drug intended for the tumor severely reducing the therapeutic impact prompting repeated doses typical of chemotherapy regimens. This represents a therapeutic and clinical paradox: The repeated administration of the drug increases the exposure of the tumor to the chemotherapy, while the inherent accumulation of the drug in skeletal muscle exacerbates the initial detrimental effects, ultimately reducing the clinical outcome. The possible manifestation of skeletal muscle toxicity before that of a cumulative and dose-dependent cardiotoxicity may have serious implications in the clinical assessment and modulation of Doxorubicin chemotherapy.

5.5 Materials and Methods

5.5.1 *Animals*

All of the experimental procedures in the study were approved by the Laurentian University Animal Care Committee. Male Sprague-Dawley rats (n=102, 434±8 g) were obtained from Charles River Laboratories (Senneville, QC) and were housed according to Standard Operating Procedures and Policies for the Housing and Environmental Enrichment of Rodents at the Laurentian University Animal Care Facility. Experiments began after a one week acclimation period.

5.5.2 *Pre-experimental procedures*

Experimental groups. Rats were injected with Doxorubicin (Doxorubicin Hydrochloride. Pfizer, Canada) at a dose of 1.5 mg kg-1 (Group 1 to 8) or 4.5 mg kg-1 (Group 9 to 16), administered intraperitoneally (IP). A sham injection of saline solution was administered to a control group (IP, n=6). Once administered, rats were randomly grouped into experimental endpoints (n=6) of 24, 48, 72, 96, 120, 144, 168 or 192 hours post-injection (Fig 5A). This dose was selected in order to examine the acute effects of the drug on skeletal muscle while minimizing the potential for cardiotoxicity.

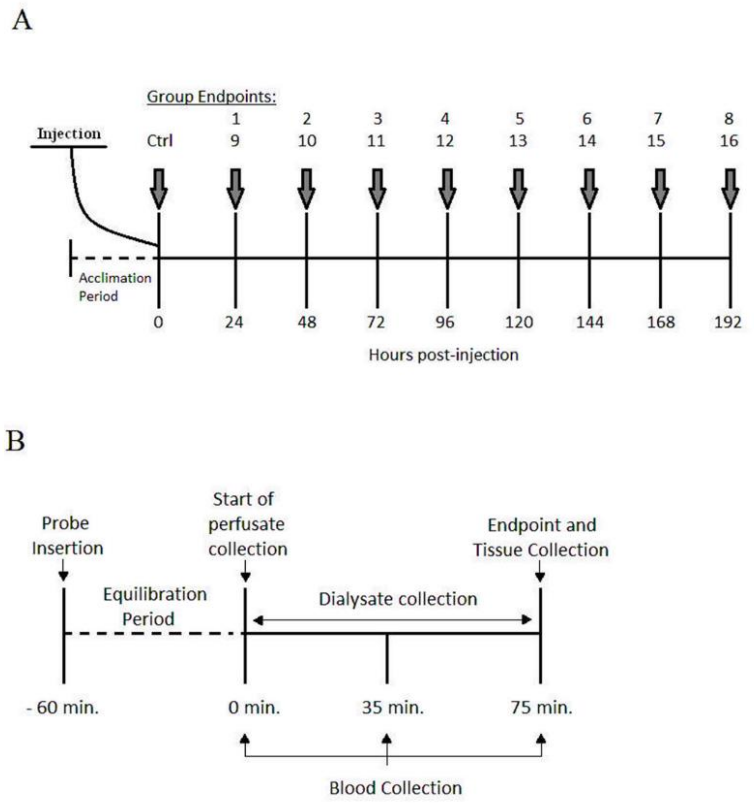

Fig 5. Organization of experimental groups and experimental procedures. (A) Schematic representation of the experimental groups receiving an injection of 1.5 mg kg-1 dose (groups 1-8) or 4.5 mg kg-1 (groups 9-16) of DOX IP. A sham injection is administered to the control group (Ctrl). (B) Representation of the experimental proceedings for dialysate, blood and tissue collection following microdialysis probe insertion and carotid artery cannulation.

Microdialysis probes. A complete description of the construction of the microdialysis probes has previously been outlined (Hellsten, Maclean, Radegran, Saltin, & Bangsbo, 1998). Briefly, microdialysis fibers were constructed using Spectra Microdialysis fibers (Spectrum, VWR International) with a molecular weight cut-off of 13 kDa and Polyamide-100II tubing (MicroLumen, Tampa FL) cut to 9.5 and 5 cm lengths. The ends of the fiber were inserted 1 cm into the hollow polyamide tube and glued. The exposed portion of the fiber (diffusible) between the polyamide tubes measured 1.0 cm in length.

5.5.3 *Experimental procedures*

Animals. On the day of the experiment, the rats were placed into an induction chamber and anaesthetized using an EZ-150 vaporizer unit (EZ-Anesthesia, Euthanex Corporation, Palmer, PA), which blends oxygen (100% O_2 Praxair, Sudbury, ON) and isoflurane (5 %). Once anaesthetized, the rats were removed from the chamber and placed onto a heated pad while its nose was placed in to a nosepiece supplying a continuous delivery of oxygen and isoflurane (2-2.5 %). The animals remained under anaesthesia throughout the experiment and the plane of anaesthesia was routinely checked by toe pinches. Heart rate and oxygen saturation were monitored throughout the experiment using a pulse oximeter (SurgiVet) attached to the base of the tail. Body temperature (between 36–37ºC) was maintained using a heated surgical bed (EZ-Anaesthesia) and a heating lamp. Following the completion of the experiment the animals were euthanized by decapitation.

Probe insertion. Using curved dissecting scissors, incisions were made at the base of the leg and the skin was manually pulled back until the entire leg was exposed (Fig 6A) and then the excess skin was removed. A 21 gauge curved cannula was inserted anteriorly into the muscle along the muscle's natural fibre orientation (Fig 6B) and acted as a guide for the microdialysis probe. Once the cannula was in place, the 9.5 cm portion of the probe is inserted caudally through the cannula and extended past the foot (Fig 6C). As soon as the diffusible portion of the probe was oriented into the muscle, then the 5 cm portion of the probe was held in place while the cannula was retracted out of the tissue leaving the probe in place (Fig 6D).

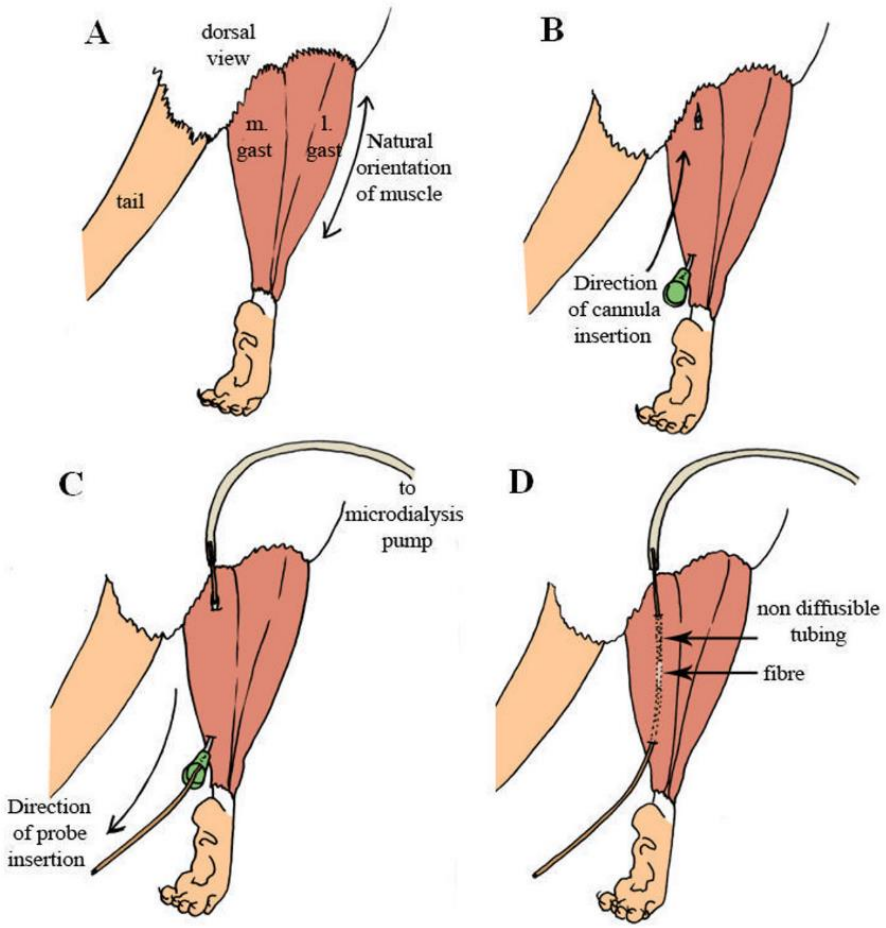

Fig 6. Experimental procedure for microdialysis probe insertion. (A) Exposing the medial and lateral gastrocnemius muscle. (B) Insertion of 21 gauge cannula. (C) Microdialysis probe insertion guided by the cannula. (D) Location of the diffusible membrane within the muscle.

Experimental protocol. Two microdialysis probes were inserted into the hind limb, one in the lateral gastrocnemius and one in the medial gastrocnemius muscle of the same limb (n=2 probes per animal) as the opposite limb was used for muscle extraction. Following probe insertion, the fibers were perfused (model 102, CMA) at a rate of 3 μL/min with Ringer's solution. It is recognized that probe insertion results in some cellular disruption therefore traditionally a 60 min. equilibration period prior to the initiation of the experiment was used to ensure that the external environment surrounding the probes had

stabilized and all cellular damage had dissipated (MacLean et al., 2001). Subsequently, the skin and tissue covering the left carotid artery was removed. A 20 gauge cannula was inserted into the exposed artery and sutured in place. Heparinized saline (100 μL) was injected into the artery to maintain patency in preparation for blood sampling.

Following the equilibration period the experimental protocol was initiated (Fig 5B) where dialysate was collected for a period of 75 minutes in order to obtain sufficient volume that was required for analysis. Dialysate samples were collected in microcentrifuge tubes and immediately sealed to prevent evaporation and stored at -80ºC until analysis. Arterial blood samples were collected during the collection of dialysate at 0, 35 and 75 minutes. Samples were spun at 15,000 rpm for 25 seconds, plasma was separated and stored at -80ºC until analysis. Upon completion of dialysate and blood collection the plantaris (PL), soleus (SOL), medial gastrocnemius (WG) and lateral gastrocnemius (RG) muscles of the opposite leg used for microdialysis were extracted and inserted into cryogenic vials then flash frozen in liquid nitrogen and stored at -80ºC until analysis.

5.5.4 *Sample analysis*

HPLC. Quantification of DOX and DOXol were determined by HPLC analysis (Waters e2695, 2475 Fluorescence Detector, Waters Corporation) with an ACE CN column (Advanced Chromatography Technologies, UK). The mobile phase was composed of a 10mM sodium phosphate monobasic (pH 4.0) solution as well as a 100 % acetonitrile solution and a volume of 90 μL was used for analysis. Detection was made by fluorescence (2475 Fluorescence Detector, Waters Corporation) at 480 nm excitation and 560 nm emission.

Interstitial DOX, DOXol. Quantification of interstitial DOX and DOXol concentrations where determined by HPLC analysis. The collected dialysate samples represent an ultra-clean filtrate and did not require any pre-analysis preparation. Dialysate and perfusate blanks as well as dialysate samples from control animals were used to confirm the quality and purity of the samples analyzed. Compounds were quantified by comparison with a standard curve (Doxorubicin Hydrochloride. Pfizer, CA; Doxorubicinol Citrate. TRC, CA).

Skeletal Muscle DOX, DOXol. Muscle samples were homogenized using a 67 μM potassium phosphate solution containing a 0.625 μM Daunorubicin (Daunorubicin hydrochloride, Sigma) internal standard, to a concentration of 125 mg muscle/mL of solution. Subsequently, 200 μL of 50:50 (v/v) 40% $ZnSO_4$ and 100% methanol was added to 150 μL homogenate and vortexed for 2 minutes. Samples were then placed in the centrifuge at 13,000 rpm for 10 minutes and supernatant was used for HPLC analysis. Compounds were quantified by comparison with a standard curve and corrected by internal standard.

Plasma DOX, DOXol. For this analysis, a 133 μL of 50:50 (v/v) 40 % $ZnSO_4$ and 100 % methanol containing 0.0625 μM Daunorubicin internal standard was added to 100 μL of plasma and vortexed for 2 minutes. Samples were then placed in the centrifuge at 13,000 rpm for 10 minutes and supernatant was used for HPLC analysis. Compounds were quantified by comparison with a standard curve and corrected by internal standard.

Probe recovery. Probe recovery was determined using an *in vitro* method previously described by Li et al. (Li, King, & Sinoway, 2003) Probes were immersed in a

Petri dish filled with a predetermined concentration of DOX and DOXol and perfused with Ringer's solution. Probe recovery was determined by dividing the concentration of DOX and DOXol in the recovered dialysate by the concentrations in the Petri dish. A flow rate of 3 μL/min was used in this experiment, yielding a 10 and 18 % recovery rate of DOX and DOXol, respectively. It is important to note that, for the scope of this study, the stability of the environment surrounding the probe is critical as it allows for the constant collection of undisturbed concentrations of the drug and its metabolite. As such, collections were done in resting conditions and after a 60 minute period of equilibration.

Statistics. Changes in plasma, interstitial and muscle DOX and DOXol concentrations in comparison to baseline, which ultimately represents zero drug concentration, were analyzed using ANOVA and significance was accepted at $P<0.05$. Similarly, the differences between doses and each time points were analyzed using ANOVA where significance was accepted at $P<0.05$. When significant changes were observed in the comparisons, a Tukey's *post hoc* test for multiple comparisons was used to determine where the significance occurred. All values used in graphical representations are displayed as mean ± SEM.

5.6 Acknowledgments

The authors wish to thank Ms. Pamela Chenard and Ms. Lindsay Anderson for their excellent technical assistance.

CHAPTER III

(Study 2)

Doxorubicin chemotherapy affects intracellular and interstitial nitric oxide concentrations in skeletal muscle.

6. Study 2 Objective: Examine the effect of Doxorubicin administration on nitric oxide concentrations in skeletal muscle and the interstitial space.

7. Overview of Study 2

Perfusion of skeletal muscle is essential in assuring the health and function of the tissue. The stringent regulation of competing local vasoconstrictive and vasodilatory molecules is necessary to meet fluctuations in metabolic demand. As a potent vasodilatory molecule, the ubiquitous production of nitric oxide in skeletal muscle plays an important role in the proper regulation of local vascular tone. Nitric oxide diffuses from the cell in which it is produced through the interstitial space to the targeted vascular smooth muscle to exert its vasodilatory effect. It is well established that alterations in nitric oxide homeostasis leads to significant physiological effects including dysregulation of local blood perfusion in the tissue, increased radical oxygen generation and peroxynitrite formation. In the previous chapter, a bolus injection of DOX resulted the sequestering of the drug in skeletal muscle up to 8 days following its administration. Doxorubicin has shown to effect nitric oxide synthase expression in cancer cells, cardiomyocytes and

skeletal muscle however direct measurements of nitric oxide following the administration of DOX has never been investigated. This study concurrently examines intracellular and interstitial concentrations of nitric oxide in skeletal muscle following the administration of DOX, highlighting the possible effects of nitric oxide dysregulation on the tissue and the potential role of nitric oxide in the timely release of the drug from the tissue.

8. Doxorubicin chemotherapy affects intracellular and interstitial nitric oxide concentrations in skeletal muscle.

(Original Research)

Sergio Fabris, David A. MacLean

[Published in *Cell Biology and Toxicology*]

Fabris, S., & MacLean, D. A. (2016). Doxorubicin chemotherapy affects intracellular and interstitial nitric oxide concentrations in skeletal muscle : Effect of doxorubicin on intracellular and interstitial NO in skeletal muscle. *Cell Biol Toxicol*, 32(2), 121-131. doi: 10.1007/s10565-016-9325-1

Contributions: Experiments where conceived, designed and conducted by Sergio Fabris. Sergio Fabris performed the analysis of the data and wrote the manuscript.

8.1 Abstract

The role of nitric oxide (NO) in Doxorubicin (DOX; cancer chemotherapeutic) induced cardiotoxicity is well established. In skeletal muscle (SM), NO regulation plays a critical role in health, biogenesis and function. Despite the increasing evidence that indicates the negative impact of DOX on SM function, the effect of DOX on NO production in SM has yet to be examined. The purpose of the current study was to simultaneously examine intracellular and interstitial NO concentrations in the SM following the administration of DOX. A single dose of 1.5 or 4.5 mg/kg was administered intraperitoneally to male Sprague-Dawley rats and interstitial (IS) and intracellular (IC) NO was quantified every 24 up to 192 hrs. post injection. There was no significant difference in IC NO following the injection of 1.5 mg/kg DOX when compared to control, however the administration of 4.5 mg/kg DOX resulted in lower ($P<0.05$) concentrations of NO in the IC. Interestingly, a consistently higher ($P<0.05$) concentration of NO in the IS was established following the administration of 1.5 mg/kg compared to control while no significant changes in IS NO resulted from the administration of the 4.5 mg/kg dose. The fluctuation of IS and IC NO where not a result of substrate availability as arginine concentrations remained stable throughout the experiment. By utilizing the microdialysis technique, we have simultaneously quantified for the first time the IS and IC concentrations of NO in SM following DOX administration. These data provide important insight in the possible mechanisms leading to DOX related SM dysfunction.

8.2 Introduction

Nitric oxide (NO) is a key signaling molecule implicated in various physiological processes including local blood flow regulation, platelet aggregation and neurotransmission (Archer et al., 1994; Calabrese et al., 2007; Riddell & Owen, 1999). In the presence of L-arginine (Arg), NADPH and molecular oxygen, NO is endogenously produced by the enzymatic activity of three nitric oxide synthase (NOS): endothelial, neuronal and inducible isoforms (eNOS, nNOS and iNOS respectively) (Stamler & Meissner, 2001). In skeletal muscle, significant physiological consequences are attributed to fluctuations in NO production, from impairment of skeletal muscle growth and differentiation to decreased muscle performance (De Palma et al., 2014; Stamler & Meissner, 2001). It has been recognized that during chemotherapeutic treatment, disruption of healthy skeletal muscle is an indicator of poor treatment results, and increased patient mortality (Antoun, Baracos, Birdsell, Escudier, & Sawyer, 2010; Prado et al., 2009).

Doxorubicin (DOX) is a widely used and highly effective cytotoxic agent used in the treatment of a broad spectrum of cancers (Carter, 1975; Gewirtz, 1999). DOX induced cytotoxicity has been attributed to the inhibition of DNA replication and RNA transcription via; 1) DNA intercalation, 2) inhibition of topoisomerase II (TOP2A) resulting in TOP2-mediated DNA damage and, 3) the formation of reactive oxygen species and hydrogen peroxide (Minotti et al., 2004; Momparler et al., 1976; S. Wang et al., 2004). The use of DOX chemotherapy is constrained by a dose-dependent and cumulative cardiotoxic effect which has been primarily attributed to its potent cytotoxic metabolite, Doxorubicinol (Minotti et al., 2004; Olson & Mushlin, 1990). Much of the attention regarding DOX and its effect on NO production has been primarily focused on its effect in cardiomyocytes

(Aldieri et al., 2002; Octavia et al., 2012; Zhang et al., 2012) where interesting progress has been made to reduce cardiotoxicity with dietary nitrates (Xi et al., 2012). Recent studies have reported a decline in muscular function, a decrease in force generation and increased muscular fatigue as a result of DOX treatment (Gilliam & St Clair, 2011; Hayward et al., 2013; van Norren et al., 2009). Similar to its well described toxic effect on myocardial tissue, significant increases in mitochondrial reactive oxygen species (ROS) as well as upregulated autophagy and apoptotic pathways are believed to be primarily responsible for DOX-related muscular dysfunction (Gilliam & St Clair, 2011; Smuder et al., 2011a; A. P. Yu et al., 2014). Little is known of the effect of DOX treatment on NO production in skeletal muscle.

In skeletal muscle, the compartment separating the myocytes from the capillary network is known as the interstitial space. The interstitial compartment plays a functional role in the regulation and integration of various substances including NO (Jackson, 2005; MacLean et al., 1999). First introduced by Delgado et al. (Delgado et al., 1972), the microdialysis technique allows for the direct *in vivo* investigation of compounds located in the interstitial space. To our knowledge, the effect of DOX administration on intracellular and interstitial concentrations of NO have not been examined. These data would greatly advance our understanding in the role of DOX chemotherapy on NO production in skeletal muscle.

As such, the purpose of the current study was simultaneously quantify intracellular and interstitial concentrations of NO in skeletal muscle as a result of the administration of DOX in order to provide insight in the possible mechanisms leading to muscle dysfunction. It is hypothesized that the administration of DOX will increase the intracellular and

interstitial concentrations of NO in skeletal muscle. The major finding in this study was a DOX dose-dependent effect on intracellular and interstitial concentrations of NO which may affect ROS generation. These data indicate that the effect of DOX on skeletal muscle, and more specifically NO production, may play a more significant role in the therapeutic impact of DOX chemotherapy than previously considered.

8.3 Materials and Methods

8.3.1 *Animals*

All of the experimental procedures in the study were approved by the Laurentian University Animal Care Committee. Male Sprague-Dawley rats (n=102, 434.3±8.3 g) were obtained from Charles River Laboratories (Senneville, QC) and were housed according to Standard Operating Procedures and Policies for the Housing and Environmental Enrichment of Rodents at the Laurentian University Animal Care Facility. Experiments began after a one week acclimation period.

8.3.2 *Pre-experimental procedures*

Experimental groups. Rats were injected intraperitoneally (i.p.) with Doxorubicin (Doxorubicin Hydrochloride. Pfizer, Canada) at a dose of 1.5 mg/kg (Groups 1 to 8, n=6 per group) or 4.5 mg/kg (Groups 9 to 16, n=6 per group). A sham injection of saline solution was administered to a control group (i.p., n=3). Once administered, rats were randomly grouped into experimental endpoints of 24, 48, 72, 96, 120, 144, 168 or 192 hrs. post-injection (Figure 1a). Previous studies have examined the cardiotoxic effect of DOX

following the administration of various doses and dose regimens. Based on these studies, the doses in the current study were selected in order to examine the acute effects of the drug on skeletal muscle NO production while minimizing the cardiotoxic potential. Further details regarding the rationale is found in the Discussion.

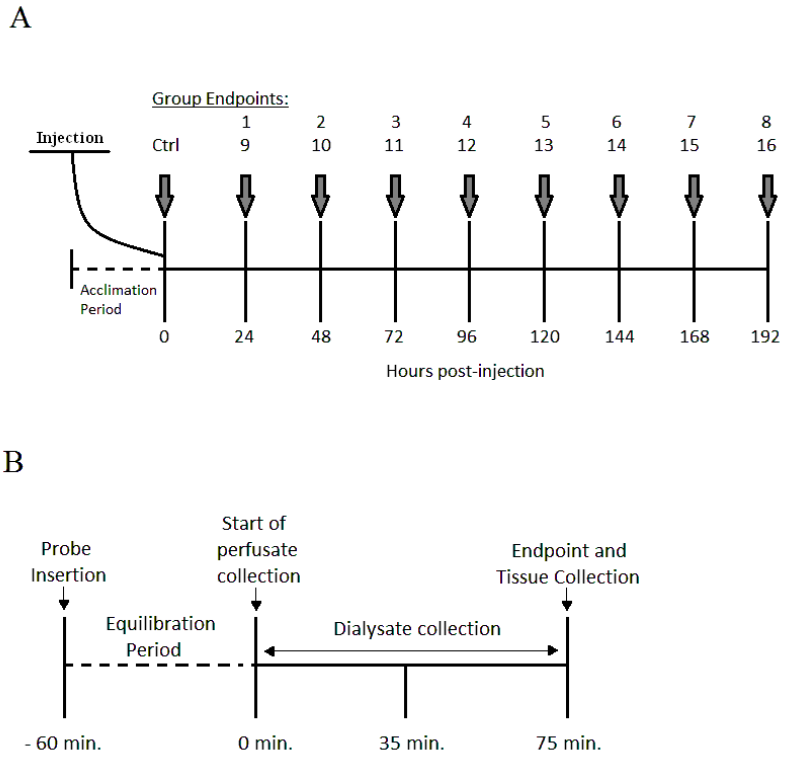

Figure 1: (A) Schematic representation of the experimental protocol, indicating groups of rats receiving an injection of 1.5 mg kg-1 dose (groups 1-8) or 4.5 mg kg-1 (groups 9-16) of DOX i.p. A sham injection is administered to the control group (Ctrl). (B) Representation of the experimental proceedings for dialysate and tissue collection following microdialysis probe insertion.

Microdialysis probes. A complete description of the construction of the microdialysis probes has previously been outlined (Hellsten et al., 1998). Briefly, microdialysis fibers were constructed using Spectra Microdialysis fibers (Spectrum, VWR International) with a molecular cutoff of 13 kDa and Polyamide-100II tubing

(MicroLumen, Tampa FL) cut to 9.5 and 5 cm lengths. The ends of the fiber were inserted 1 cm into the hollow polyamide tube and glued. The exposed portion of the fiber (diffusible) between the polyamide tubes measured 1.0 cm in length. Probe recovery was determined using an in vitro method previously described.

8.3.3 *Experimental procedures*

Animals. On the day of the experiment, the rat was placed into an induction chamber and anaesthetized with an EZ-150 vaporizer unit (EZ-Anesthesia, Euthanex Corporation, Palmer, PA), which blends oxygen (100% O_2 Praxair, Sudbury, ON) and isoflurane at a rate of 5 %. Once anaesthetized, the rat was removed from the chamber and placed onto a heated pad while its nose was placed into a nosepiece supplying a continuous delivery of oxygen and isoflurane (2-2.5 %). The animal remained under anaesthesia throughout the experiment and the plane of anaesthesia was routinely checked by toe pinches. Heart rate and oxygen saturation were monitored throughout the experiment using a pulse oximeter (SurgiVet) attached to the base of the tail. Body temperature (between 36–37^{o}C) was maintained using a heated surgical bed (EZ-Anaesthesia) and a heating lamp. Following the completion of the experiment, the animal was euthanized by decapitation.

Probe insertion. A schematic representation of the procedure for microdialysis probe insertion has previously been published by our research group (Fabris & MacLean, 2015). In short, incisions were made at the base of the leg using curved dissecting scissors and the skin was manually pulled back until the entire leg was exposed, the excess skin was then removed. A 21 gauge curved cannula was inserted anteriorly into the muscle

along the muscle's natural fibre orientation and acted as a guide for the microdialysis probe. Once the cannula was in place, the 9.5 cm portion of the probe is inserted caudally through the cannula and extended past the foot. As soon as the diffusible portion of the probe was oriented into the muscle, then the 5 cm portion of the probe was held in place while the cannula was retracted out of the tissue leaving the probe in place.

Experimental protocol. Two microdialysis probes were inserted into the hind limb for this experiment, one in the lateral gastrocnemius and one in the medial gastrocnemius muscle (n=2 probes per animal). Following probe insertion, the fibers were perfused (model 102, CMA) at a rate of 3 µL/min with Ringer's solution. It is recognized that probe insertion results in some cellular disruption therefore traditionally a 60 min. equilibration period prior to the initiation of the experiment was used to insure that the external environment surrounding the probes had stabilized and all cellular damage had dissipated (MacLean et al., 2001).

Following the equilibration period, the experimental protocol was initiated (Figure 1b) where dialysate was collected for a period of 75 minutes in order to obtain sufficient volume that was required for analysis (225 µL total). Dialysate samples were collected in microcentrifuge tubes and immediately sealed to prevent evaporation and stored at -80ºC until analysis. It is important to note that due to the nature of the procedure, the exact placement of the diffusible portion of the probe within the limb is not determined with respect to exact fibre types surrounding the probe. However is it common to describe the probe as being in a muscle group which predominantly expresses a fibre type. Upon completion of dialysate collection, the plantaris (PL), soleus (SOL), medial gastrocnemius

(WG) and muscles were extracted, inserted into cryogenic vials, flash frozen in liquid nitrogen and stored at -80ºC until analysis.

8.3.4 *Sample analysis*

Sample Preparation. Frozen muscle samples were placed in a freeze drier (Freeze Drier 4.5, Labconco) at 10 microns Hg for 24 hrs. Subsequently, samples were powdered and tweezed free of all visible connective tissue.

NO Analysis. Two mg of freeze dried skeletal muscle were added to 400 µL, 0.5 M perchloric acid for the extraction of protein. These samples were vortexed for 5 min. and then homogenized for 5 min. using a Kontes Pellet Grinder. The samples were then cooled on ice for 20 min. and centrifuged at 14 000 r.p.m. for 10 min. before analysis. The collected dialysate samples represent an ultra-clean filtrate and did not require any pre-analysis preparation. NO concentrations in skeletal muscle and dialysate samples were determined by chemiluminescence using a Sievers Model 280i Nitric Oxide Analyzer. Vanadium chloride was used to convert nitrate and nitrite (NOx) to nitric oxide. The reduction was done at 95ºC in 0.1 M hydrogen chloride. 5 µL of the prepared skeletal muscle supernatant and dialysate samples were analyzed in duplicate and quantification of NO concentrations were determined in each sample by comparison with a standard curve (sodium nitrate).

Arginine Analysis. Two mg of freeze dried skeletal muscle were added to 100 µL purified water (EMD Millipore, USA) containing L-Norleucine (Sigma-Aldrich, USA) as internal standard then homogenized for 30 sec. using a Kontes Pellet Grinder. The homogenate was then transferred into a centrifugal filtering tube (EMD Millipore, USA)

and centrifuged at 15 000 r.p.m. for 20 min. 20 µL of the filtrate was added to 60 µL borate buffer and 20 µL fluor reagent (AccQ-Tag, Waters Canada) and vortexed immediately for 30 sec. Samples were placed on a heating block at 55ºC for 10 min. before analysis. Arg concentrations were determined by HPLC using AccQ-Tag Amino Acid Analysis kits (Waters, Canada). Quantification of Arginine was determined by comparison with a standard curve and corrected by internal standard.

Statistics. Changes in NO concentrations between time points and doses were analyzed using a two-way ANOVA. When significant differences were indicated, a Tukey's *post hoc* test was used to determine where the significance occurred. Significance was accepted at $P<0.05$. All values used in graphical representations are displayed as mean ± SEM.

8.4 Results

The concentration of intracellular NO was higher ($P<0.05$) in the SOL 24 hrs. (1.25±0.15 mmol/kg dw) following the administration of 1.5 mg/kg DOX when compared to control (0.71±0.09 mmol/kg dw). The administration of 4.5 mg/kg DOX resulted in lower ($P<0.05$) intracellular NO concentrations 24 and 48 hrs. (0.35±0.04 mmol/kg dw and 0.48±0.04 mmol/kg dw, respectively) post-injection when compared to control (1.25±0.15 mmol/kg dw). When comparing between administered doses, intracellular NO conentrations were higher ($P<0.05$) following the 1.5 mg/kg after 24 (357 %), 48 (171±9 %), 168 (141±2 %) and 192 hrs. (122±2 %) when compared to the 4.5 mg/kg dose.

Concentrations of intracellular NO were higher after 96 (123±2 %) and 120 hrs. (136±6 %) following the injectin of 4.5 mg/kg when compared to the 1.5 mg/kg dose (Figure 2a).

Intracellular NO concentrations in the WG were not significantly altered at any time point by the administration of 1.5 mg/kg DOX. However, the injection of 4.5 mg/kg DOX resulted in lower ($P<0.05$) intracellular NO concentrations after 24 (0.39±0.05 mmol/kg dw) and 48 hrs (0.53±0.03 mmol/kg dw) as compared to control (0.89±0.09 μmol/kg dw). When comparing between treatments, the 4.5 mg/kg dose was lower ($P<0.05$) after 24 (267±4 %) and 48 hrs. (149±1 %) when compared to the 1.5 mg/kg dose, however NO concentrations were higher ($P<0.05$) after 96 hrs. (125±8 %). Furthermore, intracellular NO concentrations were higher ($P<0.05$) following the 1.5 mg/kg dose as compared to the 4.5 mg/kg dose after 192 hrs. (117±3 %) (Figure 2b).

The administration of either the 1.5 or 4.5 mg/kg did not affect NO concentrations in the PL when compared to control. However when comparing between administered doses, the administration of 1.5 mg/kg resulted in higher ($P<0.05$) intracellular NO concentrations after 24 hrs. (133±9 %) compared to the 4.5 mg/kg dose. Additionally, in comparison to the 1.5 mg/kg dose, intracellular NO was higher ($P<0.05$) following the 4.5 mg/kg dose after 48 and 72 hrs (130±4 % and 131±6 %, respectively) (Figure 2c).

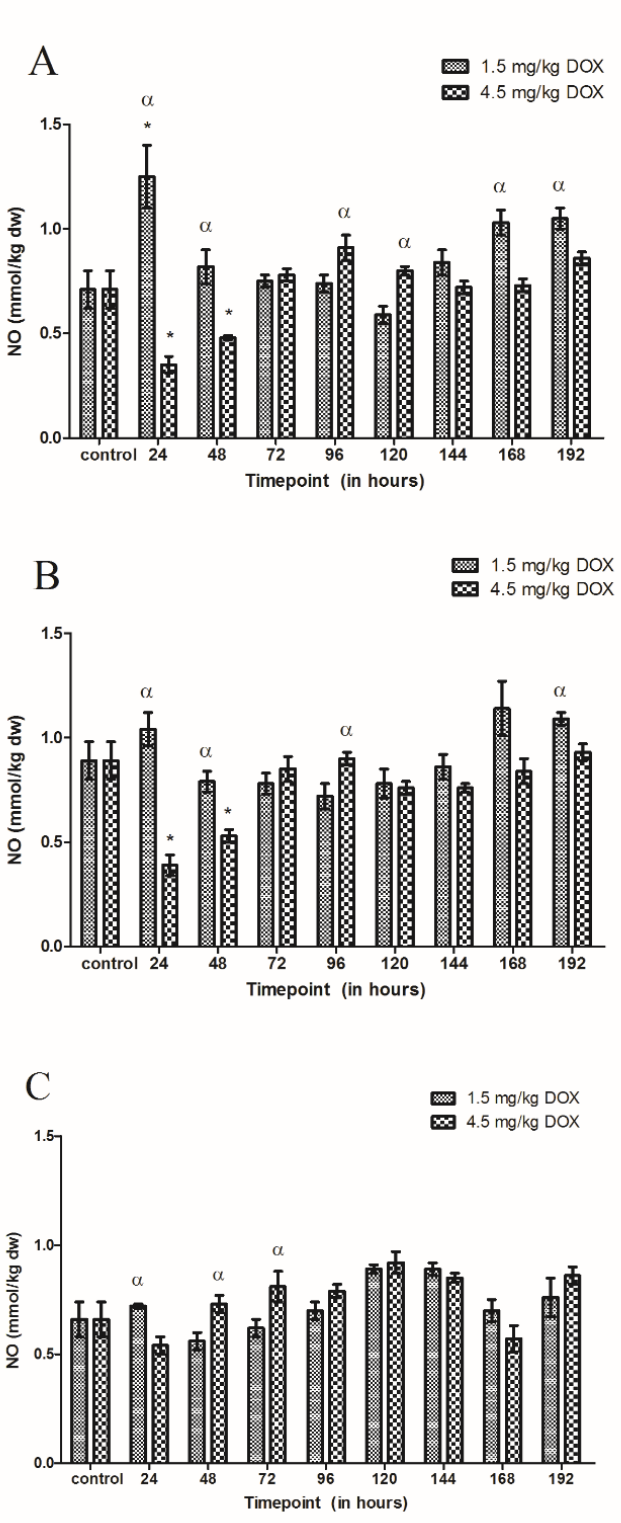

Figure 2: Intracellular concentrations of nitric oxide, quantified using chemiluminescent analysis, in the (A) Soleus, (B) White gastrocnemius and (C) Plantaris following the i.p. administration of 1.5 mg/kg DOX or 4.5 mg/kg DOX. * Denotes significance compared to control. α Denotes difference ($P<0.05$) between administered doses.

Interstitial NO concentrations were higher (P<0.05) 24, 48, 72, 96 and 120 hrs. (5.48±0.33, 7.06±0.17, 5.17±0.2, 10.11±0.62 and 6.77±0.26 μM, respectively) following the administration of 1.5 mg/kg DOX whem compared to control (2.94±0.36 μM). Surprisingly, interstitial NO was higher (P<0.05) after 96 hrs. (9.69±1.06 μM) post-injection of 4.5 mg/kg DOX when compared to control (2.94±0.36 μM) while no other differences were observed throughout the course of the experiment. When comparing between doses, interstitial concentrations of NO were increased (P<0.05) by 159±5 % after 48 hrs. and 280±2 % after 120 hrs. following the 1.5 mg/kg compared to the 4.5 mg/kg dose. However, NO concentrations were 234±6 % and 126 % higher (P<0.05) after 168 and 192 hrs. subsequent to the 4.5 mg/kg administration when compared to the 1.5 mg/kg dose (Figure 3).

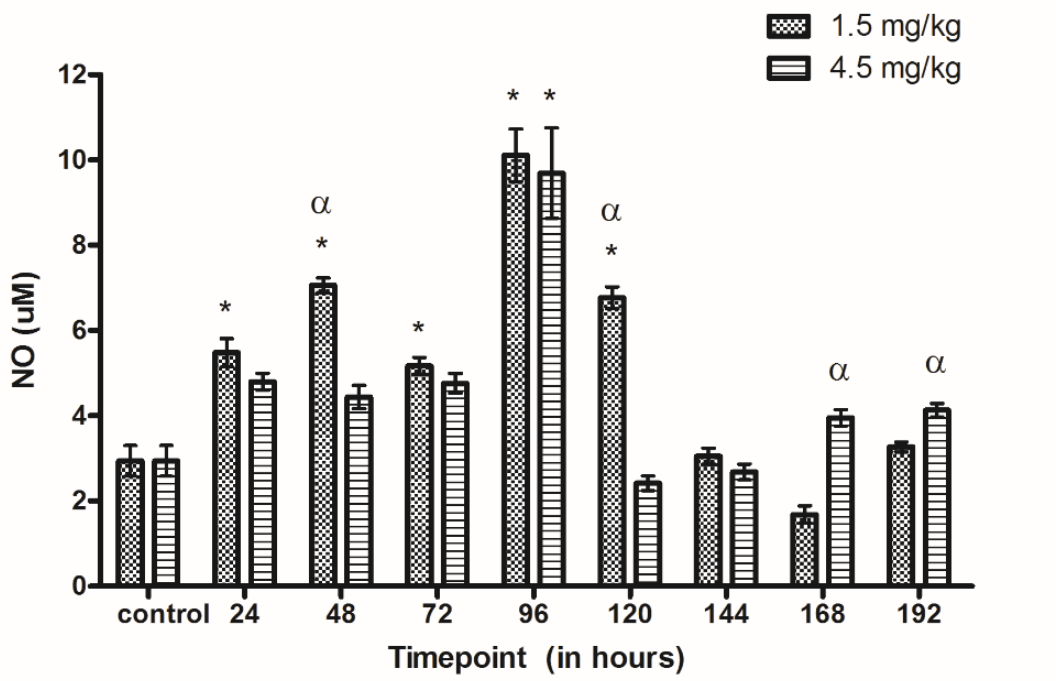

Figure 3: Skeletal muscle interstitial nitric oxide concentrations, quantified using chemiluminescent analysis, following the i.p. administration of 1.5 mg/kg DOX or 4.5 mg/kg DOX. * Denotes significance compared to control. α Denotes significance between administered doses.

Intracellular concentrations of Arg were quantified in order to determine if the variations in NO concentrations were the result of substrate availability. Following the 1.5 mg/kg dose, Arg was significantly higher ($P<0.05$) in the SOL (12±3.6 mmol/kg dw) and 72 hrs (14.5±8.9 mmol/kg dw) compared to control (6.2±0.2 mmol/kg dw). The 4.5 mg/kg dose resulted in higher ($P<0.05$) concentrations of Arg after 120 hrs. (17.7±5.5 mmol/kg dw) compared to control (6.2±0.2 mmol/kg dw). When comparing between administered doses, intracellular Arg was higher ($P<0.05$) following the 1.5 mg/kg dose after 24, 48 and 72 hrs (242±41 %, 158±279 % and 122±19 % respectively) compared to the 4.5 mg/kg dose, however concentrations were significantly higher in the 4.5 mg/kg after 120 (161±72 %) and 192 hrs. (124±4 %) (Figure 4a).

In the WG, the administration of 1.5 mg/kg DOX resulted in higher ($P<0.05$) Arg concentrations after 24 hrs. (14.8±6.8 mmol/kg dw) compared to control (4.3±2.4 mmol/kg dw) while no significant differences were observed following the 4.5 mg/kg dose. Between doses, Arg concentrations were higher ($P<0.05$)) following the 1.5 mg/kg dose after 24 and 168 hrs (320±94 % and 185±51 %, respectively) (Figure 4b).

The administration of 1.5 mg/kg DOX resulted in higher intracellular concentrations of Arg in the PL after 24 hrs (24.3±1.7 mmol/kg dw) compared to control (5.6±1.3 mmol/kg dw) whereas the 4.5 mg/kg dose elevated intracellular Arg levels 72, 96, 120 and 144 hours (13±2, 12.4±2.2, 13.4±2, 11.5±1.5 mmol/kg dw, respectively). However, when comparing doses, the 1.5 mg/kg dose increased ($P<0.05$) Arg 168±52 % compared to the 4.5 mg/kg dose after 168 hrs. Arg was more elevated ($P<0.05$) following the 4.5 mg/kg dose after 192 hrs (145±12 %) compared to the 1.5 mg/kg dose (Figure 4c).

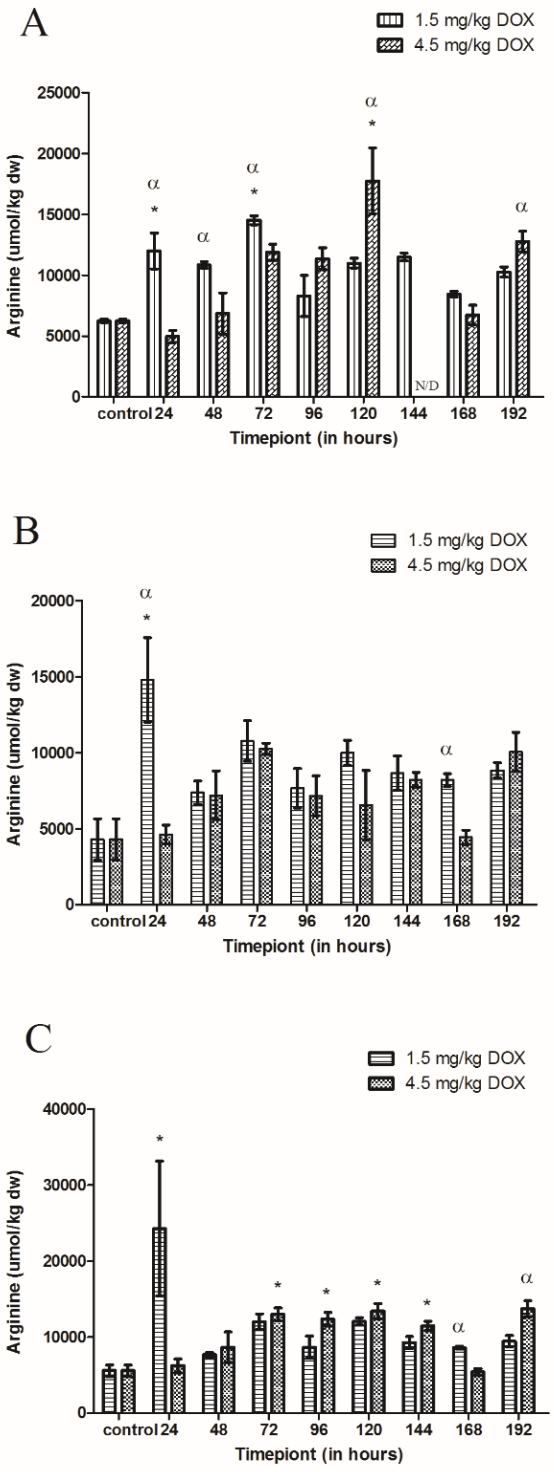

Figure 4: Intracellular concentrations of L-Arginine, quantified by HPLC analysis, in the (A) Soleus, (B) White gastrocnemius and (C) Plantaris following the i.p. administration of 1.5 mg/kg DOX or 4.5 mg/kg DOX. * Denotes significance compared to control. α Denotes significance between administered doses.

8.5 Discussion and Conclusion

The purpose of the current study was to simultaneously examine intracellular and interstitial concentrations of NO in skeletal muscle following the administration of DOX. The major finding in this study was a DOX dose-dependent effect on NO concentrations in both the intracellular and interstitial spaces in skeletal muscle. A persistent elevation (24-120 hrs.) in interstitial NO concentration was examined following the administration of 1.5 mg/kg DOX whereas an acute decrease (24-48 hrs.) in intracellular NO concentrations occured following the 4.5 mg/kg dose. These apparent alterations in NO homeostasis may lead to significant physiological effects including increased local blood perfusion in the tissue, increased ROS generation and peroxynitrite formationThe elevation in interstitial NO and increased local blood pefusion may play a key role in the removal of the drug from the tissue. By utilizing the microdialysis technique, we have simultaneously quantified for the first time the interstitial and intracellular concentrations of NO in skeletal muscle following DOX administration. These data provide important insight in the possible mechanisms leading to DOX related skeletal muscle dysfunction.

A well-documented side effect of DOX chemotherapy is a dose-dependent cardiotoxicity, which has been shown to lead to the onset of chronic cardiomyopathy and congestive cardiac failure (Kremer, van Dalen, Offringa, Ottenkamp, & Voute, 2001; Minotti et al., 2004; Paulides et al., 2006). In human and animal models, the decrease in cardiac performance has been shown to increase iNOS expression in skeletal muscle (Okutsu et al., 2014; Riede, Forstermann, & Drexler, 1998). In order to minimize the drug-induced risk of cardiotoxicity in the current study, a single dose of low concentration (1.5 mg/kg or 4.5 mg/kg) DOX was used. Former studies have utilized a variety of

concentrations and treatment regimens documenting significant cardiomyocyte damage. A single i.p. dose of 20 mg/kg (Iqbal et al., 2008) or 15 mg/kg (Nagi & Mansour, 2000) has resulted in cardiotoxicity whereas cardiomyocyte damage has not been observed as a result of a 10 mg/kg dose (Jensen et al., 1984). Minor cardiomyocyte apoptosis was reported 3 days following injection of 1.5 mg/kg and 5 mg/kg, however it remains unclear whether cardiac performance was significantly altered (Arola et al., 2000). Cumulative doses have been studied where 1 mg/kg i.p. administered 15 times over 3 weeks resulted in cardiac dysfunction (Teraoka et al., 2000) and 1.5 mg/kg for 9 weeks resulted in severe cardiomyopathy (Guerra et al., 2005). Much of the research regarding the effect of DOX administration on NO production has been focused on cardiomyocytes while the effect in skeletal muscle remains poorly understood. While providing a dose-related experimental contrast, the concentrations used in the current study greatly minimize the possibility that changes in NO concentrations are not a result of drug related cardiotoxicity.

It is apparent that the underlying mechanisms affecting the production of intracellular and interstitial NO differ between administered doses. Throughout the experiment, the administration of 1.5 mg/kg DOX did not have any sinigicant effect on the intracellular concentrations of NO however there was a persistent (24-120 hrs.) elevation of NO levels in the interstitial space. Interestingly, the threefold increase in administered dose resulted in an acute (24-48 hrs.) decrease of intracellular NO while there was no significant effect on interstitial concentrations. As a primary substrate required for the synthesis of NO by NOS isoforms, intracellular Arg concentrations were examined to determine if substrate availability was responsible for the apparent differences in NO concentrations. In all muscle groups, intracellular concentrations of Arg sharply increased

24 hrs. following the administration of 1.5 mg/kg DOX then subsequently stabilized for the remainder of the experiment. This acute increase would contribute to the incrase in NO production seen at the same time point (24 hrs.) however this would not account for the chronic elevation of NO observed 48-120 hrs. No significant changes in Arg were observed following the 4.5 mg/kg dose with the exception of the PL where Arg was increased 72-144 hrs. post injection. Though, this did not result in a significant increase intraceulluar NO production within this muscle group. Therefore, these data indicate that the differences in NO concentrations as a result of both administered doses is not the result of substrate availibility but may be the result of altered NOS activity.

The effect of DOX on NOS isoforms has been studied in cancer cells, cardiomyocites and skeletal muscle. The increase in interstitial NO observed in this study as a result of the 1.5 mg/kg dose is supported by previous research which have described the nuclear translocation of NF-κB leading to the upregulation and increased activity of iNOS as a result of DOX treatment (Riganti et al., 2005, Aldieri et al., 2002, Gilliam and St Clair, 2011). Therefore, the increase in interstitial NO may be attributed to the increased iNOS activity and subsequent diffusion of NO into the extracellular space. However, this mechanism does not describe the unexpected reduction of intracellular NO as a result of the 4.5 mg/kg dose. The reduction of NO synthesis has previously been observed in bovine aortic endothelial cells (Kalivendi, Kotamraju, Zhao, Joseph, & Kalyanaraman, 2001), cardiac myocytes (Kotamraju, Konorev, Joseph, & Kalyanaraman, 2000; Sawyer, Fukazawa, Arstall, & Kelly, 1999) and colorectal cancer cells (Jung et al., 2002). These studies describe that, eNOS transcription and activity is upregulated in the presence of DOX. The binding of DOX to the eNOS reductase domain leads to the one-electron

reduction of DOX and subsequent formation of a DOX semiquinone radical. As a result, the semiquinone activated redox cycling alters eNOS activity from NO synthesis to superoxide generator (Garner et al., 1999; Vasquez-Vivar et al., 1997). In agreement with the aforementioned studies, the more elevated administered dosage of DOX may have increase the binding of the drug to eNOS ultimately reducing the intracellular concentrations of NO as seen in the current study. Therefore, these data indicate that the changes in NO concentrations as a result of the administration of DOX may be the result of a dose dependent effect of DOX on NOS upregulation and activity.

In skeletal muscle, the production of NO is highly regulated. The dose dependent disruption in homeostasis seen in this study may lead to significant physiological ramifications. The increase in interstitial NO, as seen following the 1.5 mg/kg dose, and subsequent diffusion of NO into neighboring smooth muscle cells activates guanylyl cyclase which then catalyzes the dephosphorylation of GTP to cGMP causing relaxation and increased local blood flow (Archer et al., 1994). Also, it is well known that DOX generates high levels of oxidative stress in cardiomyocytes primarily attributed to its ability to disrupt the electron transport chain effectively resulting in the formation of ROS that includes superoxide and hydroxyl radicals (Conklin, 2004; Gille & Nohl, 1997). NO strongly reacts with superoxides (O_2^-) to produce peroxynitrite ($ONOO^-$) at a substrate diffusion-limited rate (Beckman, Beckman, Chen, Marshall, & Freeman, 1990; Evig et al., 2004). It is possible that the steady diffusion of NO into the interstitial space leading to a stable and elevated concentration, as seen in the current study, may increase the possibility of $ONOO^-$ formation. Highly reactive, the diffusion of peroxynitrites back into the cell decreases mRNA levels of myoblast determination protein (MyoD) (Di Marco et al., 2005)

required for skeletal muscle differentiation (Megeney, Kablar, Garrett, Anderson, & Rudnicki, 1996). Furthermore, the increase of iNOS expression and NO as well as peroxinitrite production has been shown to oxidize the conserved cysteine domain of transcription factor Jun-D (Buck & Chojkier, 1996). The inhibition of Jun-D decreases muscle creatine kinase (MCK) expression, important for the maintenance of ATP reserves and muscle function (Buck & Chojkier, 1996; Ramamoorthy, Donohue, & Buck, 2009; Wallimann, Wyss, Brdiczka, Nicolay, & Eppenberger, 1992) (Figure 5a). Furthermore, it is possible that the synergistic increase of iNOS and superoxide generation as a result of the effect of DOX on eNOS activity following the administration of 4.5 mg/kg DOX may amplify peroxynitrite formation and exacerbate the aforementioned physiological effects (Figure 5b).

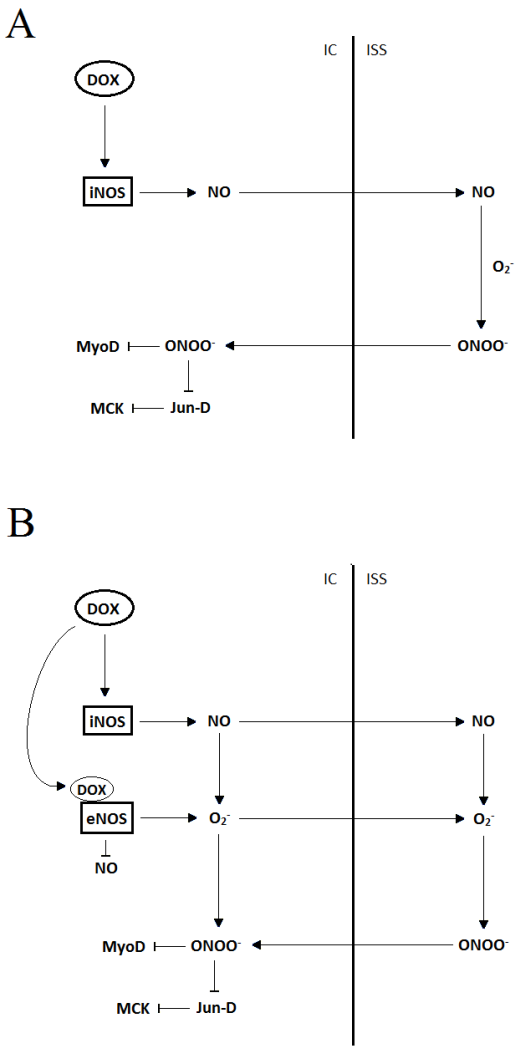

Figure 5: The effect of 1.5 mg/kg i.p. (A) and 4.5 mg/kg i.p. (B) Doxorubicin administration on nitric oxide (NO) production in the intracellular and interstitial space of skeletal muscle. (A) The upregulation of inducible nitric oxide synthase (iNOS) by Doxorubicin (DOX) increases intracellular (IC) NO production and subsequent diffusion of NO into the interstitial space (ISS). NO strongly reacts with superoxides (O_2^-) in the interstitial space to produce peroxynitrites ($ONOO^-$). The diffusion of $ONOO^-$ back into the cell decreases mRNA levels of myoblast determination protein (MyoD) and decreases muscle creatine kinase (MKC) expression via transcription factor Jun-D inhibition. (B) The effect of 4.5 mg/kg i.p. Doxorubicin administration on nitric oxide production in the intracellular and interstitial space of skeletal muscle. The upregulation of iNOS by DOX increases IC NO production. Concurrently, DOX binds to the reductase domain of eNOS altering its activity from NO production to O_2^- generator. The diffusion of NO into the ISS reacts with O_2^- in the interstitial space to produce $ONOO^-$ which may diffuse back into the cell. $ONOO^-$ formation in the cell is further exacerbated by the DOX/eNOS derived increase in IC O_2^-, which decreases mRNA levels of MyoD and decreases MKC expression via transcription factor Jun-D inhibition.

The reduction of DOX and subsequent formation of a semiquinone metabolite by eNOS (Garner et al., 1999; Vasquez-Vivar et al., 1997) may play a more significant role in the metabolic breakdown of DOX than previously considered. It is well established that aldo-keto reductase (AKR) and carbonyl reductase (CBR) activity is primarily responsible for the systemic breakdown of DOX (Kassner et al., 2008; Lim et al., 2013). To our knowledge AKR expression in skeletal muscle remains to be determined whereas as a lower affinity of CBR has been shown (Kassner et al., 2008). Much of the attention regarding the reduction of DOX to its semiquinone metabolite by eNOS is focused on the generation of ROS. However, when considering the apparent sequestering of DOX in skeletal muscle (Fabris & MacLean, 2015) and constitutive expression of eNOS (Stamler & Meissner, 2001), eNOS may play a more prominent role in the metabolic breakdown of DOX than aldo-keto and carbonyl reductases. The current study not only supports our previous notion suggesting the active role skeletal muscle on DOX availability and metabolism but provides insight into the possible physiological mechanisms involved.

This study demonstrates for the first time the effect of DOX administration on intracellular and interstitial NO concentrations simultaneously in skeletal muscle, highlighting the possible mechanisms leading to myocyte toxicity before that of a cumulative and dose-dependent cardiotoxicity. Additionally, the potential role of NO production and NOS expression in skeletal muscle and its role in the systemic availability of DOX is hypothesized. Overall, the effects of DOX on skeletal muscle may play a more important role than previously considered as NO mediation is an important factor in the quality of life and recovery of patients receiving DOX therapy.

8.6 Acknowledgements

The authors wish to thank Ms. Pamela Chenard, Ms. Talia Ryan and Ms. Josée Lalanne for their excellent technical assistance. Supported by the Natural Sciences and Engineering Research Council and the Ontario Institute for Cancer Research.

CHAPTER IV

(Study 3)

Amino Acid Metabolism in Skeletal Muscle Following the Administration of Doxorubicin Chemotherapy

9. Study 3 Objective: Investigate the amino acid response in skeletal muscle following the administration of Doxorubicin.

10. Overview of Study 3

The availability of intracellular amino acids is essential for the health and maintenance of skeletal muscle. Intramuscular amino acids derive from the exchange with the vasculature or from the endogenous breakdown of proteins from within the tissue. A net increase or decrease in total amino acid concentrations is strongly indicative of metabolic states favoring protein degradation or synthesis, respectively. The preceeding chapters have shown that DOX remained sequestered in skeletal muscle and that the sequestering of the drug in the tissue affected the production of a key local vasodilatory melocule. The current chapter examines the effect of DOX retention in skeletal muscle on the intramuscular total amino acid pool. By concurrently investigating the vacular, interstitial and intramuscular total amino acid concentrations, unique insight into the response of amino acids in communicating compartments was be obtained. The resulting

data provides a substantial foundation for future studies focused on the effect of DOX on amino acid metabolism in skeletal muscle.

11. Amino Acid Metabolism in Skeletal Muscle Following the Administration of Doxorubicin Chemotherapy

(Original Research)

Sergio Fabris, David A. MacLean

[Submitted to *Journal of Cachexia, Sarcopenia and Muscle*]

Contributions: Experiments where conceived, designed and conducted by Sergio Fabris. Sergio Fabris performed the analysis of the data and wrote the manuscript.

11.1 Abstract

Skeletal muscle (SM) health and integrity is dependent on the dynamic balance between protein synthesis and degradation, central to this process is the availability of amino acids (AA) in the free amino pool. Doxorubicin (DOX) remains one of the most widely used chemotherapeutic agents for the treatment of solid tumors and hematological malignancies. While its clinical use is constrained by a well-documented cardiotoxic side effect, little is known of the effect of the drug on SM. The purpose of the study was to examine the effect of DOX administration on intracellular, interstitial and vascular concentrations of AA in SM of the rat up to 8 days after the administration of a 1.5 or 4.5 mg/kg i.p. dose. Intracellular total amino acids (TAA), essential amino acids (EAA) and branched-chain amino acids (BCAA) where significantly increased in each muscle group analyzed, following the 1.5 and 4.5 mg/kg doses compared to control. In the plasma, TAA were significantly increased compared to control where greater ($P>0.05$) concentrations were observed following the 1.5 mg/kg dose compared to the 4.5 mg/kg dose. Compared to control, the 1.5 mg/kg dose resulted in an increase ($P<0.05$) in interstitial TAA whereas the 4.5 mg/kg resulted in a sustained decrease ($P<0.05$). This study provides important insight into the amino acid response following DOX chemotherapy and presents a substantial foundation for future studies focused on reducing (SM) damage and recovery by targeting amino acid metabolism.

11.2 Introduction

Skeletal muscle represents the largest organ in the human body, composing ~40% of the total body weight and in addition to its mechanical function, skeletal muscle plays a key role in whole body metabolism (Felig, 1973; Wolfe, 2006). Muscle mass is dependent on the dynamic balance between protein synthesis and degradation, and central to this process is the availability of amino acids in the free amino acid pool. In the human body, approximately 130 gms of free amino acids are present in the skeletal muscle intracellular space (Wagenmakers, 1998) and, in addition to its role in muscle protein turnover, amino acids participate in numerous metabolic reactions that take place in tissues throughout the body. Perturbation in the dynamic balance between protein synthesis and degradation where net protein breakdown is greater than that of synthesis in skeletal muscle can result in a cachectic, or muscle wasting, condition.

Cachexia is a serious, life-threatening condition associated with several pathologies including cancer (Esper & Harb, 2005; K. C. Fearon et al., 2012; Porporato, 2016). Cancer cachexia affects 50-80% of cancer patients and accounts for approximately 20% of cancer-related deaths (Argiles et al., 2014; Tisdale, 2002). Cachectic patients with greater than 15% weight loss exhibit impaired physiological function and a drastic reduction in quality of life. Patient death normally occurs when weight loss exceeds 30% (Tisdale, 2002). Additionally, cachectic patients are less tolerant to chemotherapy, radiation therapy and the response to these therapeutic strategies are significantly reduced (K. C. Fearon & Baracos, 2010; Vaughan et al., 2013). The use of anti-cancer chemotherapeutics such as that of Doxorubicin may play a role in the onset of cachexia in cancer patients undergoing chemotherapy.

Doxorubicin (DOX) remains one of the most widely used chemotherapeutic agents for the treatment of solid tumors and hematological malignancies (Weiss, 1992). DOX induced cytotoxicity has been attributed to DNA intercalation, inhibition of topoisomerase II (TOP2A) and the formation of reactive oxygen species (Minotti et al., 2004; Momparler et al., 1976; S. Wang et al., 2004). The clinical use of DOX is constrained by a well described dose-dependent and cumulative cardiotoxic side effect leading to the development of congestive heart failure (Lefrak et al., 1973; Singal & Iliskovic, 1998). DOX-related cardiotoxicity has been shown to be mediated by its primary circulating metabolite, Doxorubicinol (DOXol).

Recent research conducted in our laboratory has quantified the previously unreported sequestering of DOX and DOXol in skeletal muscle and described the relationship between the muscular, interstitial and vascular compartments following the administration of DOX (Fabris & MacLean, 2015). In skeletal muscle, the interstitial space represents an important active compartment located between the vasculature and the tissue and it has been shown to play a functional role in the regulation and integration of various metabolic substances. The microdialysis technique, first described by Delgado *et al.* (Delgado et al., 1972), provides a unique opportunity to quantify the availability of amino acids in this compartment *in vivo*.

The importance of skeletal muscle health and integrity on the positive prognosis and quality of life of a cancer patient is well known however the effect of chemotherapy on skeletal muscle has been relatively overlooked. Therefore, the purpose of the present study was to examine the effects of DOX administration on the intramuscular, interstitial

and vascular concentrations of amino acids in an effort to delineate the effects of DOX on protein turnover.

11.3 Materials and Methods

11.3.1 *Animals*

The experimental procedures performed in this study were approved by the Laurentian University Animal Care Committee. Male Sprague-Dawley rats (n=106, 434±60 gms) were obtained from Charles River Laboratories (Senneville, QC) and were housed and fed a 22/5 rodent diet (Envigo, WI, USA) according to Standard Operating Procedures and Policies for the Housing and Environmental Enrichment of Rodents at the Laurentian University Animal Care Facility. Experiments began following a one-week acclimation period.

11.3.2 *Pre-experimental procedures*

Experimental groups. The rats were placed into an induction chamber and anaesthetized with an EZ-150 vaporizer unit (EZ-Anesthesia, Euthanex Corporation, Palmer, PA), which blends oxygen (100% O_2 Praxair, Sudbury, ON) and isoflurane at a rate of 5 %. Once anaesthetized, the rats were removed from the chamber and placed onto a heated pad where nosepieces supplied a continuous delivery of oxygen and isoflurane (2-2.5 %). While under anaesthesia, the rats were injected intraperitoneally (i.p.) with Doxorubicin (Doxorubicin Hydrochloride. Pfizer, Canada) at a dose of 1.5 mg/kg (Groups 1 to 8) or 4.5 mg/kg (Groups 9 to 16). The administration of DOX followed an approved

injections SOP for Laurentian University. A sham injection of saline solution was administered to a control group (i.p., n=10). Once administered, rats were randomly grouped into experimental endpoints (n=6) of 24, 48, 72, 96, 120, 144, 168 or 192 hrs. post-injection (Figure 1a).

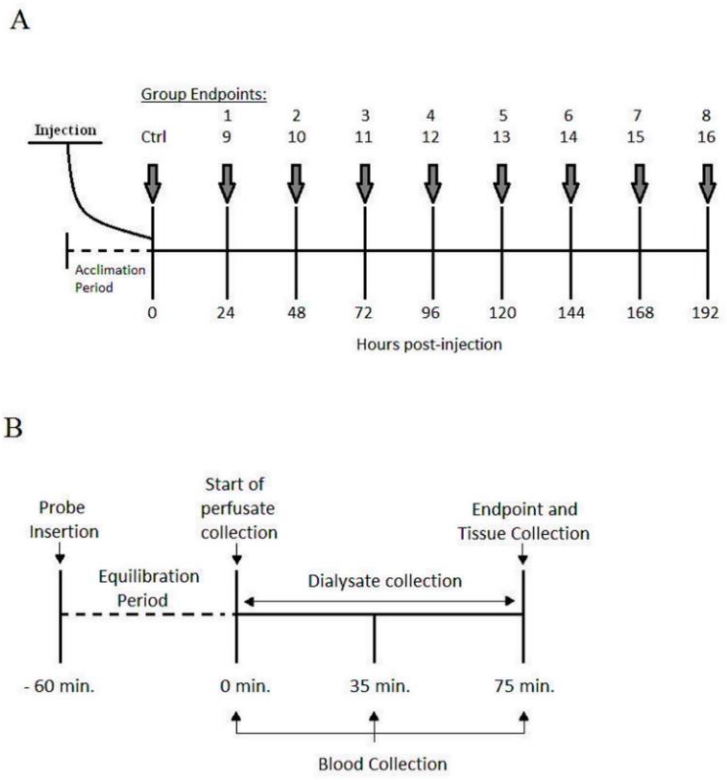

Figure 1. Schematic representation of the experimental groups and experimental procedures. (A) Representation of the experimental groups receiving an injection of 1.5 mg/kg dose (groups 1-8) or 4.5 mg/kg (groups 9-16) of DOX administered i.p. A sham injection is administered to the control group (Ctrl). (B) Representation of the experimental proceedings for dialysate, blood and tissue collection following microdialysis probe insertion and carotid artery cannulation.

Microdialysis probes. A complete description of the construction of the microdialysis probes has previously been outlined (MacLean, LaNoue, Gray, & Sinoway, 1998). Briefly, microdialysis fibers were constructed using Spectra Microdialysis fibers (Spectrum, VWR International) with a molecular cutoff of 13 kDa and Polyamide-100II

tubing (MicroLumen, Tampa FL) cut to 9.5 and 5 cm lengths. The ends of the fiber were inserted 1 cm into the hollow polyamide tube and glued. The exposed portion of the fiber (diffusible) between the polyamide tubes measured 1.0 cm in length.

11.3.3 *Experimental procedures*

Animals. On the day of the experiments, the rats were placed into an induction chamber and anaesthetized as described above. The animals remained under anaesthesia throughout the experiment and the plane of anaesthesia was routinely checked by toe pinches. Heart rate and oxygen saturation were monitored throughout the experiment using a pulse oximeter (SurgiVet) attached to the base of the tail. Body temperature (between 36–37ºC) was maintained using a heated surgical bed (EZ-Anaesthesia) and a heating lamp. Following the completion of the experiment, the animals were euthanized by decapitation.

Probe insertion. Using curved dissecting scissors, incisions were made at the base of the leg and the skin was manually pulled back until the entire leg was exposed, the excess skin was then removed. A 21 gauge curved cannula was inserted anteriorly into the muscle along the muscle's natural fibre orientation and acted as a guide for the microdialysis probe. Once the cannula was in place, the 9.5 cm portion of the probe is inserted caudally through the cannula and extended past the foot. As soon as the diffusible portion of the probe was oriented into the muscle, then the 5 cm portion of the probe was held in place while the cannula was retracted out of the tissue leaving the probe in place.

Experimental protocol. Four microdialysis probes were inserted into a single hind limb for this experiment, two in the lateral gastrocnemius and two in the medial

gastrocnemius muscle (n=4 probes per animal). Following probe insertion, the fibers were perfused (model 102, CMA) at a rate of 3 μL/min with Ringer's solution. It is recognized that probe insertion results in some cellular disruption therefore traditionally a 60 min. equilibration period prior to the initiation of the experiment was used to insure that the external environment surrounding the probes had stabilized and all cellular damage had dissipated (MacLean et al., 2001). Subsequently, the skin and tissue covering the left carotid artery was removed. A 20 gauge cannula was inserted into the exposed artery and sutured in place. Heparinized saline (100 μL) was injected into the artery to maintain patency in preparation for blood sampling.

Following the equilibration period, the experimental protocol was initiated (Figure 1b) where dialysate was collected for a period of 75 minutes in order to obtain sufficient volume that was required for analysis. Dialysate samples were collected in microcentrifuge tubes and immediately sealed to prevent evaporation and stored at -80ºC until analysis. Arterial blood samples were collected during the collection of dialysate at 0, 35 and 75 minutes. Samples were spun at 15,000 rpm for 25 seconds, plasma was separated and stored at -80°C until analysis. Upon completion of dialysate and blood collection the plantaris (PL), soleus (SOL), medial gastrocnemius (WG) and muscles from the contralateral leg used for microdialysis were excised, inserted into cryogenic vials, flash frozen in liquid nitrogen and stored at -80ºC until analysis.

11.3.4 *Sample analysis*

Skeletal Muscle. Frozen muscle samples were placed in a freeze drier (Freeze Drier 4.5, Labconco) at 10 microns Hg for 24 hrs. Subsequently, samples were powdered and

tweezed free of all visible connective tissue. Two mg of freeze dried skeletal muscle were added to 100 µL purified water (EMD Millipore, USA) containing L-Norleucine (Sigma-Aldrich, USA) as internal standard then homogenized for 30 sec. using a Kontes Pellet Grinder. The homogenate was then transferred into a centrifugal filtering tube (EMD Millipore, USA) and centrifuged at 15 000 r.p.m. for 20 min. 20 µL of the filtrate was added to 60 µL borate buffer and 20 µL fluor reagent (AccQ-Tag, Waters Canada) and vortexed immediately for 30 sec. Samples were placed on a heating block at 55ºC for 10 min. before analysis.

Plasma. Plasma samples were transferred into a centrifugal filtering tubes (EMD Millipore, USA) and centrifuged at 15 000 r.p.m. for 20 min. 20 µL of the filtrate was added to 60 µL borate buffer and 20 µL fluor reagent (AccQ-Tag, Waters Canada) and vortexed immediately for 30 sec. Samples were placed on a heating block at 55ºC for 10 min. before analysis.

Dialysate. The collected dialysate samples represent an ultra-clean filtrate and did not require any pre-analysis preparation. As such, 20 µL of dialysate was added directly to 60 µL borate buffer and 20 µL fluor reagent (AccQ-Tag, Waters Canada) and vortexed immediately for 30 sec. Samples were placed on a heating block at 55ºC for 10 min. before analysis.

Amino Acid Quantification. Amino Acid concentrations were determined by HPLC (Waters e2695, 2475 Fluorescence Detector, Waters Corporation) using AccQ-Tag Amino Acid Analysis kits (Waters, Canada). Derivatized standards include aspartate, serine, glutamate, glycine, histidine, ammonia, arginine, threonine, alanine, proline, cysteine,

tyrosine, valine, methionine, lysine, isoleucine, leucine and phenylalanine. Quantification of amino acids were determined by comparison with a standard curve and skeletal muscle amino acids where corrected by internal standard.

Statistics. Changes in amino acid concentrations between time points and doses were analyzed using a two-way ANOVA. When significant differences were indicated, a Tukey's *post hoc* test was used to determine where the significance occurred. Significance was accepted at $P<0.05$. All tabled values and values used in graphical representations are displayed as mean ± SEM.

11.4 Results

Since the direction of all the individual amino acids following the administration of DOX are similar, changes in the amino acid pool will be described via changes in total amino acids. essential amino acids and branched-chain amino acids. The total amino acids (TAA) include Asp, Ser, Glu, Gly, His, Arg, Thr, Ala, Pro, Cys, Tyr, Val, Met, Lys, Iso, Leu and Phe. The essential amino acids (EAA) in the rat are His, Arg, Thr, Val, Met, Lys, Iso, Leu, Phe and branched-chain amino acids (BCAA) are Val, Iso and Leu. It must be noted that Phe could not be quantified in the intramuscular samples due analytical limitations. Additionally, intramuscular and interstitial Arg data has previously been published (Fabris & MacLean, 2016).

The administration of the 1.5 and 4.5 mg/kg DOX resulted in a dose-related difference in arterial plasma amino acid concentrations (Table 1). Circulating arterial concentrations of TAA (Figure 2) and EAA were increased ($P<0.05$) as a result of either

administered dose compared to control however the increase in both the TAA and EAA were greater ($P<0.05$) following the 1.5 mg/kg dose compared to the 4.5 mg/kg dose. Circulating BCAA concentrations were significantly increased following the administration of both 1.5 and 4.5 mg/kg dose compared to control and were further elevated ($P<0.05$) at 96 hrs in the 4.5 mg/kg treatment group compared to the 1.5 mg/kg group. Although Ser, Cys, and Lys were increased ($P<0.05$) compared to control, their concentrations were not significantly different when compared between administered doses. Additionally, there were no changes in ammonia throughout the experiment following either administered dose.

The administration of DOX resulted in a dose-related difference in interstitial amino acids (Table 2). The 1.5 mg/kg dose resulted in a transient increase ($P<0.05$) in TAA (Figure 2), EAA and BCAA as well as ammonia from 24-96 hrs compared to control. However Cys, Lys and Leu decreased ($P<0.05$) to concentrations lower than control after 96 hrs. TAA, EAA, BCAA and ammonia decreased ($P<0.05$) 24-192 hours following the administration of 4.5 mg/kg DOX as compared to control. Ser and Glu concentrations were increased ($P<0.05$) compared to control and Met was not significantly affected.

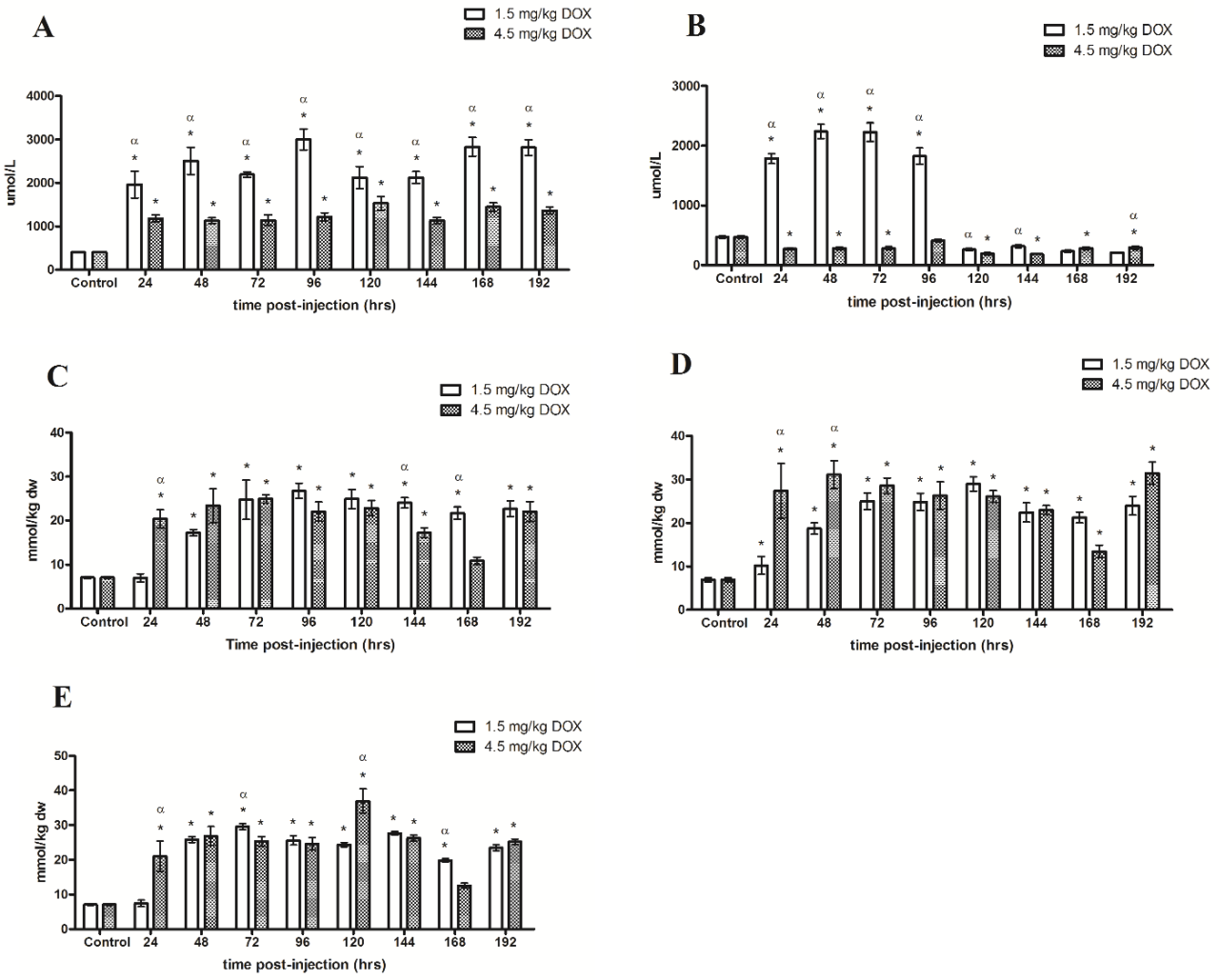

Figure 2: Total amino acid concentrations in the (A) Plasma, (B) Dialysate, (C) White gastrocnemius, (D) Plantaris and (E) Soleus following the i.p. administration of 1.5 mg/kg DOX or 4.5 mg/kg DOX. * Denotes significance compared to control. α Denotes difference ($P<0.05$) between administered doses.

In the WG (Table 3), the administration of 1.5 and 4.5 mg/kg DOX increased ($P<0.05$) TAA (Figure 2) and EAA concentrations. BCAA were significantly increased from 48-192 hrs following the 1.5 mg/kg dose whereas the 4.5 mg/kg dose increased ($P<0.05$) BCAA 48-120 hrs compared to control (Figure 3). Following the 1.5 mg/kg dose, Cys significantly decreased compared to control and was undetectable after 72 hrs.

Concentrations of Asp, Ser, Ala, Pro, Iso and Leu where greater after the 1.5 mg/kg dose compared to the 4.5 mg/kg dose and ammonia was unaffected in both treatment groups.

TAA (Figure 2) and EAA concentrations were significantly increased in the PL (Table 4) as a result of both doses as compared to control. BCAA increased ($P<0.05$) from 48-192 hrs and 24-120 hrs following the administration of 1.5 and 4.5 mg/kg DOX compared to control, respectively (Figure 3). Ser increased ($P<0.05$) whereas Cys decreased ($P<0.05$) following the 1.5 mg/kg dose. Significant increases in Ser, Pro, Val, Lys, Iso and Leu were observed following the 4.5 mg/kg dose compared to control. His, ala, Pro, Val, Lys, Iso and Leu concentrations were more elevated ($P<0.05$) in the 1.5 mg/kg compared to 4.5 mg/kg treatment groups however Cys was significantly more elevated in the 4.5 mg/kg dose group. Ammonia was unaffected throughout the experiment.

SOL (Table 5) TAA (Figure 2) and EAA concentrations were significantly increased as a result of both administered doses of DOX. Intramuscular BCAA concentrations where increased ($P<0.05$) after 48 hrs following the administrations of the 1.5 m/kg dose compared to control and remained elevated for the remainder of the experiments. BCAA were increased ($P<0.05$) 24-144 hrs following the administration of 4.5 mg/kg DOX compared to control (Figure 3). The 4.5 mgs/kg dose of DOX resulted in a transient increase ($P<0.05$) in Asp, Gly, His, Lys, Iso and Leu compared to control and subsequently returned to baseline. Asp, Gly, His, Lys, Iso and Leu concentrations were higher following the 1.5 mg/kg compared to the 4.5 mg/kg dose of DOX. No significant changes in concentrations of ammonia were observed.

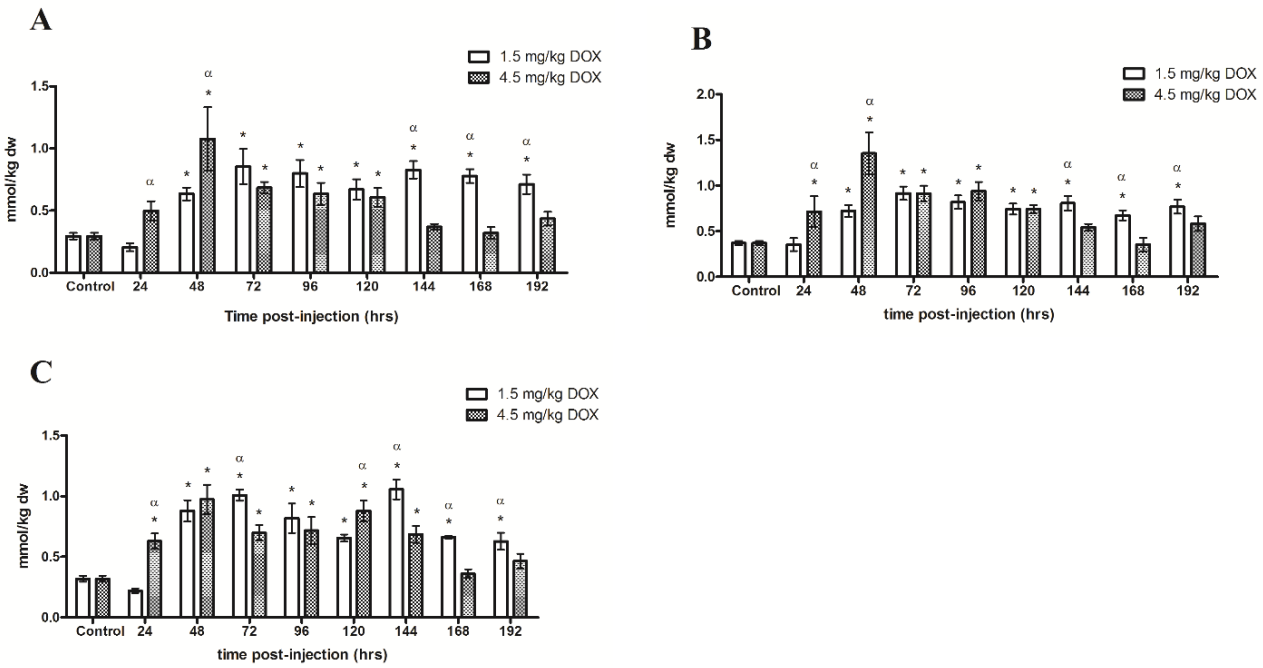

Figure 3: Total intracellular concentrations of branched-chain amino acids (Val, Iso and Leu) in the (A) White gastrocnemius, (B) Plantaris and (C) Soleus following the i.p. administration of 1.5 mg/kg DOX or 4.5 mg/kg DOX. * Denotes significance compared to control. α Denotes difference ($P<0.05$) between administered doses.

11.5 Discussion and Conclusion

The purpose of the current study was to examine the effects of DOX administration on amino acid concentrations in skeletal muscle, the interstitial space and the vasculature. The major findings were an observed increase in intramuscular TAA, EAA and BCAA concentrations, strongly suggesting that the administration of DOX resulted in a net increase in protein degradation. In addition, a dose-related difference was observed in the circulating concentration of amino acids where a greater increase was established following the administration of the 1.5 mg/kg dose of DOX compared to the 4.5 mg/kg dose. The current study provides novel insights into the response of amino acids in skeletal muscle

and their subsequent concentrations in communicating compartments through the insterstitial space and into the circulation following the administration of DOX.

The net change in amino acids in the tissue is indicative of the balance between synthesis or degradation state of proteins in the muscle. The persistent three-fold increase in total intramuscular amino acids observed in the current study as a result of either administered dose of DOX strongly suggests that the rate of protein degradation was greater than that of protein synthesis. This is further substantiated by a similar increase in intramuscular EAA concentrations as a result of either dose of drug administered. *De novo* synthesis of EAA in the muscle is not possible and changes in intramuscular concentrations must come from the exchange with the vasculature or from the endogenous breakdown of protein within the tissue (T.E. Graham, 1995). Of the EAA, the branched-chain amino acids (BCAA) Val, Iso and Leu are the dominant essential amino acids oxidized in skeletal muscle. Therefore, any change in BCAA concentrations will most likely indicate a change in overall protein balance within the tissue.

The metabolic effects of BCAAs in skeletal muscle, which range from nitrogen homeostasis to energy production and protein synthesis, are well described (Brosnan & Brosnan, 2006; Cole, 2015; T.E. Graham, 1995; MacLean et al., 1994). In the current study, both the 1.5 and 4.5 mg/kg doses of DOX resulted in an increase in the intramuscular BCAA concentrations. The mitochondrial branched-chain amino acid aminotransferase (BCAT) isoenzyme is primarily repsonbile for initiating BCAA catabolism (T. R. Hall et al., 1993). The activity of the BCAT which transfers an amino group from BCAA to α-ketoglutarate to form branched-chain ketoacids (BCKA) and Glu, responds rapidly to increases in intramuscular BCAA concentrations (Milan, 2011). The increase in Glu

synthesis is indicative of BCAT activity and formation of BCKAs. BCKA undergo irreversible oxidative decarboxylation by activated BCKA dehydrogenase complex (BCKAD) completing the the metabolism of leu (acetoacetate, acetyl-CoA), iso (propionyl-CoA, acetyl-CoA) and val (succinyl-CoA) for use in the TCA cycle (Cole, 2015).

The administration of 1.5 mg/kg DOX resulted in a substantial increase in BCAA in each muscle group whereas a transient increase was observed following the 4.5 mg/kg dose depending on the muscle group. The underlying mecahnisms responsible for the dose-related effect observed remains unclear. However, there is strong evidence to suggest that the increase in intramuscular BCAA is not due to a reduction in the rate of transamination by BCAT, which is not regulated by end-product inhibition or phosphorylation-dependent activation of inactivation mechanisms. This is made evident by the increase in Glu and Ala synthesis observed throughout the study.

In skeletal muscle, Glu is the key metabolic precursor for the synthesis of Ala and Gln via Ala aminotransferase and Gln synthase, respectively (T. E. Graham, Sgro, Friars, & Gibala, 2000). Ammonia detoxification in the muscle involves the safe transport of amino nitrogen, by Ala and Gln, to the liver for conversion to urea and subsequent excretion through the kidneys. Ala was increased in both the muscle and in the circulation which is consistent with previous research demonstrating the oxidation and release of Ala with enhanced supply of BCAA (Ruderman & Berger, 1974). Due to analytical limitations, Gln concentrations could not be determined, however no consistent changes in circulating or intracellular ammonia were observed irrespective of the administered dose suggesting that

the ammonia load was sufficiently managed via the increase in other disposal patways thus maitaining nitrogen homeostasis.

The anabolic effect of BCAAs on protein metabolism is well established. The mamalian target of rapamycin (mTOR) is a highly conserved serine-threonien kinase comprised of two disctinct mutiprotein complexes mTORC1 and mTORC2 (Catania et al., 2011; M. N. Hall, 2008). The mTORC1 complex includes mTOR, Raptor, Deptor, PRAS40 and mLST8/GβL. Intramuscular amino acid availability increases levels of Ca^{2+} which activates mTORC1 signaling via ca^{2+}/calmodulin-mediate actiavtion of PI3K (Gulati et al., 2008; Nobukuni et al., 2005). The potent BCAA-mediated stimulation of protein synthesis has been primarily attributed to the Leu regulated activation of mTORC1 by inducing the interaction of Ras-related GTP-binding protein (Rag) with ras-homolog enriched in the brain (Rheb) (Kimball & Jefferson, 2006; Norton & Layman, 2006). Recently, it has been reported that DOX causes insulin resistance mediated by AMPk inhibition (de Lima Junior et al., 2016). Additionally, it has been shown that Leu activation of mTOR is partially dependant on insulin (Kimball & Jefferson, 2006). Taken together, it is possible that mTOR activity is stunted by the sum of these effects resulting in a decrease in protein synthesis.

Collectively, the current study shows that the administration of DOX did not affect BCAA availability and has increased intramuscular BCAA concentrations. The subsequent increases in Glu and Ala indicate that the enzymatic metabolism of BCAA has not been affected. Furthermore, it is clear that the possible reduction in mTOR activity does not fully account for the increase in TAA observed in this study and that proteolysis may play a more prominent role.

Since its first clinical trials, DOX has been lauded as a highly effective anti-cancer chemotherapeutic. The fundamental concern with DOX chemotherapy, as is with most chemotherapeutic agents, is the systemic distribution of the drug following its administration. Previous research from our laboratory has demonstrated that DOX and DOXol is sequestered and retained in skeletal muscle under the same experimetal conditions as those used in the current study (Fabris & MacLean, 2015). Once in the cell, DOX intercalates between DNA base pairs effectively disrupting cell replication. (Minotti et al., 2004; S. Wang et al., 2004). It is possible that the integration of the drug in DNA may equally cause disruption in the unfolding of DNA and utimately disturbing or inhibiting protein synthesis and significantly contributing to the increase in intramuscular amino acid concentrations. The effect of DOX on regulatory mechanisms responsible for the proper formation of proteins has been studied. Recent research by Narandrula *et al.* (Narendrula et al., 2016) have shown that DOX capably induced rRNA disruption in cultured cells, suggesting that the formation of ROS and production of TNFα are likely factors responsible for the degradation of rRNA. Additionally, White and colleagues (White-Gilbertson, Kurtz, & Voelkel-Johnson, 2009) have reported that DOX affects the phosphorylation of elongation factor 2 (EF-2), a key enzyme in the modulation of protein elongation during synthesis, and capably affects the rate of translation (Ryazanov & Davydova, 1989). Furthermore, Lu *et al*. (Lu et al., 2011) have reported that DOX inhibits glucose-regulated protein 78 (GRP78) leading to the inactivation of unfolded protein response (UPR) and subsequent proteolysis via protease activity. The proteolytic outcome of protease activation may be the primary factor responsible for the significant increase in intramuscular TAA observed in this study.

Overall, the present study demonstrates that the administration of DOX increased intramuscular concentrations of BCAA which is not attributed to a reduction in BCAT activity and that the effect of the drug on BCAA-mediated protein synthesis alone does not account for the significant increase in intramuscular TAA. Seemingly, the disruption of protein synthesis by direct and indirect effects of DOX influences the dynamic balance between protein degradation and synthesis to favor the former over the latter. The resulting net protein breakdown is supported by the three-fold increase in intramuscular TAA and EAA concentrations.

Plasma concentrations of amino acids are a balance between production and elimination. Without ingestion, the largest shift in plasma amino acid concentrations come from changes in skeletal muscle protein turnover. As discussed above, the rate of protein degradation was greater than that of protein sythesis resulting in an increase of intramuscular TAA following the administration of the drug. The significant increase plasma TAA, where greater concentrations were observed following the 1.5 mg/kg dose compared to the 4.5 mg/kg dose of DOX, strongly indicates that the efflux of amino acid concentrations from the intramuscular pool into circulation were greater than that of systemic uptake resulting in the observed increase of arterial TAA.

The diffusion of amino acids between the tissue and vascular compartment must pass through the interstitial space (ISS). The interstitial compartment plays a functional role in the regualtion and integration of various endogenously produced metabolic substances (Leuenberger et al., 2008; MacLean, Sinoway, et al., 1998). The current data demonstrate, for the first time, the effect of chemotherapy on interstitial amino acid concentrations. Fabris and MacLean (Fabris & MacLean, 2015) recently measured and

sicussed the presence of DOX in the interstital space. Interestingly, in the present study, an inverse relationship was observed between doses and the ISS concentrations of TAA. For example the 1.5 mg/kg dose of DOX resulted in a significant increase of TAA in the ISS compared to control whereas the 4.5 mg/kg dose resulted in a sustained decrease when compared to control. The increase in TAA concentrations followed by the eventual decline back to baseline is consistent with the rapid efflux of TAA out of the tissue and into the interstital compartment followed by a gradual uptake from the vasculature. The decrease of TAA in the ISS following the 4.5 mg/kg dose may be the result of secondary effects of the drug on trasporter proteins responsible for the flux of amino acids out of the tissue and into the ISS or from the ISS into the vasculature. The mediation of amino acid uptake and efflux from the myocyte is regulated by the expression of the several transporter proteins encoded by the SLC superfamily (Hyde, Taylor, & Hundal, 2003; Taylor, 2014). The difference between the 1.5 and 4.5 mg/kg dose may be the result of higher concentrations of DOX affecting the normal function of the transporter proteins. This is supported by our finding that lower concentrations of TAA were observed in the ISS and in the plasma as a result of the 4.5 mg/kg dose compared to the 1.5 mg/kg dose. No studies have been conducted that have shown that an increase in DOX interferes with the normal function of the various transporter proteins associated with amino acid transport in skeletal muscle. Additionally, the systemic effect of the 4.5 mg/kg dose on other tissues would help explain the lower increase of TAA in the plasma when compared to the 1.5 mg/kg dose. Therefore, in addition to a dose-related increase of plasma TAA, the study of the interstitial space by way of microdialysis has revealed a possible dose-related effect of DOX on amino acid transport mechanisms from skeletal muscle compartment into the vasculature.

This study describes for the first time the concurrent concentrations of amino acids in skeletal muscle, the interstitial space and the vascular compartment following the administration of an anti-cancer chemotherapeutic. Traditionally, the effects of DOX chemotherapy have been examined extensively on the heart and tumor with very little attention on skeletal muscle. The summation of restricted mTOR activity and upregulated proteolytic pathways are most likely responsible for the imbalance between protein synthesis and degradation, overwhelmingly favoring protein degradation. Depressed protein synthesis and loss of skeletal muscle mass this is a hallmark characteristic attributed to cachexia, a muscle wasting pathology and significant factor in the high mortality rate of cancer patients. This may have serious clinical implications where multiple doses of DOX chemotherapy administerered in a typical treatment regimen may accelerate the onset of cachexia and exacerbate the pathology. This study provides important insight into the possible mechanisms involved in the health and maintenance of skeletal muscle integrity following DOX chemotherapy and presents a substantial foundation for future studies focused on reducing skeletal muscle damage and recovery by targetting amino acid metabolism.

11.6 Acknowledgements

The authors wish to thank Dr. Pamela Chenard for her excelent technical assistance.

11.7 Tables

Table 1. Arterial plasma amino acid concentrations.

Amino Acids	Dose	Timepoint								
	(mg/kg)	ctrl	24	48	72	96	120	144	168	192
Asp	1.5	12.5±0.6	175±31*†	230±44*†	195±10*†	298±24*†	195±27*	183±10*†	255±25*†	252±19*†
	4.5	12.5±0.6	103±5*†	102±3*†	100±10*†	135±23*†	138±14*	107±5*†	140±12*†	140±7*†
Ser	1.5	2.5±0.3	52±12*	39±7†*	23±3	30±4*	26±5*	24±3	25±3*	31±3†*
	4.5	2.5±0.3	37±1*	15±1†*	18±4*	25±4*	20±1*	15±3*	20±3*	21±1†*
Glu	1.5	0.05±0.01	194±42†	354±83*†	311±30*†	505±80*†	249±35*†	261±24*†	454±79*†	389±41*†
	4.5	0.05±0.01	65±10*†	94±23*†	81±13*†	68±6*†	143±30*†	77±8*†	119±12*†	76±7*†
Gly	1.5	11.8±0.7	135±24*	171±37†*	154±23†*	217±16†*	127±23*	94±4	155±16†*	133±12†*
	4.5	11.8±0.7	87±7*	64±12†	76±12†*	106±27†*	84±13*	75±10*	69±10†*	80±11†*
His	1.5	9.4±0.6	211±30*†	263±24*†	237±6*†	313±24*†	235±31*†	256±36*†	306±27*†	287±20*†
	4.5	9.4±0.6	100±21*†	38±7†	92±12*†	134±11*†	148±16*†	121±5*†	144±10*†	48±6†
Arg	1.5	8.7±0.7	60±13*	82±8*†	67±4*†	87±9*†	63±9*	72±14*	79±17*	96±4*†
	4.5	8.7±0.7	36±2*	34±3*†	36±5*†	36±3*†	47±6*	48±5*	45±4*	44±5*†
Thr	1.5	15.2±0.7	268±38*	306±28†*	308±14*†	381±34*†	300±41*†	354±51*†	384±15*†	369±26*†
	4.5	15.2±0.7	185±10*	161±15†*	137±15*†	182±30*†	182±17*†	163±15*†	182±9*†	189±7*†

Ala	1.5	44.1±2.8	262±40*†	320±29*†	247±8*†	340±29*†	242±34*	256±16*†	311±21*†	345±28*†
	4.5	44.1±2.8	152±12*†	139±5*†	149±12*†	156±12*†	200±22*	171±8*†	189±12*†	223±19*†
Pro	1.5	9.3±0.6	102±16*†	109±11*†	98±5*†	131±13*†	88±11*	91±5*†	120±12*†	129±9*†
	4.5	9.3±0.6	58±3*†	51±3*†	50±5*†	54±4*†	65±6*	59±7*†	67±4*†	73±3*†
Cys	1.5	193.3±4.7	8±1*	14±1*	18±3*	8±2*	14±3*	15±3*	20±3†*	14±2*
	4.5	193.3±4.7	10±1*	14±2*	12±2*	9±3*	13±3*	10±1*	10±1†*	13±1*
Tyr	1.5	1.5±0.06	38±5*†	51±7*†	43±4*†	49±3*†	34±3*	45±9*†	49±6*†	56±4*†
	4.5	1.5±0.06	24±2*†	23±3*†	21±3*†	20±2*†	23±4*	17±2*†	23±2*†	22±1*†
Val	1.5	13.8±0.9	107±16*	133±20*	122±16*	174±25*†	115±17*	151±23*†	172±16*†	179±10*†
	4.5	13.8±0.9	76±5*	98±11*	79±13*	80±14*†	97±8*	71±4*†	103±5*†	104±4*†
Met	1.5	1.4±0.04	36±5*†	41±6*†	36±2*†	44±5*†	34±5*	37±5†*	45±4*†	46±2*†
	4.5	1.4±0.04	24±0.5*†	22±2*†	20±2*†	19±2*†	23±2*	18±2†*	23±1*†	23±1*†
Lys	1.5	33.2±2	127±14*	155±13*	152±10*	197±26†*	172±14*	180±21*	207±24*†	187±7*†
	4.5	33.2±2	102±11*	123±10*	124±17*	114±13†*	164±15*	143±7*	131±12*†	135±9*†
Iso	1.5	6.4±0.4	45±7	65±11*	60±10*	87±14†*	63±8*	79±15*†	91±10*†	93±7*†
	4.5	6.4±0.4	32±2*	50±6*	39±7*	37±7†*	49±5*	35±2*†	52±3*†	53±2*†
Leu	1.5	10.7±0.7	77±12*	109±20*	101±16*	142±22*†	106±14*	131±24*†	153±17*†	155±12*†
	4.5	10.7±0.7	56±4*	83±9*	67±13*	65±13*†	84±7*	60±4*†	86±4*†	87±5*†
Phe	1.5	1.4±0.05	32±4*†	35±3*†	35±2*†	42±4*†	32±4*†	35±4*†	44±4*†	43±2*†
	4.5	1.4±0.05	22±1*†	19±2*†	16±1*†	16±1*†	19±2*†	15±1*†	21±2*†	20±0.3*†

NH_3	1.5	33.1±1.4	34±8	31±4	26±2	38±6	25±2†	23±2	28±1	27±3
	4.5	33.1±1.4	30±3	25±2	24±2	26±2	32±2†	26±1	30±3	31±3
EAA	1.5	95±5	930±131*†	1154±107*†	1084±52*†	1346±108*†	1088±120*	1249±175*†	1372±75*†	1396±44*†
	4.5	95±5	605±40*†	608±52*†	593±77*†	660±80*†	795±72*	611±38*†	765±44*†	667±46*†
BCAA	1.5	30.9±2	229.6±34*†	307±51*	284±41*†	402±61*†	283±35*	361±62*†	416±42*†	427±29*†
	4.5	30.9±2	164±11*†	231±26*	185±33*†	181±34*†	231±20*	139±29*†	240±12*†	244±11*†

All values are means ± SEM. Concentrations represented in μM concentrations. * denotes significance compared to control. † denotes significance between doses.

Table 2. Interstitial amino acid concentrations

Amino Acids	Dose	Timepoint								
	(mg/kg)	ctrl	24	48	72	96	120	144	168	192
Asp	1.5	33±2	162±9*†	202±16*†	202±13*†	219±16*†	18±1†	20±1†	18±2	16±1
	4.5	33±2	18±1*†	19±1*†	23±2*†	39±2†	11±1*†	12±1*†	18±1*	18±2*
Ser	1.5	13±1	73±5*†	59±6*†	60±6*†	75±9*†	2±0.2†	2±0.2†	1±0.1†	2±0.2†
	4.5	13±1	3±0.4*†	7±1*†	7±1*†	6±1*†	21±3*†	13±1†	14±2†	10±1†
Glu	*1.5*	2±0	58±4*†	66±5*†	55±7*†	30±3*	21±2*†	22±2*†	16±2†	13±1
	4.5	2±0	12±1*†	16±1*†	22±2*†	39±4*	10±1*†	10±1*†	11±1*†	16±2*
Gly	1.5	46±3	145±8*†	152±11*†	133±9*†	132±9*†	24±1†	26±2†	22±2†	19±1†
	4.5	46±3	20±1*†	25±2*†	23±2*†	35±2*†	15±2*†	16±1*†	30±2*†	31±3*†
His	1.5	36±2	139±9*†	161±10*†	133±9*†	132±9*†	28±2†	30±2†	22±2†	19±1†
	4.5	36±2	20±1*†	25±2*†	23±2*†	35±2†	20±2*†	20±1*†	30±2†	30±3†
Arg	1.5	47±3	147±7*†	171±10*†	202±15*†	156±13*†	54±3†	63±5†	43±3†	36±3
	4.5	47±3	44±2†	44±4†	47±6†	61±4†	29±3*†	31±2*†	32±4†	34±4
Thr	1.5	29±2	120±13*†	171±10*†	38±5†	19±3†	22±2†	25±2†	14±4	20±2
	4.5	29±2	4±1*†	3±0.5*†	11±1*†	7±1*†	14±2*†	8±1*†	22±3	21±2
Ala	1.5	64±4	332±19*†	444±31*†	454±42*†	398±34*†	31±2†	42±3†	29±3†	27±2†
	4.5	64±4	37±3*†	40±3*†	36±3*†	67±5†	17±2*†	24±2*†	35±3*†	47±7*†

Pro	1.5	24±1	71±4*†	80±5*†	89±7*†	82±7*†	8±0.5†	11±1†	9±1	9±1
	4.5	24±1	10±1*†	12±1*†	10±1*†	17±1*†	5±1*†	6±0.4*†	9±1*	10±1*
Cys	1.5	8±1	24±1*†	27±2*†	28±2*†	20±2*†	3±0.1*†	3±0.2*†	2±0.2*†	2±0.1*†
	4.5	8±1	3±0.2*†	3±0.2*†	3±0.4*†	4±0.4*†	2±0.3*†	2±0.1*†	5±0.4*†	5±0.5*†
Tyr	1.5	4±0	16±1*†	15±1*†	14±1*†	13±1*†	2±0.1†	3±0.2†	2±0.2	2±0.1
	4.5	4±0	3±0.1*†	3±0.3*†	3±0.2*†	4±0.3†	1±0.2*†	2±0.1*†	2±0.3*	2±0.2*
Val	1.5	27±1	75±3*†	103±8*†	126±10*†	102±11*†	11±1†	14±1†	12±1	11±1
	4.5	27±1	22±1†	17±1*†	16±2*†	19±1*†	8±1*†	8±0.4*†	12±1*	12±1*
Met	1.5	3±0	21±1*†	20±1*†	21±2*†	19±2*†	3±0.1†	3±0.2†	2±0.2	2±0.1
	4.5	3±0	3±0.2†	3±0.2†	3±0.3†	4±0.3†	1±0.2*†	1±0.1*†	3±0.2	2±0.2
Lys	1.5	66±2	158±9*†	227±14*†	273±24*†	222±18*†	15±1*†	16±1†	16±2	12±1*†
	4.5	66±2	24±2*†	19±2*†	222±2*†	30±2*†	12±1*†	13±1*†	17±1*	17±2*†
Iso	1.5	11±1	25±1*†	43±4*†	52±5*†	37±5*†	5±0.3†	6±1†	6±0.5	5±0.3
	4.5	11±1	10±1†	6±0.4*†	7±1*†	8±1*†	3±0.5*†	4±0.2*†	6±1*	6±1*
Leu	1.5	19±1	51±2*	79±7*	94±8*	66±7*†	9±0.5*	11±1*†	10±1*†	9±1*†
	4.5	19±1	17±1*	11±1*	12±2*	14±1*†	6±1*	6±0.3*†	12±1*†	10±1*†
Phe	1.5	3±0	11±1*†	9±0.5*†	10±1*†	8±1*†	3±0.2†	3±0.2†	2±0.2	2±0.1
	4.5	3±0	2±0.2*†	3±0.2†	3±0.2*†	3±0.2†	2±0.2*†	1±0.1*†	2±0.2*	2±0.2*
NH_3	1.5	36±3	156±9*†	215±11*†	254±17*†	107±8*†	22±1†	22±1†	16±1†	13±1†
	4.5	36±3	22±4*†	26±1*†	19±1*†	26±1*†	15±1*†	15±1*†	28±1*†	23±2*†

EAA	1.5	195±8	601±35*†	812±45*†	738±55*†	593±47*†	87.1±5.6†	106±8†	75.1±7.8	72.3±3.5†
	4.5	195±8	100±5*†	87.4±5.8*†	92.8±8.3*†	117±6*†	64.5±7.8*†	55.9±4*†	100±9*	93.7±9.5*†
BCAA	1.5	57.3±2.6	151±7*†	225±18*†	272±23*†	204±24*†	24±1.4†	40±2.8†	26.7±2.6	24.7±1.4
	4.5	57.3±2.6	48.3±2.8†	34.3±2.2*†	34.9±4.6*†	40.1±2.7*†	17.2±2.2*†	17.3±0.9*†	30.6±3.2*	28.1±2.7*

All values are means ± SEM. Concentrations represented in μM concentrations. * denotes significance compared to control. † denotes significance between doses.

Table 3. Intracellular amino acids in the medial gastrocnemius.

Amino Acids	Dose	Time post-injection (in hours)								
	(mg/kg)	ctrl	24	48	72	96	120	144	168	192
Asp	1.5	0.19±0.01	0.28±0.05	0.63±0.09*	0.78±0.2*	0.99±0.05*†	0.67±0.1*†	0.71±0.1*†	0.64±0.08*†	0.53±0.05
	4.5	0.19±0.01	0.43±0.07	0.64±0.13*	0.65±0.06*	0.71±0.07*†	0.68±0.09*†	0.38±0.03†	0.28±0.04†	0.4±0.05
Ser	1.5	0.35±0.04	0.33±0.05	0.82±0.18	0.73±0.07	0.69±0.04	0.55±0.10	1.16±0.35*†	0.44±0.03†	0.86±0.18
	4.5	0.35±0.04	0.56±0.11	0.77±0.21*	0.53±0.05	0.57±0.05	0.37±0.09	0.29±0.05†	0.29±0.04†	0.57±0.08
Glu	1.5	0.03±0.01	0.15±0.02†	0.27±0.04*	0.45±0.10*	0.47±0.04*	0.46±0.03*	0.47±0.08*	0.38±0.05*†	0.37±0.05*
	4.5	0.03±0.01	0.32±0.05†	0.29±0.05	0.47±0.07*	0.55±0.1*	0.86±0.19*	0.43±0.05*	0.21±0.02†	0.45±0.04*
Gly	1.5	0.68±0.04	0.47±0.11†	1.65±0.41	2.22±0.62*	2.96±0.15*†	1.87±0.3*	1.8±0.29	1.63±0.24†	1.82±0.18
	4.5	0.68±0.04	1.66±0.3*†	1.64±0.31*	2.07±0.23*	2.23±0.24*†	2.07±0.25*	1.24±0.08	0.52±0.06†	1.8±0.22*
His	1.5	0.21±0.01	0.48±0.08†	1.28±0.26*	1.19±0.20*	1.56±0.12*	1.44±0.29*	1.48±0.27*	1.11±0.17*†	1.0±0.98*†
	4.5	0.21±0.01	0.79±0.1†	1.69±0.63*	1.17±0.1	1.4±0.17*	1.43±0.23*	0.93±0.05	0.61±0.12†	1.53±0.19*†
Thr	1.5	0.92±0.02	1.03±0.17†	2.76±0.63	3.82±0.57*	3.84±0.18*	5.33±0.95*	4.40±0.47*	4.11±0.64*†	4.98±0.49*
	4.5	0.92±0.02	3.35±0.32*†	4.65±0.93*	4.59±0.92*	3.79±0.46*	5.73±0.5*	4.08±0.47*	2.16±0.31†	4.59±0.57*
Ala	1.5	0.72±0.06	0.9±0.12†	1.6±0.16	2.08±0.57*	2.54±0.19*†	1.28±0.19	1.54±0.14†	1.28±0.17†	1.42±0.21
	4.5	0.72±0.06	1.81±0.29*†	2.2±0.51*	1.65±0.34	1.47±0.12†	1.49±0.22	0.76±0.07†	0.65±0.1†	1.06±0.07
Pro	1.5	0.11±0.01	0.08±0.01†	0.18±0.02	0.25±0.06*	0.27±0.02*	0.2±0.01	0.23±0.02*†	0.2±0.02†	0.18±0.02†
	4.5	0.11±0.01	0.18±0.03†	0.23±0.05*	0.26±0.01*	0.22±0.03*	0.22±0.04*	0.11±0.002†	0.08±0.01†	0.11±0.02†

Cys	1.5	0.47±0.02	0.02±0.001*†	0.04±0.004*†	n/d	n/d	n/d	n/d	n/d	n/d
	4.5	0.47±0.02	0.92±0.14*†	0.67±0.08†	0.38±0.09	n/d	n/d	n/d	n/d	n/d
Tyr	1.5	0.03±0.002	n/d	0.06±0.01†	0.11±0.03*	0.11±0.01*	0.09±0.003*	0.09±0.01*†	0.07±0.01*†	0.09±0.01*
	4.5	0.03±0.002	n/d	0.17±0.04*†	0.08±0.01	0.1±0.02	0.14±0.02*	0.06±0.01†	0.05±0.01†	0.1±0.01
Val	1.5	0.12±0.01	0.09±0.01†	0.26±0.03*	0.34±0.06*	0.33±0.05*	0.28±0.03*	0.34±0.03*†	0.31±0.03*†	0.29±0.03*
	4.5	0.12±0.01	0.2±0.03†	0.42±0.1*	0.29±0.02*	0.26±0.03	0.29±0.02*	0.16±0.01†	0.13±0.02†	0.2±0.03
Met	1.5	0.03±0.002	0.04±0.001†	0.07±0.01†	0.11±0.03*	0.1±0.01*	0.08±0.01*†	0.09±0.002*†	0.08±0.01*†	0.08±0.01*†
	4.5	0.03±0.002	0.07±0.01†	0.2±0.04*†	0.1±0.01*	0.1±0.02*	0.11±0.01*†	0.05±0.003†	0.04±0.01†	0.05±0.01†
Lys	1.5	0.42±0.04	0.27±0.03†	1.39±0.21*	0.94±0.42	1.51±0.21*	1.06±0.08	1.25±0.1*†	1.32±0.15*†	0.8±0.13
	4.5	0.42±0.04	0.72±0.13†	1.01±0.3	2.22±0.38*	1.21±0.26*	1.0±0.21	0.43±0.04†	0.35±0.01†	0.85±0.09
Iso	1.5	0.06±0.01	0.05±0.01†	0.14±0.01*	0.18±0.03*	0.16±0.03*	0.14±0.02*	0.18±0.02*†	0.16±0.01*†	0.15±0.02*†
	4.5	0.06±0.01	0.1±0.02†	0.24±0.06*	0.15±0.01	0.14±0.02	0.17±0.02*	0.08±0.01†	0.07±0.01†	0.08±0.01†
Leu	1.5	0.14±0.01	0.09±0.01†	0.24±0.02	0.33±0.06*	0.3±0.04*	0.26±0.04	0.31±0.03*†	0.3±0.02*†	0.27±0.03†
	4.5	0.14±0.01	0.2±0.03†	0.42±0.1*	0.25±0.02	0.23±0.04	0.23±0.02	0.13±0.01†	0.12±0.02†	0.16±0.03†
NH_3	1.5	1.29±0.11	0.35±0.02†	0.71±0.1	2.03±0.78	2.23±0.34†	1.42±0.23†	1.35±0.15†	1.55±0.23†	0.98±0.16
	4.5	1.29±0.11	1.41±0.19†	1.26±0.26	1.21±0.06	0.86±0.09†	0.77±0.09†	0.61±0.04*†	0.83±0.11†	1.19±0.18
EAA	1.5	3.14±0.15	4.58±0.8†	11.5±1.4*	16.1±2.3*	17.1±1.0*	18.6±1.6*	16.7±1.2*	15.6±1.1*†	16.4±1.2*
	4.5	3.14±0.15	13.1±1.4*†	15.7±2.4*	17.8±0.5*	15.3±1.7*	16.2±1.1*	13.4±1.0*	8.0±0.6†	16.5±1.9*

All values are means ± SEM. Concentrations represented in mmol/kg dry weight. * denotes significance compared to control. † denotes significance between doses. n/d denotes not detectable.

Table 4. Intracellular amino acids in the plantaris

Amino Acids	Dose	Time post-injection (in hours)								
	(mg/kg)	ctrl	24	48	72	96	120	144	168	192
Asp	1.5	0.32±0.03	0.41±0.08	0.79±0.1*	1.01±0.06*	1.17±.0.12*	1.15±0.08*	0.99±0.1*	0.95±0.07*	1.03±0.13*
	4.5	0.32±0.02	0.81±0.19	1.29±0.19*	1.07±0.09*	1.31±0.12*	0.95±0.05*	0.78±0.08	0.6±0.15	1.1±0.13*
Ser	1.5	0.89±0.09	0.99±0.22	1.65±0.39	2.37±0.38*	1.80±0.31	3.24±0.42*†	2.53±0.49*†	2.32±0.28	3.02±0.43*
	4.5	0.89±0.09	2.44±0.61*	2.7±0.44*	2.64±0.14*	2.0±0.16	1.29±0.11†	1.29±0.2†	1.46±0.39	2.73±0.25*
Glu	1.5	0.05±0.01	0.32±0.08*	0.31±0.04*†	0.65±0.1*	0.49±0.03*†	0.78±0.03*†	0.59±0.04*†	0.57±0.03*	0.65±0.08*†
	4.5	0.05±0.01	0.61±0.18*	0.61±0.09*†	0.57±0.05*	0.78±0.09*†	1.05±0.04*†	1.1±0.04*†	0.62±0.16*	1.7±0.2*†
Gly	1.5	0.27±0.01	0.27±0.05†	0.5±0.07	0.70±0.07*	0.83±0.09*	0.74±0.04*†	0.63±0.05*	0.62±0.03*	0.62±0.09*
	4.5	0.27±0.01	0.71±0.15*†	0.78±0.14*	0.71±0.08*	0.87±0.06*	0.6±0.05†	0.52±0.04	0.55±0.18	0.91±0.12*
His	1.5	0.45±0.02	0.7±0.15	1.58±0.22*	2.06±0.2*	2.31±0.25*	2.95±0.19*	2.19±0.15*	1.89±0.16*†	2.21±0.26*†
	4.5	0.45±0.02	2.0±0.53	4.83±1.83*	2.38±0.21	2.81±0.27	2.51±0.19	2.18±0.13	1.16±0.22†	3.79±0.43*†
Thr	1.5	0.5±0.03	1.04±0.6	1.31±0.1*	1.83±0.2*	1.65±0.11*	2.53±0.2*	1.93±0.13*	1.88±0.1*	2.0±0.22*
	4.5	0.5±0.03	2.12±0.52*	2.35±0.45*	2.09±0.17*	2.04±0.16*	2.56±0.23*	2.15±0.12*	1.67±0.45	2.19±0.15*
Ala	1.5	0.96±0.05	1.18±0.26	1.99±0.11*†	2.49±0.17*	2.73±0.27*	2.06±0.17*	1.83±0.23*	1.89±0.16*	2.09±0.2*
	4.5	0.96±0.05	2.55±0.53*	3.34±0.53*†	2.88±0.3*	2.22±0.16	1.76±0.09	1.43±0.11	1.24±0.42	2.1±0.29
Pro	1.5	0.11±0.01	0.12±0.02	0.18±0.02†	0.22±0.02*	0.26±0.03*	0.18±0.01	0.21±0.03*	0.21±0.02*†	0.22±0.03*
	4.5	0.11±0.01	0.21±0.05	0.37±0.07*†	0.3±0.04*	0.27±0.03*	0.22±0.02	0.15±0.01	0.1±0.03†	0.17±0.02

Cys	1.5	0.41±0.01	0.03±0.01*†	n/d	n/d	n/d	n/d	n/d	n/d	n/d
	4.5	0.41±0.01	1.13±0.29*†	3.6±0.33*	0.38±0.04	n/d	n/d	n/d	n/d	n/d
Tyr	1.5	0.03±0.002	n/d	0.06±0.01*†	0.10±0.01*	0.11±0.01*	0.09±0.01*†	0.08±0.01*	0.08±0.01*†	0.09±0.01*
	4.5	0.03±0.002	n/d	0.15±0.02*†	0.09±0.01*	0.13±0.02*	0.12±0.004*†	0.07±0.01*	0.05±0.01†	0.12±0.01*
Val	1.5	0.13±0.01	0.13±0.03	0.28±0.03*†	0.34±0.03*	0.32±0.03*	0.29±0.03*	0.32±0.03*†	0.3±0.03*†	0.29±0.03*
	4.5	0.13±0.01	0.26±0.06	0.5±0.09*†	0.35±0.03*	0.36±0.02*	0.3±0.02*	0.22±0.01†	0.14±0.03†	0.23±0.03
Met	1.5	0.003±0.002	0.05±0.01	0.07±0.01*†	0.1±0.01*	0.1±0.01*†	0.08±0.01*†	0.08±0.01*	0.08±0.01*†	0.08±0.01*
	4.5	0.003±0.002	0.97±0.03*	0.16±0.02*†	0.12±0.01*	0.13±0.01*†	0.11±0.01*†	0.07±0.01	0.05±0.01†	0.07±0.01
Lys	1.5	0.04±0.03	0.42±0.09	1.4±0.16*	1.38±0.21*	1.06±0.1*	1.43±0.19*†	1.52±0.16*†	1.51±0.03*†	1.23±0.14*
	4.5	0.04±0.03	0.970.25	1.75±0.24*	2.05±0.23*	1.1±0.04*	0.94±0.12†	0.87±0.12†	0.47±0.12†	1.19±0.14*
Iso	1.5	0.07±0.01	0.07±0.01	0.15±0.01*†	0.19±0.02*	0.17±0.02*	0.15±0.01*	0.17±0.02*†	0.16±0.01*†	0.16±0.02*
	4.5	0.07±0.02	0.14±0.03	0.29±0.05*†	0.2±0.02*	0.2±0.02*	0.16±0.01	0.12±0.01†	0.08±0.02†	0.13±0.02
Leu	1.5	0.19±0.01	0.15±0.03	0.29±0.03*†	0.38±0.03*	0.33±0.03*	0.3±0.02*	0.32±0.03*†	0.29±0.01*†	0.31±0.03*
	4.5	0.19±0.01	0.31±0.08	0.56±0.09*†	0.36±0.04*	0.38±0.04*	0.28±0.02	0.2±0.02†	0.13±0.03†	0.22±0.03
NH_3	1.5	1.12±0.08	0.33±0.02	0.81±0.22†	1.09±0.16	1.66±0.52	0.96±0.11†	0.57±0.05	0.79±0.06	0.53±0.03†
	4.5	1.12±0.08	1.33±0.33	1.82±0.53†	1.26±0.06	0.91±0.09	0.51±0.013†	0.56±0.03	0.8±0.19	1.07±0.02†
EAA	1.5	2.9±0.3	6.6±1.4†	12.5±0.8*†	16.5±1.4*	15.9±1.1*	19.8±1.0*	15.2±1.4*	14.1±0.6*†	15.7±1.3*†
	4.5	2.9±0.3	17.6±4.2*†	19.2±1.6*†	19.0±1.3*	18.2±2.8*	20.0±1.4*	17.3±0.7*	8.2±1.0†	21.7±1.6*†

All values are means ± SEM. Concentrations represented in mmol/kg dry weight. * denotes significance compared to control. † denotes significance between doses. n/d denotes not detectable.

Table 5. Intracellular amino acids in the soleus.

Amino Acids	Dose	Time post-injection (in hours)								
	(mg/kg)	ctrl	24	48	72	96	120	144	168	192
Asp	1.5	0.18±0.02	0.21±0.02†	0.79±0.08*	0.89±0.13*	0.99±0.01*	0.63±0.02*	0.84±0.07*†	0.59±0.01*†	0.61±0.07*
	4.5	0.18±0.02	0.59±0.05*†	0.6±0.05*	0.6±0.06*	0.84±0.11*	0.87±0.17*	0.64±0.04*†	0.29±0.01†	0.5±0.09*
Ser	1.5	0.43±0.04	0.37±0.05†	1.4±0.3*	1.25±0.13*†	0.93±0.1	0.68±0.03	0.97±0.13†	0.74±0.12†	1.31±0.26*
	4.5	0.43±0.04	1.28±0.24*†	0.93±0.16	0.8±0.11†	1.12±0.31*	0.55±0.14	0.47±0.04†	0.4±0.07†	0.81±0.08
Glu	1.5	0.02±0.003	0.13±0.02†	0.32±0.02*†	0.48±0.03*†	0.39±0.05*	0.49±0.03*†	0.52±0.03*	0.34±0.03*	0.4±0.02*
	4.5	0.02±0.003	0.3±0.01†	0.25±0.02†	0.35±0.04*†	0.43±0.01*	1.05±0.15*†	0.58±0.04*	0.25±0.02	0.61±0.*
Gly	1.5	0.39±0.02	0.28±0.05†	1.17±0.14*	1.53±0.17*†	1.65±0.1*†	1.20±0.09*	1.56±0.04*†	1.05±0.1*†	1.15±0.13*
	4.5	0.39±0.02	0.94±0.12*†	0.94±0.1*	1.1±0.09*†	1.12±0.08*†	1.42±0.17*	0.88±0.06†	0.53±0.09†	1.23±0.23*
His	1.5	0.24±0.02	0.37±0.04†	1.79±0.28*	1.72±0.15*†	1.7±0.14*	1.45±0.03*†	1.89±0.18*	1.17±0.09*†	1.41±0.14*
	4.5	0.24±0.02	1.23±0.06†	1.93±0.53*	1.26±0.12*†	1.82±0.23*	2.23±0.35*†	1.68±0.14*	0.76±0.09†	1.7±0.09*
Thr	1.5	0.83±0.03	0.86±0.18†	3.64±0.09*	4.39±0.29*	3.4±0.18*	4.89±0.44*†	4.59±0.21*	3.77±0.25*†	4.51±0.3*
	4.5	0.83±0.03	3.06±0.58*†	4.09±0.55*	4.26±0.25*	3.55±0.32*	7.25±0.57*†	4.61±0.25*	2.71±0.2*†	4.34±0.11*
Ala	1.5	0.72±0.05	0.85±0.11†	2.16±0.29*	2.32±0.41*	2.48±0.19*†	1.15±0.06†	1.79±0.15*†	1.08±0.16†	1.42±0.11
	4.5	0.72±0.05	2.12±0.16*†	1.91±0.2*	1.8±0.28*	1.66±0.26*†	1.75±0.19*†	1.25±0.15†	0.61±0.11†	1.27±0.16
Pro	1.5	0.1±0.01	0.07±0.01†	0.23±0.03*	0.27±0.03*	0.27±0.01*	0.18±0.01†	0.28±0.02*†	0.21±0.01*†	0.22±0.03*†
	4.5	0.1±0.01	0.15±0.01†	0.21±0.02*	0.24±0.02*	0.23±0.03*	0.26±0.03*†	0.18±0.01†	0.08±0.004†	0.13±0.02†

Cys	1.5	0.48±0.03	0.2±0.001*†	n/d	n/d	n/d	n/d	n/d	n/d	n/d
	4.5	0.48±0.03	1.12±0.12†	1.91±0.36*	0.46±0.07	n/d	n/d	n/d	n/d	n/d
Tyr	1.5	0.03±0.002	n/d	0.08±0.01*†	0.11±0.01*†	0.11±0.01*	0.09±0.004*†	0.11±0.01*	0.07±0.004*†	0.07±0.01*†
	4.5	0.03±0.002	n/d	0.16±0.01*†	0.08±0.01*†	0.1±0.01*	0.16±0.01*†	0.1±0.01*	0.05±0.003†	0.1±0.01*†
Val	1.5	0.11±0.01	0.09±0.01†	0.36±0.04*	0.4±0.02*†	0.33±0.05*	0.27±0.01*†	0.42±0.03*†	0.27±0.01*†	0.24±0.03*
	4.5	0.11±0.01	0.24±0.02*†	0.37±0.05*	0.29±0.03*†	0.3±0.05*	0.37±0.04*†	0.28±0.03*†	0.15±0.02†	0.2±0.02
Met	1.5	0.03±0.003	0.04±0.004†	0.09±0.01*†	0.11±0.01*	0.11±0.01*	0.08±0.01*†	0.11±0.01*	0.07±0.003*†	0.07±0.01*†
	4.5	0.03±0.003	0.09±0.01*†	0.16±0.01*†	0.1±0.01*	0.12±0.01*	0.14±0.01*†	0.1±0.01*	0.05±0.01†	0.05±0.004†
Lys	1.5	0.39±0.07	0.22±0.02†	1.53±0.14*†	1.59±0.1*	0.97±0.15*	1.01±0.07*	1.55±0.07*†	1.19±0.09*†	0.86±0.05*†
	4.5	0.39±0.07	0.73±0.09†	0.89±0.07*†	1.71±0.17*	0.69±0.1	1.03±0.17*	0.89±0.14*†	0.39±0.03†	0.7±0.03†
Iso	1.5	0.06±0.01	0.04±0.004†	0.19±0.02*	0.21±0.01*†	0.17±0.03*	0.14±0.01*†	0.23±0.02*†	0.14±0.003*†	0.15±0.01*†
	4.5	0.06±0.01	0.12±0.01†	0.22±0.03*	0.16±0.02*†	0.16±0.03*	0.2±0.02*†	0.15±0.02*†	0.08±0.01†	0.1±0.01†
Leu	1.5	0.15±0.01	0.09±0.01†	0.34±0.03*	0.39±0.02*†	0.32±0.05*	0.25±0.01*	0.41±0.03*†	0.25±0.01*†	0.26±0.02*†
	4.5	0.15±0.01	0.27±0.03*†	0.39±0.05*	0.26±0.02†	0.27±0.04	0.31±0.03*	0.25±0.03†	0.13±0.01†	0.17±0.02†
NH_3	1.5	1.38±0.12	0.36±0.06*†	0.92±0.04*†	1.54±0.15	1.05±0.09	1.06±0.04	1.3±0.1	0.67±0.05*†	0.66±0.04*†
	4.5	1.38±0.12	1.69±0.29†	1.94±0.21†	1.57±0.14	1.05±0.11	1.13±0.17	1.14±0.09	1.02±0.11†	1.65±0.08†
EAA	1.5	3.4±0.1	5.1±0.7†	18.8±0.4*	21.1±0.6*	17.9±1.1*	19.1±0.7*†	20.7±0.5*	15.2±0.4*†	17.6±0.6*
	4.5	3.4±0.1	14.2±3.1*†	18.1±2.0*	18.5±1.1*	18.3±1.4*	29.8±2.8*†	21.0±0.7*	9.4±0.8†	18.9±0.7*

All values are means ± SEM. Concentrations represented in mmol/kg dry weight. * denotes significance compared to control. † denotes significance between doses. n/d denotes not detectable.

CHAPTER V

12. Discussion and Conclusion

It is well accepted that the health and maintenance of skeletal muscle in cancer patients is clinically important; however, the effect of anti-cancer chemotherapy on skeletal muscle is poorly understood. Le Bricon *et al.* (Le Bricon, Gugins, Cynober, & Baracos, 1995) have reported that various chemotherapeutic agents (cyclophosphamide, cisplatinum, methotrexate and 5-fluorouracil) caused a transient weight loss as well as a drug-specific negative nitrogen balance in patients. Additionally, Damrauer *et al.* (S Damrauer et al., 2008) and Klose *et al.* (Klose et al., 2016) have noted that muscle wasting persisted after the reduction of the tumor burden and that cisplatin chemotherapy treatment frequently exacerbated the onset of cachexia. These reports suggest that chemotherapeutic agents disrupt metabolic pathways which are responsible for the health and preservation of the muscle. It also appears that these effects occur in concert with the drug's anti-tumor activity. However, it should be noted that in the aforementioned studies, the amount of drug in the muscle was not quantified nor was the retention of the drug in the tissue determined. It is evident that cancer chemotherapeutic agents affect healthy skeletal muscle; however, the accumulation of drug in the tissue and the possible sequestering of drug in skeletal muscle has not been investigated. This thesis highlights the role that skeletal muscle plays in DOX chemotherapy and the reciprocal effect that this drug has on the tissue.

In this thesis, a single low dose of DOX was used to minimize the drug-induced risk of cardiotoxicity by remaining below the reported threshold of cardiotoxicity. Previous studies have

utilized a variety of concentrations and treatment regimens documenting significant cardiomyocyte damage. Iqbal *et al.* (Iqbal et al., 2008) administered a single 20 mg/kg dose i.p. and observed the induction of acute cardiotoxicity after 48 hours and up to 7 days post administration. A study by Nagi *et al.* (Nagi & Mansour, 2000) reported that a single dose of 15 mg/kg i.p. induced cardiotoxicity after 24 and 48 hours and Jensen *et al.* (Jensen et al., 1984) noted that a 10 mg/kg or less total dosage did not cause cardiac failure. Arola *et al.* (Arola et al., 2000) reported minor cardiomyocyte apoptosis after 3 days following the injection of 1.5 mg/kg and 5 mg/kg, although it remains unclear whether this significantly altered cardiac performance. The concentrations of 1.5 mg/kg and 4.5 mg/kg used in this thesis provided a dose-related experimental contrast while minimizing the drug-induced risk of cardiac dysfunction associated with the higher doses. Furthermore, the aforementioned studies, as well as those employing cumulative doses (Guerra et al., 2005; Teraoka et al., 2000) focused on the long term effects of DOX in cardiomyocytes where little attention has been given to the early stages of DOX accumulation in skeletal muscle. As such, this thesis investigated the effects of DOX on skeletal muscle every 24 hours up to 192 hours. This time frame allowed for the examination of the acute effects of DOX accumulation on skeletal muscle as well as the dynamic interaction between the circulation and the interstitial space within skeletal muscle. A highlight of this thesis is the novel finding that a single low dose administration of DOX caused a persistent and significant accumulation of the drug in skeletal muscle throughout the entire timeline of the experiment (8 days). Passive diffusion of the drug into the tissue alone cannot explain the magnitude of increase of drug in the tissue when compared to its concentration in the circulation and in the interstitial space.

Further support for the rational for the accumulation of Dox can be found in the fact that in addition to the nuclei-rich characteristic of skeletal muscle, it is also rich in mitochondria and

mitochondrial DNA. The binding of DOX to DNA, mitochondrial DNA and its high affinity for cardiolipin would explain the sequestering of drug in the tissue beyond that of concentrations resulting from passive diffusion into the cell. As skeletal muscle represents the largest organ in the human body, the sequestering of DOX in the tissue greatly decreases the systemic availability of the drug intended for the tumor. This effectively reduces the therapeutic impact of the drug prompting the need for repeated doses. This presents an important clinical paradox; the repeated administration of the drug increases the exposure of the tumor to the chemotherapeutic agent while the intrinsic nature of DOX consequently increases accumulation of the drug in skeletal muscle, exacerbating the detrimental effects of the preceding dose. This prolonged accumulation of DOX in the muscle may lead to wasting of the tissue ultimately progressing to a cachectic condition.

A single low-dose administration of DOX, as shown in Chapter IV, caused a remarkable 3-4 fold increase in the intramuscular total amino acid pool. The overall net change of amino acids in the tissue is a key indicator of the synthesis or degradation state of proteins in the muscle. The reported increase in total amino acids strongly indicates that the rate of protein breakdown in the tissue was greater than that of synthesis. This is consistent with results reported by Hellin *et al.* (Hellin, Calmant, Gielen, Bours, & Merville, 1998) who has noted that daunomycin, an anthracycline similar to DOX, was a potent inducer of NF-κB transcription factors in a colon carcinoma cell line. In addition to its role in reducing tumor cell sensitivity to chemotherapy by inhibiting the apoptotic response (Camp et al., 2004; J. C. Cusack, Jr. et al., 2001), the upregulation of NF-κB has been shown to cause severe skeletal muscle wasting (Cai et al., 2004; Guttridge, Mayo, Madrid, Wang, & Baldwin, 2000; Hunter & Kandarian, 2004). The potential increase of NF-κB as a result of the accumulation of DOX in the muscle has been discussed in Chapter IV, where the increase in iNOS activity may be indicative of NF-κB upregulation. Taken together, the

persistent accumulation of a single dose of DOX in the muscle, the possible upregulation of NF-κB transcription factors as reported by Hellin *et al.* in addition to the regulatory mechanisms of protein synthesis potentially affected by DOX discussed in Chapter IV, this thesis establishes the potent myotoxicity of DOX. The resulting decrease in muscular integrity and potential loss of muscle mass, following DOX chemotherapeutic treatment, is of significant importance in cancer patients receiving chemotherapy as it reduces the effectiveness of the treatment, affects the quality of life of the patient and prolongs the recovery process following the cessation of treatment. More importantly, however is the loss of muscle mass and integrity which is indicative of the early onset of cachexia.

The accumulation and impact of DOX was not limited to the intracellular compartment of the tissue. The study of the interstitial space by way of the microdialysis technique revealed that a static pool of DOX was established in the interstitial space following the administration of a single dose of DOX. The rate of appearance of DOX in the interstitial space from the vasculature appeared to be matched by the rate of disappearance of the drug from the interstitial space into skeletal muscle. This formed a dynamic equilibrium resulting in a no net accumulation of DOX in the interstitial compartment. The concentration of DOX in the IC was greater than that of the ISS suggesting that despite its ability to passively diffuse through the cellular membrane, it was retained in the cell. This is further indication of the strong affinity of DOX to base pairs of the DNA as well as other molecules such as cardiolipin found in the mitochondria (as discussed in Chapter II). Additionally, the use of microdialysis helped clarify a confounding result in the acute removal of DOX from the tissue into the vasculature by identifying a concurrent increase in interstitial nitric oxide concentrations. This indicates that the increase in perfusion of the tissue mediated by local vasodilatory mechanisms play an important role in the removal of the drug from

the tissue and back into the circulation. Furthermore, microdialysis revealed a possible dose-related effect of DOX on amino acid transport mechanisms from the skeletal muscle compartment into the vasculature. The application of the microdialysis technique to study the interstitial space has proven to be a unique and powerful analytical tool in its ability to help elucidate the delivery kinetics of anti-cancer drugs in the tissue as well as provide insight into the local mechanisms affected by chemotherapy drugs.

The study of DOX and cardiomyocyte toxicity has deservedly received much of the focus of DOX-related research. As a vital organ it is imperative to conduct research to better understand and minimize cardiotoxicity for the benefit of the cancer patient receiving treatment. With this objective in mind, it is equally imperative to acknowledge the role that skeletal muscle plays in DOX bioavailability and the ability of the drug to overwhelmingly activate protein degradation contributing to the onset of cachexia. Further elucidation of these relationships would greatly improve the effectiveness of the drug, the health of the patient undergoing treatment and ultimately favor a positive prognosis.

In conclusion, the major contributions of this thesis include the quantification of a single dose of Doxorubicin in skeletal muscle. In addition, the accumulatin of intramuscular DOX resulted in significant protein degradation and demonstrates for the first time the adverse effect of this drug on Skeleltal muscle health and maintenance. In closing, these studies helped to better understand the relationship between chemotherapy and skeletal muscle and represents a major contribution to the field.

13. Limitations and Future Directions

One inherent limiatation to the studies performed in this thesis was due to sample size and allocation which resulted in analytical constraints. For example, it would have been beneficial to be able to perform fiber type analysis of the excised skeletal muscle groups, which would have allowed for greater insight into the potential role that the fiber type differences may play in the accumulation of DOX in skeletal muscle. Furthermore, as the samples were collected under basal metabolic conditions (the samples were collected while animals were under aneasthesia), concurrent sampling during the electrical stimulation of the muscle would provide even greater insight on the effects that increased metabolic demand and increased blood flow would have had on the accumulation of the drug in the tissue. This thesis presents a substantial foundation for future studies focused on reducing skeletal muscle damage as a result of DOX chemotherapy. As noted in Study 1 (Chapter II), the presence of drug in the tissue persisted up to 8 days following a single treatment, however the length of time that the drug remains sequestered in the tissue has yet to be determined. The natural progression of the studies presented in this thesis is to utilize a multiple treatment experimental design. As DOX is already sequestered in skeletal muscle as a result of the initial administration, subsequent doses may or may not elicit the same biphasic accumulation response in the tissue. Additionally, the subsequent administrations of drug may prolong the amount of time that the drug is sequestered in the tissue which may lead to cytotoxic effects that last beyond the cessation of the chemotherapeutic regimen. Furthermore, it is of particular clinical interest to determine whether repeated doses will induce the same degree of increase in amino acids as noted in Study 3 (Chapter IV). Finally, the next logical step is to move

into a xenograft model to determine weather the result of drug administration on skeletal muscle reported in this thesis are affected by the presence of a tumor in the system.

14. References

Acharyya, S., Ladner, K. J., Nelsen, L. L., Damrauer, J., Reiser, P. J., Swoap, S., & Guttridge, D. C. (2004). Cancer cachexia is regulated by selective targeting of skeletal muscle gene products. *J Clin Invest, 114*(3), 370-378. doi: 10.1172/JCI20174

Ahn, H. S., Foster, M., Cable, M., Pitts, B. J., & Sybertz, E. J. (1991). Ca/CaM-stimulated and cGMP-specific phosphodiesterases in vascular and non-vascular tissues. *Adv Exp Med Biol, 308*, 191-197.

Aldieri, E., Bergandi, L., Riganti, C., Costamagna, C., Bosia, A., & Ghigo, D. (2002). Doxorubicin induces an increase of nitric oxide synthesis in rat cardiac cells that is inhibited by iron supplementation. *Toxicol Appl Pharmacol, 185*(2), 85-90.

Anderson, A. B., Xiong, G., & Arriaga, E. A. (2004). Doxorubicin accumulation in individually electrophoresed organelles. *J Am Chem Soc, 126*(30), 9168-9169. doi: 10.1021/ja0492539

Antoun, S., Baracos, V. E., Birdsell, L., Escudier, B., & Sawyer, M. B. (2010). Low body mass index and sarcopenia associated with dose-limiting toxicity of sorafenib in patients with renal cell carcinoma. *Ann Oncol, 21*(8), 1594-1598. doi: 10.1093/annonc/mdp605

Arcamone, F., Cassinelli, G., Fantini, G., Grein, A., Orezzi, P., Pol, C., & Spalla, C. (1969). Adriamycin, 14-hydroxydaunomycin, a new antitumor antibiotic from S. peucetius var. caesius. *Biotechnol Bioeng, 11*(6), 1101-1110. doi: 10.1002/bit.260110607

Archer, S. L., Huang, J. M., Hampl, V., Nelson, D. P., Shultz, P. J., & Weir, E. K. (1994). Nitric oxide and cGMP cause vasorelaxation by activation of a charybdotoxin-sensitive K channel by cGMP-dependent protein kinase. *Proc Natl Acad Sci U S A, 91*(16), 7583-7587.

Argiles, J. M., Busquets, S., Stemmler, B., & Lopez-Soriano, F. J. (2014). Cancer cachexia: understanding the molecular basis. *Nat Rev Cancer, 14*(11), 754-762. doi: 10.1038/nrc3829

Armsey, T. D., Jr., & Grime, T. E. (2002). Protein and amino Acid supplementation in athletes. *Curr Sports Med Rep, 1*(4), 253-256.

Arnold, R. D., Slack, J. E., & Straubinger, R. M. (2004). Quantification of Doxorubicin and metabolites in rat plasma and small volume tissue samples by liquid chromatography/electrospray tandem mass spectroscopy. *J Chromatogr B Analyt Technol Biomed Life Sci, 808*(2), 141-152. doi: 10.1016/j.jchromb.2004.04.030

Arola, O. J., Saraste, A., Pulkki, K., Kallajoki, M., Parvinen, M., & Voipio-Pulkki, L. M. (2000). Acute doxorubicin cardiotoxicity involves cardiomyocyte apoptosis. *Cancer Res, 60*(7), 1789-1792.

Awasthi, S., Singhal, S. S., Awasthi, Y. C., Martin, B., Woo, J. H., Cunningham, C. C., & Frankel, A. E. (2008). RLIP76 and Cancer. *Clin Cancer Res, 14*(14), 4372-4377. doi: 10.1158/1078-0432.CCR-08-0145

Bains, O. S., Karkling, M. J., Lubieniecka, J. M., Grigliatti, T. A., Reid, R. E., & Riggs, K. W. (2010). Naturally occurring variants of human CBR3 alter anthracycline in vitro metabolism. *J Pharmacol Exp Ther, 332*(3), 755-763. doi: 10.1124/jpet.109.160614

Baker, J. S., McCormick, M. C., & Robergs, R. A. (2010). Interaction among Skeletal Muscle Metabolic Energy Systems during Intense Exercise. *J Nutr Metab, 2010*, 905612. doi: 10.1155/2010/905612

Balligand, J. L., Feron, O., & Dessy, C. (2009). eNOS activation by physical forces: from short-term regulation of contraction to chronic remodeling of cardiovascular tissues. *Physiol Rev, 89*(2), 481-534. doi: 10.1152/physrev.00042.2007

Baltgalvis, K. A., Berger, F. G., Pena, M. M., Davis, J. M., Muga, S. J., & Carson, J. A. (2008). Interleukin-6 and cachexia in ApcMin/+ mice. *Am J Physiol Regul Integr Comp Physiol, 294*(2), R393-401. doi: 10.1152/ajpregu.00716.2007

Beckman, J. S., Beckman, T. W., Chen, J., Marshall, P. A., & Freeman, B. A. (1990). Apparent hydroxyl radical production by peroxynitrite: implications for endothelial injury from nitric oxide and superoxide. *Proc Natl Acad Sci U S A, 87*(4), 1620-1624.

Biolo, G., Bosutti, A., Iscra, F., Toigo, G., Gullo, A., & Guarnieri, G. (2000). Contribution of the ubiquitin-proteasome pathway to overall muscle proteolysis in hypercatabolic patients. *Metabolism, 49*(6), 689-691. doi: 10.1053/meta.2000.6236

Bloemberg, D., & Quadrilatero, J. (2012). Rapid determination of myosin heavy chain expression in rat, mouse, and human skeletal muscle using multicolor immunofluorescence analysis. *PLoS One, 7*(4), e35273. doi: 10.1371/journal.pone.0035273

Blomstrand, E., Eliasson, J., Karlsson, H. K., & Kohnke, R. (2006). Branched-chain amino acids activate key enzymes in protein synthesis after physical exercise. *J Nutr, 136*(1 Suppl), 269S-273S.

Boucek, R. J., Jr., Olson, R. D., Brenner, D. E., Ogunbunmi, E. M., Inui, M., & Fleischer, S. (1987). The major metabolite of doxorubicin is a potent inhibitor of membrane-associated ion pumps. A correlative study of cardiac muscle with isolated membrane fractions. *J Biol Chem, 262*(33), 15851-15856.

Brosnan, J. T., & Brosnan, M. E. (2006). Branched-chain amino acids: enzyme and substrate regulation. *J Nutr, 136*(1 Suppl), 207S-211S.

Buck, M., & Chojkier, M. (1996). Muscle wasting and dedifferentiation induced by oxidative stress in a murine model of cachexia is prevented by inhibitors of nitric oxide synthesis and antioxidants. *EMBO J, 15*(8), 1753-1765.

Cai, D., Frantz, J. D., Tawa, N. E., Jr., Melendez, P. A., Oh, B. C., Lidov, H. G., . . . Shoelson, S. E. (2004). IKKbeta/NF-kappaB activation causes severe muscle wasting in mice. *Cell, 119*(2), 285-298. doi: 10.1016/j.cell.2004.09.027

Calabrese, V., Mancuso, C., Calvani, M., Rizzarelli, E., Butterfield, D. A., & Stella, A. M. (2007). Nitric oxide in the central nervous system: neuroprotection versus neurotoxicity. *Nat Rev Neurosci, 8*(10), 766-775. doi: 10.1038/nrn2214

Camp, E. R., Li, J., Minnich, D. J., Brank, A., Moldawer, L. L., MacKay, S. L., & Hochwald, S. N. (2004). Inducible nuclear factor-kappaB activation contributes to chemotherapy resistance in gastric cancer. *J Am Coll Surg, 199*(2), 249-258. doi: 10.1016/j.jamcollsurg.2004.04.015

Carpenter, A. J., & Porter, A. C. (2004). Construction, characterization, and complementation of a conditional-lethal DNA topoisomerase IIalpha mutant human cell line. *Mol Biol Cell, 15*(12), 5700-5711. doi: 10.1091/mbc.E04-08-0732

Carter, S. K. (1975). Adriamycin-a review. *J Natl Cancer Inst, 55*(6), 1265-1274.

Catania, C., Binder, E., & Cota, D. (2011). mTORC1 signaling in energy balance and metabolic disease. *Int J Obes (Lond), 35*(6), 751-761. doi: 10.1038/ijo.2010.208

Chaires, J. B., Fox, K. R., Herrera, J. E., Britt, M., & Waring, M. J. (1987). Site and sequence specificity of the daunomycin-DNA interaction. *Biochemistry, 26*(25), 8227-8236.

Chala, E., Manes, C., Iliades, H., Skaragkas, G., Mouratidou, D., & Kapantais, E. (2006). Insulin resistance, growth factors and cytokine levels in overweight women with breast cancer before and after chemotherapy. *Hormones (Athens), 5*(2), 137-146.

Chen, K. X., Gresh, N., & Pullman, B. (1986). A theoretical investigation on the sequence selective binding of mitoxantrone to double-stranded tetranucleotides. *Nucleic Acids Res, 14*(9), 3799-3812.

Chromiak, J. A., & Antonio, J. (2002). Use of amino acids as growth hormone-releasing agents by athletes. *Nutrition, 18*(7-8), 657-661.

Ciaccio, M., Valenza, M., Tesoriere, L., Bongiorno, A., Albiero, R., & Livrea, M. A. (1993). Vitamin A inhibits doxorubicin-induced membrane lipid peroxidation in rat tissues in vivo. *Arch Biochem Biophys, 302*(1), 103-108. doi: 10.1006/abbi.1993.1186

Clausen, T. (1986). Regulation of active Na+-K+ transport in skeletal muscle. *Physiol Rev, 66*(3), 542-580.

Clifford, P. S., & Hellsten, Y. (2004). Vasodilatory mechanisms in contracting skeletal muscle. *J Appl Physiol (1985), 97*(1), 393-403. doi: 10.1152/japplphysiol.00179.2004

Coldwell, K. E., Cutts, S. M., Ognibene, T. J., Henderson, P. T., & Phillips, D. R. (2008). Detection of Adriamycin-DNA adducts by accelerator mass spectrometry at clinically relevant Adriamycin concentrations. *Nucleic Acids Res, 36*(16), e100. doi: 10.1093/nar/gkn439

Cole, J. T. (2015). Metabolism of BCAAs *Branched Chain Amino Acids in Clinical Nutrition* (Vol. Volume 1, pp. 13-24). New York: Springer Science.

Conklin, K. A. (2004). Chemotherapy-associated oxidative stress: impact on chemotherapeutic effectiveness. *Integr Cancer Ther, 3*(4), 294-300. doi: 10.1177/1534735404270335

Cusack, B. J., Young, S. P., Driskell, J., & Olson, R. D. (1993). Doxorubicin and doxorubicinol pharmacokinetics and tissue concentrations following bolus injection and continuous infusion of doxorubicin in the rabbit. *Cancer Chemother Pharmacol, 32*(1), 53-58.

Cusack, J. C., Jr., Liu, R., Houston, M., Abendroth, K., Elliott, P. J., Adams, J., & Baldwin, A. S., Jr. (2001). Enhanced chemosensitivity to CPT-11 with proteasome inhibitor PS-341: implications for systemic nuclear factor-kappaB inhibition. *Cancer Res, 61*(9), 3535-3540.

de Lima Junior, E. A., Yamashita, A. S., Pimentel, G. D., De Sousa, L. G., Santos, R. V., Goncalves, C. L., . . . Rosa Neto, J. C. (2016). Doxorubicin caused severe hyperglycaemia and insulin resistance, mediated by inhibition in AMPk signalling in skeletal muscle. *J Cachexia Sarcopenia Muscle, 7*(5), 615-625. doi: 10.1002/jcsm.12104

De Palma, C., Morisi, F., Pambianco, S., Assi, E., Touvier, T., Russo, S., . . . Clementi, E. (2014). Deficient nitric oxide signalling impairs skeletal muscle growth and performance: involvement of mitochondrial dysregulation. *Skelet Muscle, 4*(1), 22. doi: 10.1186/s13395-014-0022-6

Delgado, J. M., DeFeudis, F. V., Roth, R. H., Ryugo, D. K., & Mitruka, B. M. (1972). Dialytrode for long term intracerebral perfusion in awake monkeys. *Arch Int Pharmacodyn Ther, 198*(1), 9-21.

Di Marco, S., Mazroui, R., Dallaire, P., Chittur, S., Tenenbaum, S. A., Radzioch, D., . . . Gallouzi, I. E. (2005). NF-kappa B-mediated MyoD decay during muscle wasting requires nitric oxide synthase mRNA stabilization, HuR protein, and nitric oxide release. *Mol Cell Biol, 25*(15), 6533-6545. doi: 10.1128/MCB.25.15.6533-6545.2005

Doroshow, J. H. (1983). Effect of anthracycline antibiotics on oxygen radical formation in rat heart. *Cancer Res, 43*(2), 460-472.

Doroshow, J. H., Tallent, C., & Schechter, J. E. (1985). Ultrastructural features of Adriamycin-induced skeletal and cardiac muscle toxicity. *Am J Pathol, 118*(2), 288-297.

Erzen, I., Janacek, J., & Kubinova, L. (2011). Characterization of the capillary network in skeletal muscles from 3D data. *Physiol Res, 60*(1), 1-13.

Esper, D. H., & Harb, W. A. (2005). The cancer cachexia syndrome: a review of metabolic and clinical manifestations. *Nutr Clin Pract, 20*(4), 369-376. doi: 10.1177/0115426505020004369

Evans, W. J., Morley, J. E., Argiles, J., Bales, C., Baracos, V., Guttridge, D., . . . Anker, S. D. (2008). Cachexia: a new definition. *Clin Nutr, 27*(6), 793-799. doi: 10.1016/j.clnu.2008.06.013

Evig, C. B., Kelley, E. E., Weydert, C. J., Chu, Y., Buettner, G. R., & Burns, C. P. (2004). Endogenous production and exogenous exposure to nitric oxide augment doxorubicin cytotoxicity for breast cancer cells but not cardiac myoblasts. *Nitric Oxide, 10*(3), 119-129. doi: 10.1016/j.niox.2004.03.006

Fabris, S., & MacLean, D. A. (2015). Skeletal Muscle an Active Compartment in the Sequestering and Metabolism of Doxorubicin Chemotherapy. *PLoS One, 10*(9), e0139070. doi: 10.1371/journal.pone.0139070

Fabris, S., & MacLean, D. A. (2016). Doxorubicin chemotherapy affects intracellular and interstitial nitric oxide concentrations in skeletal muscle : Effect of doxorubicin on intracellular and interstitial NO in skeletal muscle. *Cell Biol Toxicol, 32*(2), 121-131. doi: 10.1007/s10565-016-9325-1

Fearon, K., Strasser, F., Anker, S. D., Bosaeus, I., Bruera, E., Fainsinger, R. L., . . . Baracos, V. E. (2011). Definition and classification of cancer cachexia: an international consensus. *Lancet Oncol, 12*(5), 489-495. doi: 10.1016/S1470-2045(10)70218-7

Fearon, K. C., & Baracos, V. E. (2010). Cachexia in pancreatic cancer: new treatment options and measures of success. *HPB (Oxford), 12*(5), 323-324. doi: 10.1111/j.1477-2574.2010.00178.x

Fearon, K. C., Glass, D. J., & Guttridge, D. C. (2012). Cancer cachexia: mediators, signaling, and metabolic pathways. *Cell Metab, 16*(2), 153-166. doi: 10.1016/j.cmet.2012.06.011

Felig, P. (1973). The glucose-alanine cycle. *Metabolism, 22*(2), 179-207.

Feng, J. P., Yuan, X. L., Li, M., Fang, J., Xie, T., Zhou, Y., . . . Ye, D. W. (2013). Secondary diabetes associated with 5-fluorouracil-based chemotherapy regimens in non-diabetic patients with colorectal cancer: results from a single-centre cohort study. *Colorectal Dis, 15*(1), 27-33. doi: 10.1111/j.1463-1318.2012.03097.x

Forstermann, U., & Sessa, W. C. (2012). Nitric oxide synthases: regulation and function. *Eur Heart J, 33*(7), 829-837, 837a-837d. doi: 10.1093/eurheartj/ehr304

Furchgott, R. F. (1999). Endothelium-derived relaxing factor: discovery, early studies, and identification as nitric oxide. *Biosci Rep, 19*(4), 235-251.

Garner, A. P., Paine, M. J., Rodriguez-Crespo, I., Chinje, E. C., Ortiz De Montellano, P., Stratford, I. J., . . . Wolf, C. R. (1999). Nitric oxide synthases catalyze the activation of redox cycling and bioreductive anticancer agents. *Cancer Res, 59*(8), 1929-1934.

Georges, E., Bradley, G., Gariepy, J., & Ling, V. (1990). Detection of P-glycoprotein isoforms by gene-specific monoclonal antibodies. *Proc Natl Acad Sci U S A, 87*(1), 152-156.

Gewirtz, D. A. (1999). A critical evaluation of the mechanisms of action proposed for the antitumor effects of the anthracycline antibiotics adriamycin and daunorubicin. *Biochem Pharmacol, 57*(7), 727-741.

Ghofrani, H. A., Osterloh, I. H., & Grimminger, F. (2006). Sildenafil: from angina to erectile dysfunction to pulmonary hypertension and beyond. *Nat Rev Drug Discov, 5*(8), 689-702. doi: 10.1038/nrd2030

Gibson, N. M., Quinn, C. J., Pfannenstiel, K. B., Hydock, D. S., & Hayward, R. (2013). Effects of age on multidrug resistance protein expression and doxorubicin accumulation in cardiac and skeletal muscle. *Xenobiotica*. doi: 10.3109/00498254.2013.846489

Gille, L., & Nohl, H. (1997). Analyses of the molecular mechanism of adriamycin-induced cardiotoxicity. *Free Radic Biol Med, 23*(5), 775-782.

Gilliam, L. A., & St Clair, D. K. (2011). Chemotherapy-induced weakness and fatigue in skeletal muscle: the role of oxidative stress. *Antioxid Redox Signal, 15*(9), 2543-2563. doi: 10.1089/ars.2011.3965

Goormaghtigh, E., Huart, P., Praet, M., Brasseur, R., & Ruysschaert, J. M. (1990). Structure of the adriamycin-cardiolipin complex. Role in mitochondrial toxicity. *Biophys Chem, 35*(2-3), 247-257.

Graham, M. A., Newell, D. R., Butler, J., Hoey, B., & Patterson, L. H. (1987). The effect of the anthrapyrazole antitumour agent CI941 on rat liver microsome and cytochrome P-450 reductase mediated free radical processes. Inhibition of doxorubicin activation in vitro. *Biochem Pharmacol, 36*(20), 3345-3351.

Graham, T. E. (1995). *Skeletal muscle amino acid metabolism and ammonia production during exercise*. Champaign: Human Kinetics.

Graham, T. E., Sgro, V., Friars, D., & Gibala, M. J. (2000). Glutamate ingestion: the plasma and muscle free amino acid pools of resting humans. *Am J Physiol Endocrinol Metab, 278*(1), E83-89.

Guerra, J., De Jesus, A., Santiago-Borrero, P., Roman-Franco, A., Rodriguez, E., & Crespo, M. J. (2005). Plasma nitric oxide levels used as an indicator of doxorubicin-induced cardiotoxicity in rats. *Hematol J, 5*(7), 584-588. doi: 10.1038/sj.thj.6200573

Gulati, P., Gaspers, L. D., Dann, S. G., Joaquin, M., Nobukuni, T., Natt, F., . . . Thomas, G. (2008). Amino acids activate mTOR complex 1 via Ca2+/CaM signaling to hVps34. *Cell Metab, 7*(5), 456-465. doi: 10.1016/j.cmet.2008.03.002

Guttridge, D. C., Mayo, M. W., Madrid, L. V., Wang, C. Y., & Baldwin, A. S., Jr. (2000). NF-kappaB-induced loss of MyoD messenger RNA: possible role in muscle decay and cachexia. *Science, 289*(5488), 2363-2366.

Hall, M. N. (2008). mTOR-what does it do? *Transplant Proc, 40*(10 Suppl), S5-8. doi: 10.1016/j.transproceed.2008.10.009

Hall, T. R., Wallin, R., Reinhart, G. D., & Hutson, S. M. (1993). Branched chain aminotransferase isoenzymes. Purification and characterization of the rat brain isoenzyme. *J Biol Chem, 268*(5), 3092-3098.

Han, Y., Weinman, S., Boldogh, I., Walker, R. K., & Brasier, A. R. (1999). Tumor necrosis factor-alpha-inducible IkappaBalpha proteolysis mediated by cytosolic m-calpain. A mechanism parallel to the ubiquitin-proteasome pathway for nuclear factor-kappab activation. *J Biol Chem, 274*(2), 787-794.

Harper, A. E., Miller, R. H., & Block, K. P. (1984). Branched-chain amino acid metabolism. *Annu Rev Nutr, 4*, 409-454. doi: 10.1146/annurev.nu.04.070184.002205

Hayward, R., Hydock, D., Gibson, N., Greufe, S., Bredahl, E., & Parry, T. (2013). Tissue retention of doxorubicin and its effects on cardiac, smooth, and skeletal muscle function. *J Physiol Biochem, 69*(2), 177-187. doi: 10.1007/s13105-012-0200-0

Heibein, A. D., Guo, B., Sprowl, J. A., Maclean, D. A., & Parissenti, A. M. (2012). Role of aldo-keto reductases and other doxorubicin pharmacokinetic genes in doxorubicin resistance, DNA binding, and subcellular localization. *BMC Cancer, 12*, 381. doi: 10.1186/1471-2407-12-381

Hellin, A. C., Calmant, P., Gielen, J., Bours, V., & Merville, M. P. (1998). Nuclear factor - kappaB-dependent regulation of p53 gene expression induced by daunomycin genotoxic drug. *Oncogene, 16*(9), 1187-1195. doi: 10.1038/sj.onc.1201638

Hellsten, Y., Maclean, D., Radegran, G., Saltin, B., & Bangsbo, J. (1998). Adenosine concentrations in the interstitium of resting and contracting human skeletal muscle. *Circulation, 98*(1), 6-8.

Hunter, R. B., & Kandarian, S. C. (2004). Disruption of either the Nfkb1 or the Bcl3 gene inhibits skeletal muscle atrophy. *J Clin Invest, 114*(10), 1504-1511. doi: 10.1172/JCI21696

Hyde, R., Taylor, P. M., & Hundal, H. S. (2003). Amino acid transporters: roles in amino acid sensing and signalling in animal cells. *Biochem J, 373*(Pt 1), 1-18.

Iqbal, M., Dubey, K., Anwer, T., Ashish, A., & Pillai, K. K. (2008). Protective effects of telmisartan against acute doxorubicin-induced cardiotoxicity in rats. *Pharmacol Rep, 60*(3), 382-390.

Jackson, M. J. (2005). Use of microdialysis to study interstitial nitric oxide and other reactive oxygen and nitrogen species in skeletal muscle. *Methods Enzymol, 396*, 514-525. doi: 10.1016/S0076-6879(05)96043-6

Jensen, R. A., Acton, E. M., & Peters, J. H. (1984). Doxorubicin cardiotoxicity in the rat: comparison of electrocardiogram, transmembrane potential, and structural effects. *J Cardiovasc Pharmacol, 6*(1), 186-200.

Juel, C. (1996). Lactate/proton co-transport in skeletal muscle: regulation and importance for pH homeostasis. *Acta Physiol Scand, 156*(3), 369-374. doi: 10.1046/j.1365-201X.1996.206000.x

Jung, I. D., Lee, J. S., Yun, S. Y., Park, C. G., Han, J. W., Lee, H. W., & Lee, H. Y. (2002). Doxorubicin inhibits the production of nitric oxide by colorectal cancer cells. *Arch Pharm Res, 25*(5), 691-696.

Kalivendi, S. V., Kotamraju, S., Zhao, H., Joseph, J., & Kalyanaraman, B. (2001). Doxorubicin-induced apoptosis is associated with increased transcription of endothelial nitric-oxide synthase. Effect of antiapoptotic antioxidants and calcium. *J Biol Chem, 276*(50), 47266-47276. doi: 10.1074/jbc.M106829200

Kassner, N., Huse, K., Martin, H. J., Godtel-Armbrust, U., Metzger, A., Meineke, I., . . . Wojnowski, L. (2008). Carbonyl reductase 1 is a predominant doxorubicin reductase in the human liver. *Drug Metab Dispos, 36*(10), 2113-2120. doi: 10.1124/dmd.108.022251

Kimball, S. R., & Jefferson, L. S. (2006). Signaling pathways and molecular mechanisms through which branched-chain amino acids mediate translational control of protein synthesis. *J Nutr, 136*(1 Suppl), 227S-231S.

Klose, R., Krzywinska, E., Castells, M., Gotthardt, D., Putz, E. M., Kantari-Mimoun, C., . . . Stockmann, C. (2016). Targeting VEGF-A in myeloid cells enhances natural killer cell responses to chemotherapy and ameliorates cachexia. *Nat Commun, 7*, 12528. doi: 10.1038/ncomms12528

Koopman, R., Verdijk, L., Manders, R. J., Gijsen, A. P., Gorselink, M., Pijpers, E., . . . van Loon, L. J. (2006). Co-ingestion of protein and leucine stimulates muscle protein synthesis rates to the same extent in young and elderly lean men. *Am J Clin Nutr, 84*(3), 623-632.

Kotamraju, S., Konorev, E. A., Joseph, J., & Kalyanaraman, B. (2000). Doxorubicin-induced apoptosis in endothelial cells and cardiomyocytes is ameliorated by nitrone spin traps and ebselen. Role of reactive oxygen and nitrogen species. *J Biol Chem, 275*(43), 33585-33592. doi: 10.1074/jbc.M003890200

Kremer, L. C., van Dalen, E. C., Offringa, M., Ottenkamp, J., & Voute, P. A. (2001). Anthracycline-induced clinical heart failure in a cohort of 607 children: long-term follow-up study. *J Clin Oncol, 19*(1), 191-196.

Le Bricon, T., Gugins, S., Cynober, L., & Baracos, V. E. (1995). Negative impact of cancer chemotherapy on protein metabolism in healthy and tumor-bearing rats. *Metabolism, 44*(10), 1340-1348.

Lefrak, E. A., Pitha, J., Rosenheim, S., & Gottlieb, J. A. (1973). A clinicopathologic analysis of adriamycin cardiotoxicity. *Cancer, 32*(2), 302-314.

Leuenberger, U. A., Johnson, D., Loomis, J., Gray, K. S., & MacLean, D. A. (2008). Venous but not skeletal muscle interstitial nitric oxide is increased during hypobaric hypoxia. *Eur J Appl Physiol, 102*(4), 457-461. doi: 10.1007/s00421-007-0601-x

Levy, J. (1999). Abnormal cell calcium homeostasis in type 2 diabetes mellitus: a new look on old disease. *Endocrine, 10*(1), 1-6. doi: 10.1385/ENDO:10:1:1

Li, J., King, N. C., & Sinoway, L. I. (2003). ATP concentrations and muscle tension increase linearly with muscle contraction. *J Appl Physiol (1985), 95*(2), 577-583. doi: 10.1152/japplphysiol.00185.2003

Lim, S., Shin, J. Y., Jo, A., Jyothi, K. R., Nguyen, M. N., Choi, T. G., . . . Kim, S. S. (2013). Carbonyl reductase 1 is an essential regulator of skeletal muscle differentiation and regeneration. *Int J Biochem Cell Biol, 45*(8), 1784-1793. doi: 10.1016/j.biocel.2013.05.025

Lorite, M. J., Thompson, M. G., Drake, J. L., Carling, G., & Tisdale, M. J. (1998). Mechanism of muscle protein degradation induced by a cancer cachectic factor. *Br J Cancer, 78*(7), 850-856.

Lu, M., Merali, S., Gordon, R., Jiang, J., Li, Y., Mandeli, J., . . . Holland, J. F. (2011). Prevention of Doxorubicin cardiopathic changes by a benzyl styryl sulfone in mice. *Genes Cancer, 2*(10), 985-992. doi: 10.1177/1947601911436199

MacLean, D. A., Bangsbo, J., & Saltin, B. (1999). Muscle interstitial glucose and lactate levels during dynamic exercise in humans determined by microdialysis. *J Appl Physiol (1985), 87*(4), 1483-1490.

MacLean, D. A., Graham, T. E., & Saltin, B. (1994). Branched-chain amino acids augment ammonia metabolism while attenuating protein breakdown during exercise. *Am J Physiol, 267*(6 Pt 1), E1010-1022.

MacLean, D. A., LaNoue, K. F., Gray, K. S., & Sinoway, L. I. (1998). Effects of hindlimb contraction on pressor and muscle interstitial metabolite responses in the cat. *J Appl Physiol (1985), 85*(4), 1583-1592.

MacLean, D. A., Sinoway, L. I., & Leuenberger, U. (1998). Systemic hypoxia elevates skeletal muscle interstitial adenosine levels in humans. *Circulation, 98*(19), 1990-1992.

MacLean, D. A., Vickery, L. M., & Sinoway, L. I. (2001). Elevated interstitial adenosine concentrations do not activate the muscle reflex. *Am J Physiol Heart Circ Physiol, 280*(2), H546-553.

Mahnik, S. N., Rizovski, B., Fuerhacker, M., & Mader, R. M. (2006). Development of an analytical method for the determination of anthracyclines in hospital effluents. *Chemosphere, 65*(8), 1419-1425. doi: http://dx.doi.org/10.1016/j.chemosphere.2006.03.069

Matthews, D. E., Bier, D. M., Rennie, M. J., Edwards, R. H., Halliday, D., Millward, D. J., & Clugston, G. A. (1981). Regulation of leucine metabolism in man: a stable isotope study. *Science, 214*(4525), 1129-1131.

Megeney, L. A., Kablar, B., Garrett, K., Anderson, J. E., & Rudnicki, M. A. (1996). MyoD is required for myogenic stem cell function in adult skeletal muscle. *Genes Dev, 10*(10), 1173-1183.

Michel, J. B., Feron, O., Sacks, D., & Michel, T. (1997). Reciprocal regulation of endothelial nitric-oxide synthase by Ca2+-calmodulin and caveolin. *J Biol Chem, 272*(25), 15583-15586.

Milan, H. (2011). Branched-chain Amino Acid Oxidation in Skeletal Muscle – Physiological and Clinical Importance of its Modulation by Reactant Availability. *Current Nutrition & Food Science, 7*(1), 50-56. doi: http://dx.doi.org/10.2174/157340111794941139

Minotti, G., Menna, P., Salvatorelli, E., Cairo, G., & Gianni, L. (2004). Anthracyclines: molecular advances and pharmacologic developments in antitumor activity and cardiotoxicity. *Pharmacol Rev, 56*(2), 185-229. doi: 10.1124/pr.56.2.6

Minotti, G., Recalcati, S., Mordente, A., Liberi, G., Calafiore, A. M., Mancuso, C., . . . Cairo, G. (1998). The secondary alcohol metabolite of doxorubicin irreversibly inactivates aconitase/iron regulatory protein-1 in cytosolic fractions from human myocardium. *FASEB J, 12*(7), 541-552.

Mitch, W. E., & Goldberg, A. L. (1996). Mechanisms of muscle wasting. The role of the ubiquitin-proteasome pathway. *N Engl J Med, 335*(25), 1897-1905. doi: 10.1056/NEJM199612193352507

Mohan, P., & Rapoport, N. (2010). Doxorubicin as a molecular nanotheranostic agent: effect of doxorubicin encapsulation in micelles or nanoemulsions on the ultrasound-mediated intracellular delivery and nuclear trafficking. *Mol Pharm, 7*(6), 1959-1973. doi: 10.1021/mp100269f

Momparler, R. L., Karon, M., Siegel, S. E., & Avila, F. (1976). Effect of adriamycin on DNA, RNA, and protein synthesis in cell-free systems and intact cells. *Cancer Res, 36*(8), 2891-2895.

Mordente, A., Meucci, E., Silvestrini, A., Martorana, G. E., & Giardina, B. (2009). New developments in anthracycline-induced cardiotoxicity. *Curr Med Chem, 16*(13), 1656-1672.

Murakami, S., Fujino, H., Takeda, I., Momota, R., Kumagishi, K., & Ohtsuka, A. (2010). Comparison of capillary architecture between slow and fast muscles in rats using a confocal laser scanning microscope. *Acta Med Okayama, 64*(1), 11-18.

Mushlin, P. S., Cusack, B. J., Boucek, R. J., Jr., Andrejuk, T., Li, X., & Olson, R. D. (1993). Time-related increases in cardiac concentrations of doxorubicinol could interact with doxorubicin to depress myocardial contractile function. *Br J Pharmacol, 110*(3), 975-982.

Nagi, M. N., & Mansour, M. A. (2000). Protective effect of thymoquinone against doxorubicin-induced cardiotoxicity in rats: a possible mechanism of protection. *Pharmacol Res, 41*(3), 283-289. doi: 10.1006/phrs.1999.0585

Narendrula, R., Mispel-Beyer, K., Guo, B., Parissenti, A. M., Pritzker, L. B., Pritzker, K., . . . Lanner, C. (2016). RNA disruption is associated with response to multiple classes of chemotherapy drugs in tumor cell lines. *BMC Cancer, 16*, 146. doi: 10.1186/s12885-016-2197-1

Nicholson, C., & Phillips, J. M. (1981). Ion diffusion modified by tortuosity and volume fraction in the extracellular microenvironment of the rat cerebellum. *J Physiol, 321*, 225-257.

Nobukuni, T., Joaquin, M., Roccio, M., Dann, S. G., Kim, S. Y., Gulati, P., . . . Thomas, G. (2005). Amino acids mediate mTOR/raptor signaling through activation of class 3 phosphatidylinositol 3OH-kinase. *Proc Natl Acad Sci U S A, 102*(40), 14238-14243. doi: 10.1073/pnas.0506925102

Norton, L. E., & Layman, D. K. (2006). Leucine regulates translation initiation of protein synthesis in skeletal muscle after exercise. *J Nutr, 136*(2), 533S-537S.

Octavia, Y., Tocchetti, C. G., Gabrielson, K. L., Janssens, S., Crijns, H. J., & Moens, A. L. (2012). Doxorubicin-induced cardiomyopathy: from molecular mechanisms to therapeutic strategies. *J Mol Cell Cardiol, 52*(6), 1213-1225. doi: 10.1016/j.yjmcc.2012.03.006

Okutsu, M., Call, J. A., Lira, V. A., Zhang, M., Donet, J. A., French, B. A., . . . Yan, Z. (2014). Extracellular superoxide dismutase ameliorates skeletal muscle abnormalities, cachexia, and exercise intolerance in mice with congestive heart failure. *Circ Heart Fail, 7*(3), 519-530. doi: 10.1161/CIRCHEARTFAILURE.113.000841

Olson, R. D., & Mushlin, P. S. (1990). Doxorubicin cardiotoxicity: analysis of prevailing hypotheses. *FASEB J, 4*(13), 3076-3086.

Olson, R. D., Mushlin, P. S., Brenner, D. E., Fleischer, S., Cusack, B. J., Chang, B. K., & Boucek, R. J., Jr. (1988). Doxorubicin cardiotoxicity may be caused by its metabolite, doxorubicinol. *Proc Natl Acad Sci U S A, 85*(10), 3585-3589.

Paulides, M., Kremers, A., Stohr, W., Bielack, S., Jurgens, H., Treuner, J., . . . Langer, T. (2006). Prospective longitudinal evaluation of doxorubicin-induced cardiomyopathy in sarcoma patients: a report of the late effects surveillance system (LESS). *Pediatr Blood Cancer, 46*(4), 489-495. doi: 10.1002/pbc.20492

Peters, J. H., Gordon, G. R., Kashiwase, D., & Acton, E. M. (1981). Tissue distribution of doxorubicin and doxorubicinol in rats receiving multiple doses of doxorubicin. *Cancer Chemother Pharmacol, 7*(1), 65-69.

Pilegaard, H., Domino, K., Noland, T., Juel, C., Hellsten, Y., Halestrap, A. P., & Bangsbo, J. (1999). Effect of high-intensity exercise training on lactate/H+ transport capacity in human skeletal muscle. *Am J Physiol, 276*(2 Pt 1), E255-261.

Pommier, Y., Leo, E., Zhang, H., & Marchand, C. (2010). DNA topoisomerases and their poisoning by anticancer and antibacterial drugs. *Chem Biol, 17*(5), 421-433. doi: 10.1016/j.chembiol.2010.04.012

Porporato, P. E. (2016). Understanding cachexia as a cancer metabolism syndrome. *Oncogenesis, 5*, e200. doi: 10.1038/oncsis.2016.3

Prado, C. M., Baracos, V. E., McCargar, L. J., Reiman, T., Mourtzakis, M., Tonkin, K., . . . Sawyer, M. B. (2009). Sarcopenia as a determinant of chemotherapy toxicity and time to tumor progression in metastatic breast cancer patients receiving capecitabine treatment. *Clin Cancer Res, 15*(8), 2920-2926. doi: 10.1158/1078-0432.CCR-08-2242

Ramamoorthy, S., Donohue, M., & Buck, M. (2009). Decreased Jun-D and myogenin expression in muscle wasting of human cachexia. *Am J Physiol Endocrinol Metab, 297*(2), E392-401. doi: 10.1152/ajpendo.90529.2008

Rennie, M. J., Wackerhage, H., Spangenburg, E. E., & Booth, F. W. (2004). Control of the size of the human muscle mass. *Annu Rev Physiol, 66*, 799-828. doi: 10.1146/annurev.physiol.66.052102.134444

Riddell, D. R., & Owen, J. S. (1999). Nitric oxide and platelet aggregation. *Vitam Horm, 57*, 25-48.

Riede, U. N., Forstermann, U., & Drexler, H. (1998). Inducible nitric oxide synthase in skeletal muscle of patients with chronic heart failure. *J Am Coll Cardiol, 32*(4), 964-969.

Ruderman, N. B., & Berger, M. (1974). The formation of glutamine and alanine in skeletal muscle. *J Biol Chem, 249*(17), 5500-5506.

Ryazanov, A. G., & Davydova, E. K. (1989). Mechanism of elongation factor 2 (EF-2) inactivation upon phosphorylation. Phosphorylated EF-2 is unable to catalyze translocation. *FEBS Lett, 251*(1-2), 187-190.

S Damrauer, J., Stadler, M., Acharyya, S., S Baldwin, A., E Couch, M., & Guttridge, D. (2008). *Chemothrapy-induced muscle wasting: association with NF-kB and cancer cachexia* (Vol. 18).

Sacco, G., Giampietro, R., Salvatorelli, E., Menna, P., Bertani, N., Graiani, G., . . . Minotti, G. (2003). Chronic cardiotoxicity of anticancer anthracyclines in the rat: role of secondary metabolites and reduced toxicity by a novel anthracycline with impaired metabolite formation and reactivity. *Br J Pharmacol, 139*(3), 641-651. doi: 10.1038/sj.bjp.0705270

Sawyer, D. B., Fukazawa, R., Arstall, M. A., & Kelly, R. A. (1999). Daunorubicin-induced apoptosis in rat cardiac myocytes is inhibited by dexrazoxane. *Circ Res, 84*(3), 257-265.

Shin, M., Matsunaga, H., & Fujiwara, K. (2010). Differences in accumulation of anthracyclines daunorubicin, doxorubicin and epirubicin in rat tissues revealed by immunocytochemistry. *Histochem Cell Biol, 133*(6), 677-682. doi: 10.1007/s00418-010-0700-3

Sinacore, D. R., & Gulve, E. A. (1993). The role of skeletal muscle in glucose transport, glucose homeostasis, and insulin resistance: implications for physical therapy. *Phys Ther, 73*(12), 878-891.

Singal, P. K., & Iliskovic, N. (1998). Doxorubicin-induced cardiomyopathy. *N Engl J Med, 339*(13), 900-905. doi: 10.1056/NEJM199809243391307

Singal, P. K., Li, T., Kumar, D., Danelisen, I., & Iliskovic, N. (2000). Adriamycin-induced heart failure: mechanism and modulation. *Mol Cell Biochem, 207*(1-2), 77-86.

Skovsgaard, T., & Nissen, N. I. (1982). Membrane transport of anthracyclines. *Pharmacol Ther, 18*(3), 293-311.

Smuder, A. J., Kavazis, A. N., Min, K., & Powers, S. K. (2011a). Exercise protects against doxorubicin-induced markers of autophagy signaling in skeletal muscle. *J Appl Physiol (1985), 111*(4), 1190-1198. doi: 10.1152/japplphysiol.00429.2011

Smuder, A. J., Kavazis, A. N., Min, K., & Powers, S. K. (2011b). Exercise protects against doxorubicin-induced oxidative stress and proteolysis in skeletal muscle. *J Appl Physiol (1985), 110*(4), 935-942. doi: 10.1152/japplphysiol.00677.2010

Stamler, J. S., & Meissner, G. (2001). Physiology of nitric oxide in skeletal muscle. *Physiol Rev, 81*(1), 209-237.

Taylor, P. M. (2014). Role of amino acid transporters in amino acid sensing. *Am J Clin Nutr, 99*(1), 223S-230S. doi: 10.3945/ajcn.113.070086

Temparis, S., Asensi, M., Taillandier, D., Aurousseau, E., Larbaud, D., Obled, A., . . . Attaix, D. (1994). Increased ATP-ubiquitin-dependent proteolysis in skeletal muscles of tumor-bearing rats. *Cancer Res, 54*(21), 5568-5573.

Teraoka, K., Hirano, M., Yamaguchi, K., & Yamashina, A. (2000). Progressive cardiac dysfunction in adriamycin-induced cardiomyopathy rats. *Eur J Heart Fail, 2*(4), 373-378.

Thorn, C. F., Oshiro, C., Marsh, S., Hernandez-Boussard, T., McLeod, H., Klein, T. E., & Altman, R. B. (2011). Doxorubicin pathways: pharmacodynamics and adverse effects. *Pharmacogenet Genomics, 21*(7), 440-446. doi: 10.1097/FPC.0b013e32833ffb56

Tisdale, M. J. (2002). Cachexia in cancer patients. *Nat Rev Cancer, 2*(11), 862-871. doi: 10.1038/nrc927

Uehara, A., Sekiya, C., Takasugi, Y., Namiki, M., & Arimura, A. (1989). Anorexia induced by interleukin 1: involvement of corticotropin-releasing factor. *Am J Physiol, 257*(3 Pt 2), R613-617.

van Asperen, J., van Tellingen, O., Tijssen, F., Schinkel, A. H., & Beijnen, J. H. (1999). Increased accumulation of doxorubicin and doxorubicinol in cardiac tissue of mice lacking mdr1a P-glycoprotein. *Br J Cancer, 79*(1), 108-113. doi: 10.1038/sj.bjc.6690019

van Norren, K., van Helvoort, A., Argiles, J. M., van Tuijl, S., Arts, K., Gorselink, M., . . . van der Beek, E. M. (2009). Direct effects of doxorubicin on skeletal muscle contribute to fatigue. *Br J Cancer, 100*(2), 311-314. doi: 10.1038/sj.bjc.6604858

Vasquez-Vivar, J., Martasek, P., Hogg, N., Masters, B. S., Pritchard, K. A., Jr., & Kalyanaraman, B. (1997). Endothelial nitric oxide synthase-dependent superoxide generation from adriamycin. *Biochemistry, 36*(38), 11293-11297. doi: 10.1021/bi971475e

Vaughan, V. C., Martin, P., & Lewandowski, P. A. (2013). Cancer cachexia: impact, mechanisms and emerging treatments. *J Cachexia Sarcopenia Muscle, 4*(2), 95-109. doi: 10.1007/s13539-012-0087-1

Volpi, E., Kobayashi, H., Sheffield-Moore, M., Mittendorfer, B., & Wolfe, R. R. (2003). Essential amino acids are primarily responsible for the amino acid stimulation of muscle protein anabolism in healthy elderly adults. *Am J Clin Nutr, 78*(2), 250-258.

Wagenmakers, A. J. (1998). Protein and amino acid metabolism in human muscle. *Adv Exp Med Biol, 441*, 307-319.

Wallimann, T., Wyss, M., Brdiczka, D., Nicolay, K., & Eppenberger, H. M. (1992). Intracellular compartmentation, structure and function of creatine kinase isoenzymes in tissues with high and fluctuating energy demands: the 'phosphocreatine circuit' for cellular energy homeostasis. *Biochem J, 281 (Pt 1)*, 21-40.

Wang, H., Li, T. L., Hsia, S., Su, I. L., Chan, Y. L., & Wu, C. J. (2015). Skeletal muscle atrophy is attenuated in tumor-bearing mice under chemotherapy by treatment with fish oil and selenium. *Oncotarget, 6*(10), 7758-7773. doi: 10.18632/oncotarget.3483

Wang, S., Konorev, E. A., Kotamraju, S., Joseph, J., Kalivendi, S., & Kalyanaraman, B. (2004). Doxorubicin induces apoptosis in normal and tumor cells via distinctly different mechanisms. intermediacy of H(2)O(2)- and p53-dependent pathways. *J Biol Chem, 279*(24), 25535-25543. doi: 10.1074/jbc.M400944200

Weiss, R. B. (1992). The anthracyclines: will we ever find a better doxorubicin? *Semin Oncol, 19*(6), 670-686.

Weissman, B. A., Jones, C. L., Liu, Q., & Gross, S. S. (2002). Activation and inactivation of neuronal nitric oxide synthase: characterization of Ca(2+)-dependent [125I]Calmodulin binding. *Eur J Pharmacol, 435*(1), 9-18.

Westerblad, H., Bruton, J. D., & Katz, A. (2010). Skeletal muscle: energy metabolism, fiber types, fatigue and adaptability. *Exp Cell Res, 316*(18), 3093-3099. doi: 10.1016/j.yexcr.2010.05.019

White-Gilbertson, S., Kurtz, D. T., & Voelkel-Johnson, C. (2009). The role of protein synthesis in cell cycling and cancer. *Mol Oncol, 3*(5-6), 402-408. doi: 10.1016/j.molonc.2009.05.003

Williams, A., Sun, X., Fischer, J. E., & Hasselgren, P. O. (1999). The expression of genes in the ubiquitin-proteasome proteolytic pathway is increased in skeletal muscle from patients with cancer. *Surgery, 126*(4), 744-749; discussion 749-750.

Wolfe, R. R. (2006). The underappreciated role of muscle in health and disease. *Am J Clin Nutr, 84*(3), 475-482.

Xi, L., Zhu, S. G., Das, A., Chen, Q., Durrant, D., Hobbs, D. C., . . . Kukreja, R. C. (2012). Dietary inorganic nitrate alleviates doxorubicin cardiotoxicity: mechanisms and implications. *Nitric Oxide, 26*(4), 274-284. doi: 10.1016/j.niox.2012.03.006

Yang, F., Teves, S. S., Kemp, C. J., & Henikoff, S. (2014). Doxorubicin, DNA torsion, and chromatin dynamics. *Biochim Biophys Acta, 1845*(1), 84-89. doi: 10.1016/j.bbcan.2013.12.002

Yen, H. C., Oberley, T. D., Vichitbandha, S., Ho, Y. S., & St Clair, D. K. (1996). The protective role of manganese superoxide dismutase against adriamycin-induced acute cardiac toxicity in transgenic mice. *J Clin Invest, 98*(5), 1253-1260. doi: 10.1172/JCI118909

Yu, A. P., Pei, X. M., Sin, T. K., Yip, S. P., Yung, B. Y., Chan, L. W., . . . Siu, P. M. (2014). Acylated and unacylated ghrelin inhibit doxorubicin-induced apoptosis in skeletal muscle. *Acta Physiol (Oxf), 211*(1), 201-213. doi: 10.1111/apha.12263

Yu, Z., Zhang, W., & Kone, B. C. (2002). Signal transducers and activators of transcription 3 (STAT3) inhibits transcription of the inducible nitric oxide synthase gene by interacting with nuclear factor kappaB. *Biochem J, 367*(Pt 1), 97-105. doi: 10.1042/BJ20020588

Zhang, S., Liu, X., Bawa-Khalfe, T., Lu, L. S., Lyu, Y. L., Liu, L. F., & Yeh, E. T. (2012). Identification of the molecular basis of doxorubicin-induced cardiotoxicity. *Nat Med, 18*(11), 1639-1642. doi: 10.1038/nm.2919